EVALUATION OF CYTOCHROME *BC_1* AS A TARGET FOR SINGLE-DOSE ANTIMALARIAL THERAPY: A COMPARATIVE ASSESSMENT OF Q_I VS. Q_O SITE INHIBITION IN *PLASMODIUM*

Allison M. Stickles, M.S.

A DISSERTATION

Presented to the Department of Physiology and Pharmacology

Oregon Health & Science University

School of Medicine

In partial fulfillment of the requirements for the degree of

Doctor of Philosophy

June 2014

School of Medicine

Oregon Health & Science University

CERTIFICATE OF APPROVAL

This is to certify that the PhD dissertation of

Allison M. Stickles

has been approved

_____
Mentor/Advisor

_____
Member

_____
Member

_____
Member

_____
Member

TABLE OF CONTENTS

LIST OF ABBREVIATIONS

ACT	Artemisinin Combination Therapy
ATV	Atovaquone
cLogP	Calculated LogP (solubility measure)
CQ	Chloroquine
CRI	Cross-Resistance Index
Cyt *bc*$_1$	Cytochrome *bc*$_1$
DDM	n-dodecyl β-D-maltoside
DDT	Dichlorodiphenyltrichloroethane (insecticide)
DHODH	Dihydroorotate Dehydrogenase
DMF	Dimethylformamide
DMSO	Dimethyl Sulfoxide
ED$_{50}$/ED$_{99}$	50% and 90% Effective Dose
ELQ	Endochin-like Quinolone
GDP	Gross Domestic Product
GSK	GlaxoSmithKline
G6PD	Glucose-6-Phosphate Dehydrogenase
HDQ	1-hydroxyl-2-dodecyl-4(*1H*)-quinolone
HEK	Human Embryonic Kidney
HFF	Human Foreskin Fibroblasts
IC$_{50}$	50% Inhibitory Concentration
ISP	Rieske Iron Sulfur Protein

LC/MS	Liquid Chromatography / Mass Spectrometry
MMV	Medicines for Malaria Venture
NMR	Nuclear Magnetic Resonance Imaging
Q	Ubiquinone
QH	Semiquinone
QH_2	Ubiquinol
PEG	Polyethylene Glycol
PRR	Parasite Reduction Ratio
RBC	Red Blood Cell
SAR	Structure-Activity Relationship
WHO	World Health Organization

LIST OF FIGURES

CHAPTER 1

CHAPTER 2

CHAPTER 3

CHAPTER 4

CHAPTER 5

CHAPTER 6

APPENDIX A

LIST OF TABLES

CHAPTER 3

CHAPTER 4

CHAPTER 5

APPENDIX B

ACKNOWLEDGEMENTS

This work would not have been possible without the support of my many teachers, collaborators, and colleagues. I would especially like to thank our friends at Drexel University, Albert Einstein College of Medicine, Columbia University, and the Medicines for Malaria venture for their crucial roles in supporting the development of ELQ-300 and ELQ-400. Dr. Akhil Vaidya and his team at Drexel have been instrumental in assessing the resistance propensity and enzyme-level mutations associated with these compounds, and their previous work with cytochrome bc_1 provided an invaluable foundation for this research. Dr. Kami Kim and her colleagues at Albert Einstein have greatly extended the impact of this work by evaluating the transmission-blocking and prophylactic capabilities of our compounds, and without Dr. Fidock's group at Columbia I would not have had access to the invaluable D1 clone that drove much of my research and provided initial insight into the site-specific targeting of the ELQs.

Within my own group, I would like to acknowledge Drs. Rolf Winter and Aaron Nilsen for their tireless work in synthesizing and diversifying the ELQ library, and express my gratitude to Aaron for teaching me the basics of medicinal chemistry that will be invaluable in my future career. I would also like to thank Dr. Isaac Forquer for his patience and extensive knowledge of enzyme biophysics, and Dr. Yuexin Li for her help with the many in vivo studies required for this project. To

my mentor, Dr. Mike Riscoe, I cannot express enough gratitude for the intellectual freedom and support you have offered me, and I know that your unique blend of realism and tireless enthusiasm will be something that I dearly attempt to replicate in my own career. To the members of my dissertation committee, colleagues within the MD/PhD program, and all of my teachers at Oregon Health & Science University, I would like to acknowledge and thank you for the support, guidance, and unique perspectives that have been offered to me. Finally, to the members of the broader parasitology community, it has been an absolute pleasure to be embraced by this field, and I look forward to many more years of excitement, collaboration, and research.

On a personal level, I would like to thank all of my teachers outside of the world of science. I would like to thank my family for teaching me the value of hard work, and tell my parents that I am so grateful to them for always supporting my choices, even when they were difficult to understand. To my martial arts family, I want to acknowledge all of the life lessons I have learned on the training floor. Without you, I may not know that pain and struggle can be positive things and I may have never learned to confront challenges with my eyes open. To all of you, friends, family, teachers, collaborators, and colleagues: thank you. I simply cannot say that enough.

ABSTRACT

Malaria is a devastating parasitic disease that affects more than 200 million people and is a leading cause of mortality in the developing world. Although many potent antimalarial therapies exist, the effectiveness of these compounds has been limited by the emergence of drug resistant *Plasmodium* parasites, the cost of multi-day treatment, and restrictive mechanisms of action, which often fail to protect against the sexual or liver stage parasites that are responsible for disease transmission. A major priority for antimalarial drug development, and this project, is the identification of multi-stage therapies that are broadly effective as treatments, prophylactics, and transmission blocking agents following a single, oral dose.

This project focuses specifically on the cytochrome bc_1 complex (cyt bc_1) as a target for single-dose, multi-stage therapy. Biologically, cyt bc_1 is essential for the regeneration of ubiquinone, which plays an essential role in major metabolic processes for *P. falciparum*, including heme and pyrimidine biosynthesis. While various cyt bc_1 inhibitors, including atovaquone (ATV) and ELQ-300, are effective single-dose prophylactics, they have not previously demonstrated single-dose, curative activity against blood-stage parasites. For that reason, I first evaluated the 4(*1H*)-quinolone compound, ELQ-400, as a more potent, in vivo alternative to ATV and ELQ-300.

In single-dose murine models, ELQ-400 rapidly reduced blood-stage parasitemia and prevented recrudescence at low doses of 1 mg/kg. In order to understand the mechanism of the single-dose response to ELQ-400, I next assessed how 4(*1H*)-quinolones interacted with cyt bc_1. I used drug sensitivity screens against *P. falciparum* clones containing selective mutations at either the oxidative (Q_o) or reductive (Q_i) sites of cyt bc_1 to create a structure activity (SAR) profile of Q_o vs. Q_i targeting for the ELQs. I found that, while 5 and 7-position substituents were broadly associated with Q_o-targeting, aryl side chains and 6-halogens contributed to Q_i site inhibition. Intriguingly, ELQ-400 contained both Q_o and Q_i directing features, suggesting a role as potential dual-site inhibitor of cyt bc_1. Accordingly, ELQ-400 demonstrated signs of both Q_i and Q_o site inhibition in cytochrome *b* reduction assays conducted in *P. denitrificans*.

Strikingly, I found that the single-dose activity of ELQ-400 could be effectively replicated by co-administration of the respective Q_o and Q_i site inhibitors, ATV and ELQ-300. Acute assessment of ATV vs. ELQ-300 therapy also revealed several specific differences that may be attributable to general Q_o vs. Q_i site inhibition. While ATV therapy initiated more rapid parasite clearance, ELQ-300 treatment was associated with both a lower resistance propensity and a cumulative multi-day dosing effect. Importantly, both ELQ-400 and ATV:ELQ-300 combination therapy combined the desirable clinical features of ATV and ELQ-300 monotherapy, suggesting that dual-site inhibition of cyt bc_1 is a viable strategy for multi-stage, single-dose antimalarial treatment.

CHAPTER ONE: INTRODUCTION AND LITERATURE REVIEW

INTRODUCTION

Malaria is a global parasitic disease that affects approximately 200 million people and is responsible for more than half a million deaths every year[1]. Mechanistically, malaria is caused by *Plasmodium* parasites, which are transmitted by the bite of an infected *Anopheles* mosquito and progress through a series of biologically distinct stages within the liver and red blood cells (RBCs) of the human host. Although malaria is treatable, resistance has developed against many hallmark therapies, including quinine, chloroquine, mefloquine, and pyrimethamine[2], which has severely limited treatment options for patients in endemic areas. As a result, there is an urgent need for new antimalarial compounds, particularly those that effectively inhibit drug-resistant parasites and function throughout multiple stages of the parasite life cycle to provide simultaneous treatment, prophylaxis, and transmission blocking activity against malaria.

Complex III of the mitochondrial electron transport chain, also known as the cytochrome bc_1 complex (cyt bc_1), is a validated target for multi-stage antimalarial therapy. **This project focuses specifically on cyt bc_1, with the major goal of optimizing inhibitors of this complex for single-dose use**. The following sections provide an overview of malaria and highlight several biological,

clinical, and historical features that impact modern drug development. This chapter also describes the major cellular roles of cyt bc_1 and concludes with a general strategy for identifying and characterizing single-dose cyt bc_1 inhibitors.

LITERATURE REVIEW

Plasmodium Parasites

Plasmodium parasites are obligate intracellular, single-celled eukaryotes that belong to the phylum, *Apicomplexa*. Although dozens of *Plasmodium* species have been documented, only five are responsible for malaria in humans: *P. falciparum, P. vivax, P. ovale, P. malariae, and P. knowlesi*[3,4]. For each of these species, the *Plasmodium* life cycle consists of a sexual replication phase within the *Anopheles* mosquito and several asexual replication and differentiation stages within the secondary host (Figure 1). In humans, infection begins when sporozoites are introduced from the salivary glands of an infected *Anopheles* mosquito. These sporozoites migrate to the liver where they undergo initial maturation and asexual reproduction within hepatocytes and, after approximately one week, merozoites exit the liver and invade either reticulocytes or mature RBCs within the bloodstream[5]. These blood-stage parasites then undergo multiple rounds of rapid asexual reproduction in what is known as the erythrocytic cycle.

CHAPTER ONE: INTRODUTION AND LITERATURE REVIEW

Erythrocytic cycle parasites can be divided into several subtypes based on morphology. Ring-stage parasites are discernable shortly after RBC invasion and are characterized by their faint, circular (ring-like) appearance. During the maturation process, ring-stage parasites develop into trophozoites, which are larger in size and contain distinctive acidic vacuoles used for heme digestion and detoxification. Ultimately, trophozoite parasites undergo mitotic replication to produce schizonts and, upon schizont rupture, multiple merozoites are released into the blood stream to initiate new rounds of erythrocytic infection[6].

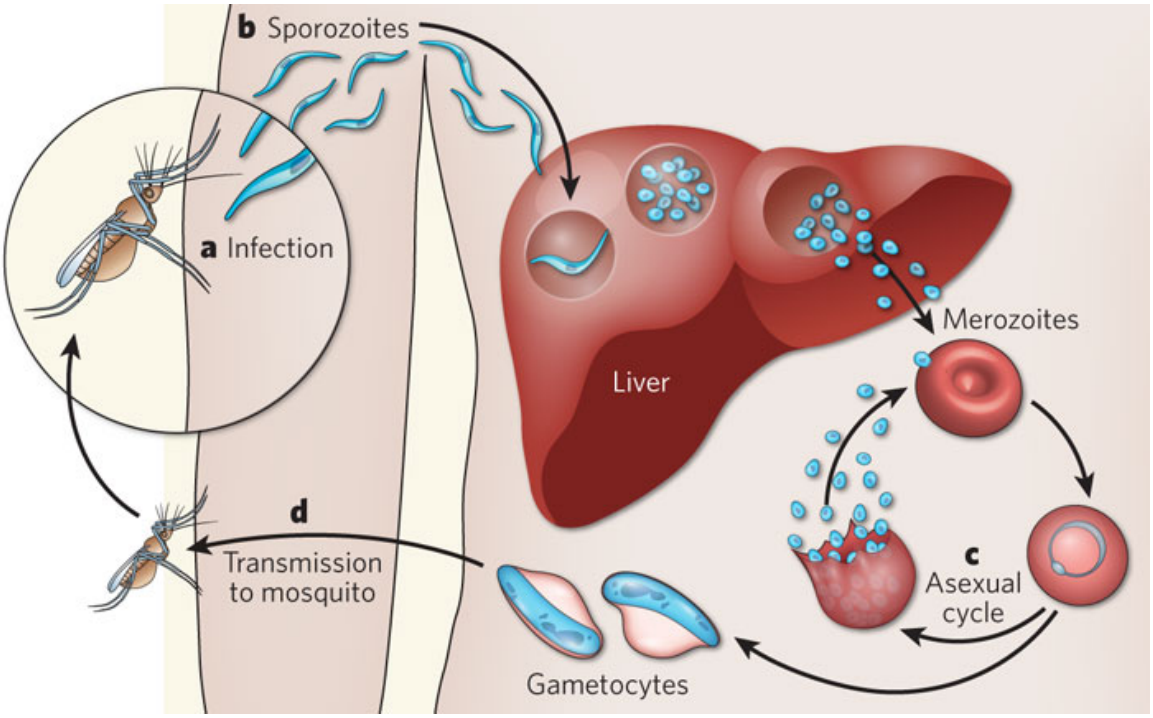

Figure 1: Life cycle of *Plasmodium* parasites[7], depicting liver-stage, blood-stage, and sexual-stage (gametocyte) parasites.

CHAPTER ONE: INTRODUTION AND LITERATURE REVIEW

Although the majority of blood-stage parasites continue through the erythrocytic cycle, a subset will differentiate into sexual-stage gametocytes, which can be transmitted back to the *Anopheles* mosquito during a blood meal. These sexual-stage parasites then complete gamete differentiation, sexual reproduction, and oocyst formation within the mosquito midgut, and within 1-2 weeks, newly formed sporozoites migrate to the *Anopheles* salivary glands where they can be transmitted to a new host[8].

Clinical Malaria

The symptoms of malaria can be largely attributed to RBC lysis and antigen presentation that occurs as *Plasmodium* parasites progress through the erythrocytic cycle. The clinical presentation of disease varies widely, but often includes headaches, nausea, fatigue, and high fever[9]. Although these symptoms are not unique to malaria and are frequently misdiagnosed, a subset of patients exhibit precise fever/chill cycles that are characteristic of *Plasmodium* infection. In these patients, fevers align with periods of RBC lysis[10], and the specific frequency of each fever cycle reflects the replication time of blood-stage parasites, which can serve as a preliminary diagnostic tool. Of the five *Plasmodium* species capable of infecting humans, *P. falciparum, P. vivax*, and *P. ovale* are associated with 48 hour cycles, while *P. malariae* and *P. knowlesi* exhibit 72 and 24 hour cycles, respectively[3]. Clinically, most cases of malaria are

caused by either *P. falciparum* or *P. vivax*, and these have been the most extensively characterized malaria subtypes.

Falciparum Malaria

While the vast majority of malaria cases are non-fatal, severe manifestations of disease have been associated with *P. falciparum* infection. Unlike other *Plasmodium* species, *P. falciparum* parasites have the ability to express adhesion proteins on the RBC surface as a mechanism for immune evasion[11,12]. As a result, blood-vessel occlusion is a side effect of *falciparum* malaria, and damage can occur as a result of ischemia to major organs[13]. When occlusion occurs in the brain, it is termed “cerebral malaria” and may be associated with coma or even death in affected patients[14]. Occlusion of placental vessels is also a significant concern, and is a major factor contributing to the increased malaria mortality observed among pregnant women[15].

Vivax Malaria

Vivax malaria is distinct from *falciparum* malaria, both clinically and biologically. While *P. vivax* infection is rarely fatal and does not cause cytoadherence or blood-vessel occlusion, it has been associated with several manifestations of severe disease including anemia, thrombocytopenia, and acute lung injury[16,17]. Most challengingly, *vivax* malaria is also complicated by disease relapse that

may occur weeks or years after a patient has received treatment and left an endemic area. This potential for relapse is attributable to latent, "hypnozoite" parasites within the liver that exist in *P. vivax* and *P. ovale* infections[18]. Very little is known about the biological behavior of hypnozoites, and they can only be targeted by "radical cure" antimalarial therapies such as primaquine, which are limited by their extreme redox activity and associated toxicity in glucose-6-phosphate dehydrogenase (G6PD) deficient patients[19].

Falciparum vs. Vivax

Another relevant difference between *P. vivax* and *P. falciparum* is their mechanism of RBC invasion and associated blood cell preference. While *P. falciparum* parasites predominantly infect mature RBCs, *P. vivax* interacts with Duffy antigen during cell invasion and preferentially targets reticulocytes, which are Duffy antigen positive[18]. Although this reticulocyte-preference limits the parasite burden carried by patients, it creates unique challenges for research, which relies heavily on the ability to culture parasites in vitro.

Malaria Epidemiology

Geographically, tropical and subtropical regions have the highest malaria prevalence, due largely to abundance of the *Anopheles* mosquito vector and the potential for continuous, "stable" transmission. Of the 99 countries classified as

malaria endemic in 2011, the vast majority are on the African continent, where more than 90% of malaria-related fatalities occur[20].

Numerous classification systems are used to gauge the extent and severity of malaria burden within infected communities. Infection rate divides malaria-positive regions into hypoendemic (<10%), mesoendemic (11-50%), hyperendemic (51-75%), and holoendemic (>75%) areas[21], while political intent and infrastructure are used to classify nations as either malaria-eliminating (where evidence-based elimination programs are in place), or as malaria-controlling (where there is no official policy for disease control)[22] (Figure 2).

Measures of disease burden are clinically relevant because high-frequency exposure to *Plasmodium* parasites is associated with partial immunity and is protective against the development of severe malaria[9,21]. Although the immune response is poorly understood and does not prevent individuals from carrying patent, transmissible infections, many malaria-infected adults in hyperendemic and holoendemic regions are fully asymptomatic[9]. As a result, malaria fatalities are largely limited to immune-naïve individuals, including young children and travelers from low-transmission or non-endemic regions.

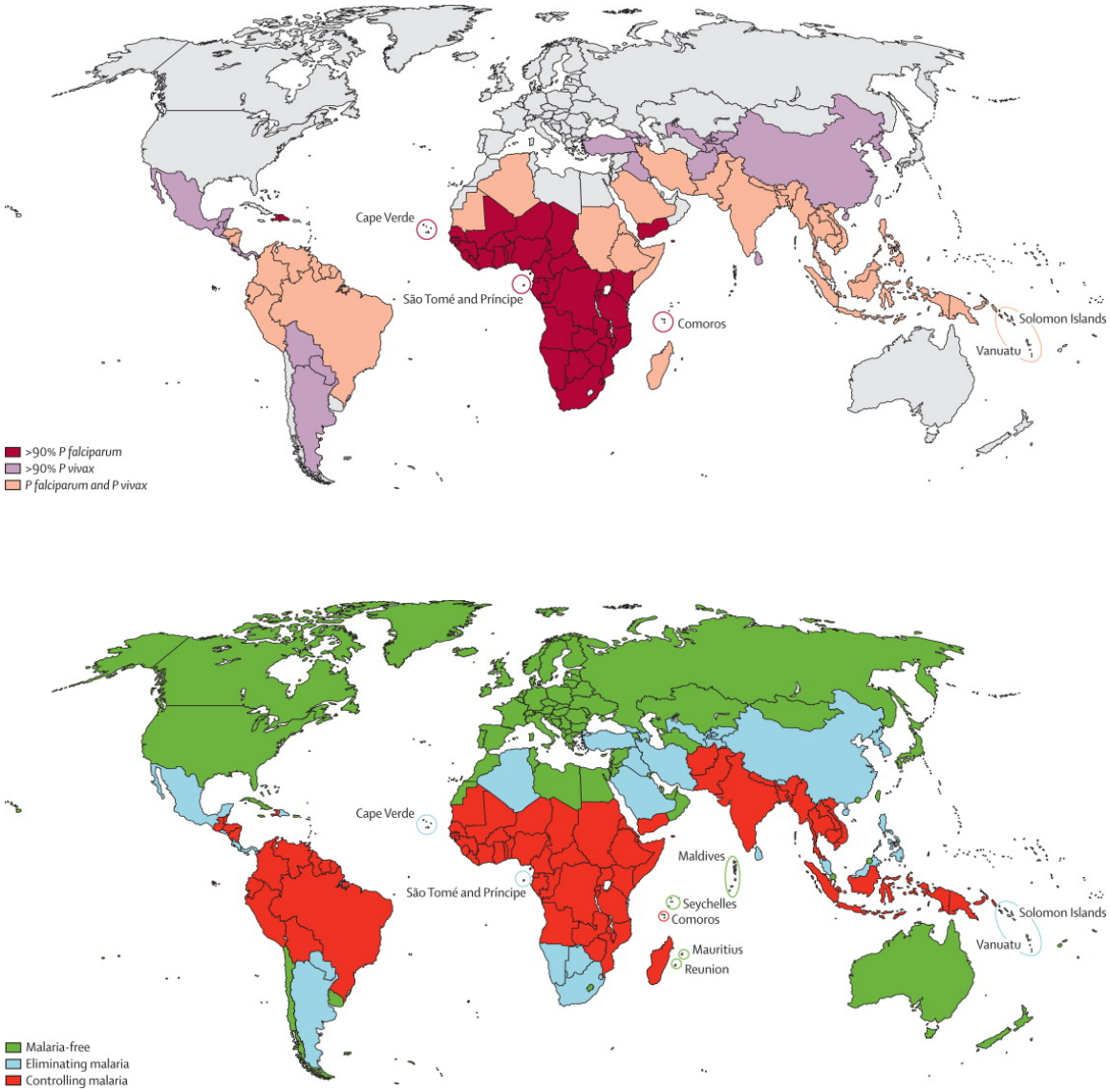

Figure 2: Geographical distribution of human malaria. Top panel: Distribution of *P. falciparum* (red), *P. vivax* (purple), or both *P. falciparum* and *P. vivax* (tan). Bottom panel: Classification of malaria-free (green), malaria-eliminating (blue), and malaria-controlling (red) regions[22].

Several genetic factors have also been implicated in partial protection against malaria. In Sub-Saharan Africa, the high frequency of the Duffy-negative phenotype has resulted in the essential absence of *P. vivax* infection[23]. More broadly, genes associated with sickle-cell anemia, thalassemia, and G6PD deficiency have all been associated with moderate protection against both *vivax* and *falciparum* malaria[24], presumably by altering the morphology of RBCs and complicating the process of merozoite invasion or by increasing RBC turnover.

Malaria Eradication

Historical Perspective

While malaria remains a devastating, widespread disease, coordinated eradication programs have played a significant role in decreasing the global malaria burden over the past century. The first of these efforts was the Global Malaria Eradication Program, launched by the World Health Organization (WHO) in 1955. During this period, chloroquine and DDT were extensively used to treat patients and decrease the *Anopheles* population[25], respectively. Chloroquine is a quinoline compound, which functions by accumulating within the acidic digestive vacuole of trophozoite parasites. Biologically, this accumulation both interferes with the process of heme detoxification and disrupts osmotic balance, causing rapid lysis of blood-stage parasites[26]. Unfortunately, the evolution of efflux pumps in *P. falciparum* has rendered chloroquine and similar quinolone derivatives

ineffective in many endemic regions and it they are not viable options for ongoing drug eradication efforts.

Current Standard of Care

In endemic areas, artemisinin and its analogs currently play a dominant role in the acute treatment of malaria[27]. Aretmisinin combination therapies (ACTs) are endoperoxide-based and cause oxidative damage and alkylation of multiple cellular organelles as a result of endoperoxide activation by free iron within the digestive vacuole[28]. ACTs have an incredibly rapid onset of action and artesunate, which can be administered via IV injection, is especially useful for the treatment of infants or patients with severe disease[29]. Unfortunately, ACTs fail to inhibit liver-stage parasites, and provide no prophylactic protection against malaria[30]. More problematically, ACT resistance has also recently emerged in the South Pacific[31], and there is a desperate need for new first-line therapies, especially multi-stage compounds that provide both acute treatment and prophylactic protection against malaria.

To date, several multi-stage antimalarials have been identified, including atovaquone, pyrimethamine, and proguanil, which function throughout the *Plasmodium* life cycle by inhibiting major metabolic processes such as electron transport and folate metabolism[32,33]. Unfortunately, treatment is often cost-

prohibitive and, as a result, these multi-stage therapies are mainly used as prophylactics for travellers from non-endemic regions (Figure 3).

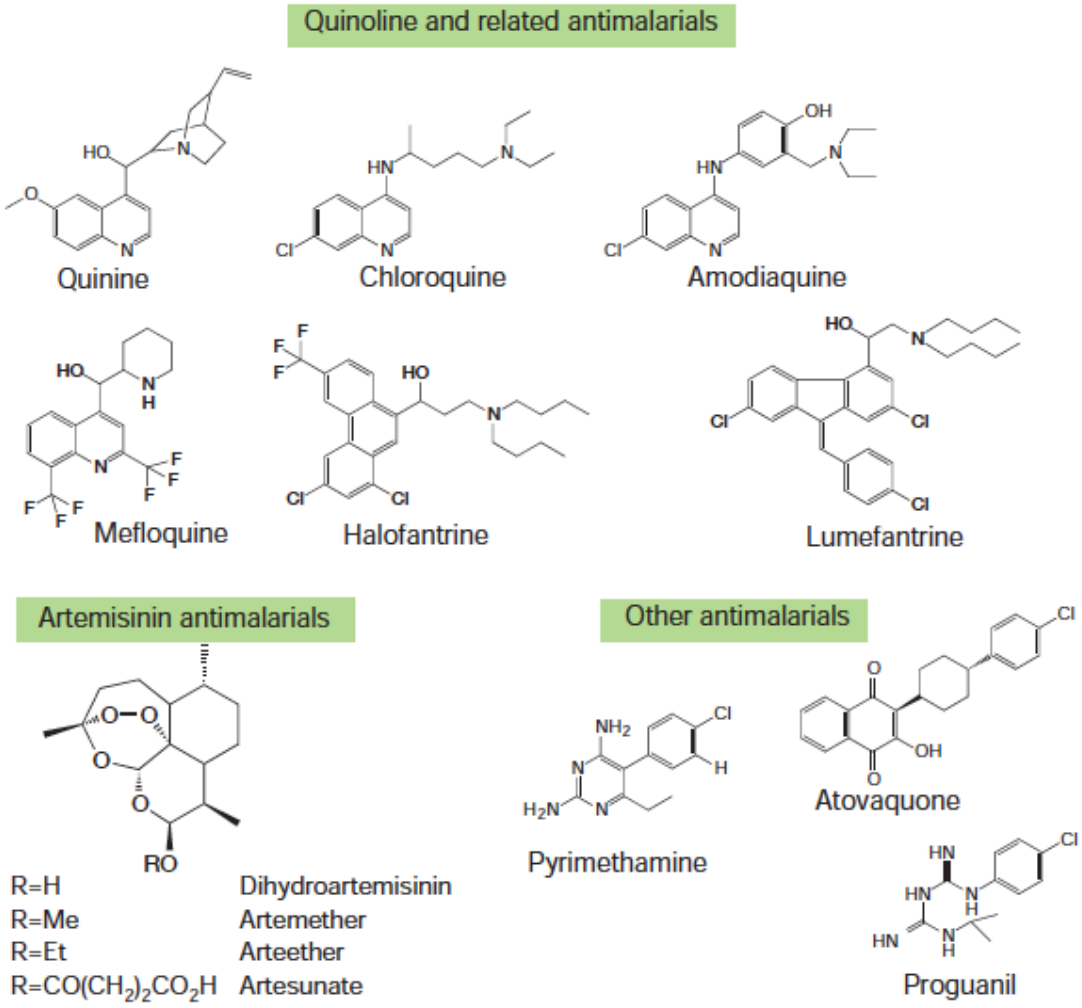

Figure 3: Structures of common antimalarial therapies, including chloroquine, artemisinin, and the multi-stage inhibitors pyrimethamine, atovaquone, and proguanil[34].

CHAPTER ONE: INTRODUTION AND LITERATURE REVIEW

Current Eradication Initiative

Although early eradication efforts were responsible for eliminating malaria from nearly 100 low-transmission countries, including the United States[35], the remaining malaria-endemic nations face a range of severe problems including widespread DDT and chloroquine resistance, low GDP[36], unpredictable access to healthcare providers, and a high incidence of HIV co-infection[37]. Ongoing treatment efforts require billions of dollars each year[38], yet have not effectively reduced disease burden in these highly endemic areas.

In an effort to address these problems, various international organizations, including the Gates Foundation, the Medicines for Malaria Venture, and the WHO have launched a second malaria eradication initiative and have outlined several priorities for ongoing drug development. Ultimately, these guidelines emphasize features that maximize the impact of antimalarial therapy in high-transmission areas. While cost is a major concern for use in the developing world, multi-stage efficacy and low potential for treatment failure are also key elements of the desired antimalarial target profile[39] (Figure 4).

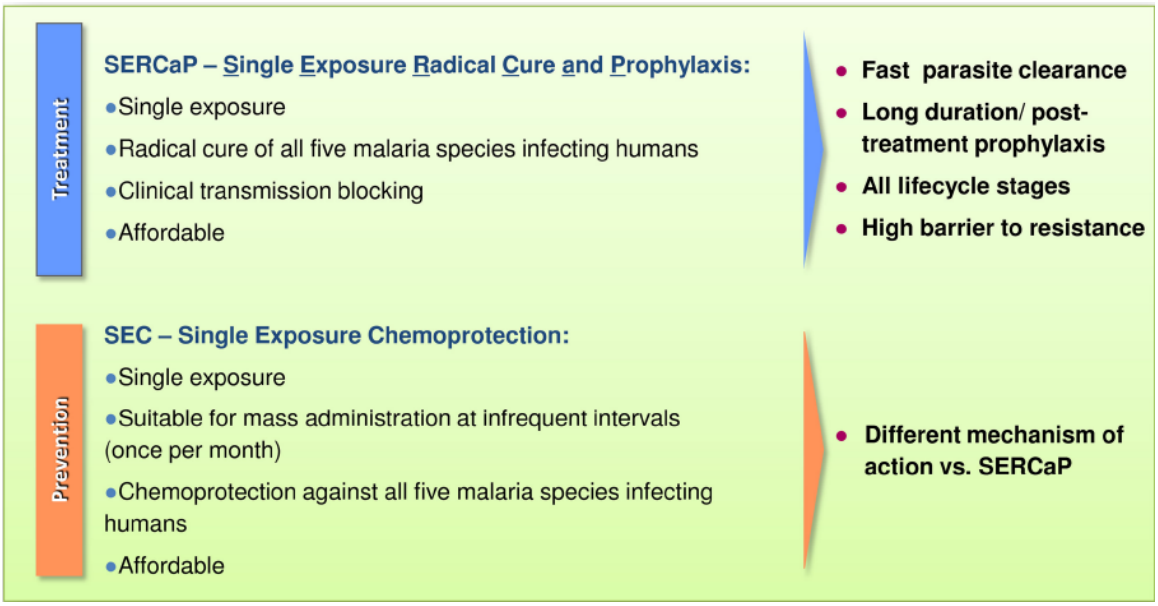

Figure 4: Target profiles for single-dose antimalarial therapy, as outlined by the Medicines for Malaria Venture[39].

Single Dose Antimalarial Therapy

Single dose therapy is one proposed way to reduce the risk of antimalarial treatment failure, specifically by simplifying dosing schedules and preventing medication noncompliance[40]. With multi-day dosing, compliance varies widely among patients and, in the most extreme cases, fewer than 50% of individuals take antimalarial drugs as directed[41]. Although there may be several reasons for noncompliance, cost is likely a dominant factor, especially in India and Africa where antimalarials may be purchased over the counter in variable quantities.

Several single dose compounds are currently being assessed for use in humans. For acute therapy, the endoperoxide OZ439[42], the aminopyridine MMV390048[43], and the spiroindolone NITD609[44], all effectively clear blood-stage parasites with respective curative doses of 20, 30, and 100 mg/kg in mouse models. Although these compounds all demonstrate secondary (human to mosquito) transmission-blocking activity, they do not provide single-dose causal prophylaxis[30]. In contrast, single dose prophylactic compounds, including atovaquone[73], 8-aminoquinolines[72], and imidazolopiperazines[45,46], are limited by their incomplete single-dose activity against blood-stage malaria. To date, no compound has exhibited combined treatment, prophylactic, and transmission-blocking activity following a single dose. **One major hypothesis of this research is that metabolic inhibitors can be optimized to provide single-dose, multi-stage activity against malaria, including inhibitors of the parasite cyt *bc$_1$* complex.**

Cytochrome *bc$_1$* Complex

Cyt *bc$_1$* is the third component of the mitochondrial electron transport chain, and is the specific molecular target of the multi-stage antimalarial drug, atovaquone. The main enzymatic function of cyt *bc$_1$* is to regenerate the local electron acceptor ubiquinone by transferring electrons from its reduced form, ubiquinol, to cytochrome *c.* This process is known as the Q cycle and involves the concerted

activity of three major catalytic subunits: cytochrome *b,* cytochrome c_1, and the Rieske iron sulfur protein (ISP) (Figure 5). Mechanistically, the Q cycle begins when ubiquinone and ubiquinol respectively bind to reductive (Q_i) and oxidative (Q_o) sites on opposite sides of the cytochrome *b* subunit. At the Q_o site, electrons are removed from ubiquinol and divergently transferred to the ISP and to local (b_H and b_L) heme groups within cytochrome *b*. ISP electrons are subsequently passed to cytochrome *c* via the cytochrome c_1 subunit, while cytochrome *b* electrons are ultimately used to regenerate ubiquinol at the Q_i site.

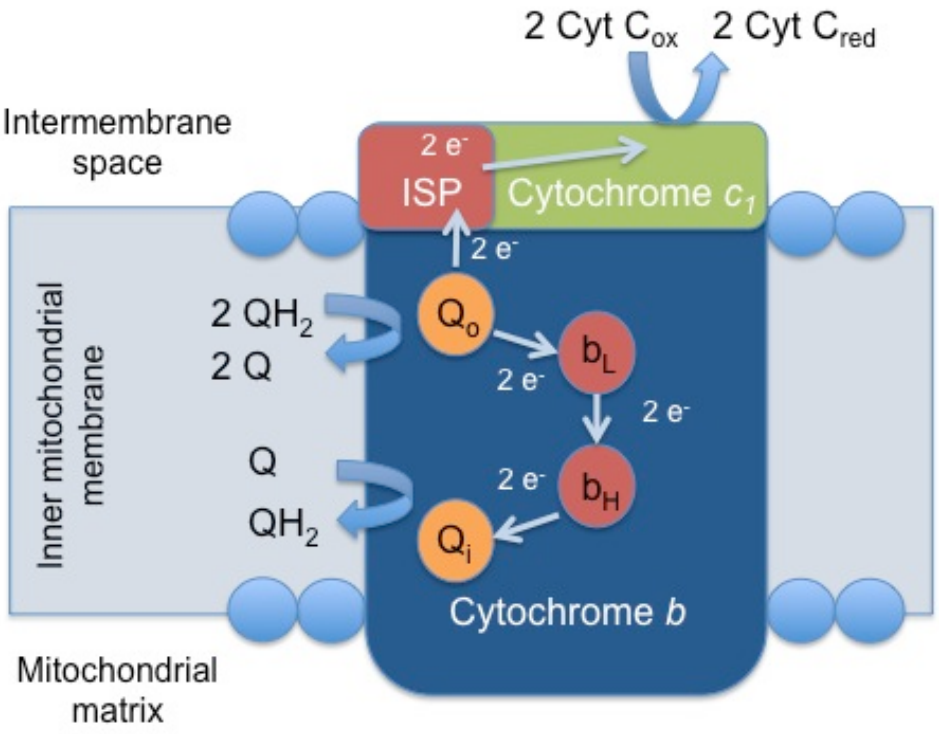

Figure 5: Schematic representation of the Q cycle, showing the conversion of ubiquinol (QH_2) to ubiquinone (Q) and the associated reduction of cytochrome *c*.

CHAPTER ONE: INTRODUTION AND LITERATURE REVIEW

While electron transport plays no significant role in ATP formation for *Plasmodium*, cyt bc_1 function is essential for both pyrimidine and heme biosynthesis for *P. falciparum* parasites. The link to pyrimidine biosynthesis is attributable to the type II dihydroorotate dehydrogenase (DHODH) enzyme, which is linked to the inner mitochondrial membrane and requires ubiquinone as a terminal electron acceptor. Because *P. falciparum* parasites lack a functional pyrimidine salvage pathway[47], inhibition of either DHODH or of downstream electron transport (at cyt bc_1) eliminates the pyrimidine supply necessary for nucleic acid synthesis, and this is believed to be ATV's primary mechanism of action in blood-stage parasites. Consistently, transgenic expression of cytosolic, yeast DHODH is sufficient to rescue blood-stage parasites from even high concentrations of ATV and other cyt bc_1 inhibitors[48].

Although blood-stage parasites have a clear demand for pyrimidines, the effects of cyt bc_1 inhibition in liver-stage and gametocyte parasites may be more directly linked to heme biosynthesis and TCA cycle function. While the overall role of the TCA cycle in *Plasmodium* remains unclear, it has been established that glutamate effectively feeds into the cycle and supports heme biosynthesis through its conversion to succinyl CoA[49]. It has also been reported that *P. falciparum* gametocytes undergo glucose catabolism via the TCA cycle and that both sporozoite and ookinete parasites upregulate expression of numerous TCA

enzymes relative to blood-stage forms[50]. In each of these contexts, TCA cycle function is linked to the activity of cyt bc_1 because it is the sole enzyme responsible for regenerating ubiquinone, which is a required electron acceptor for both succinate dehydrogenase and malate:quinone oxidoreductase (Figure 6).

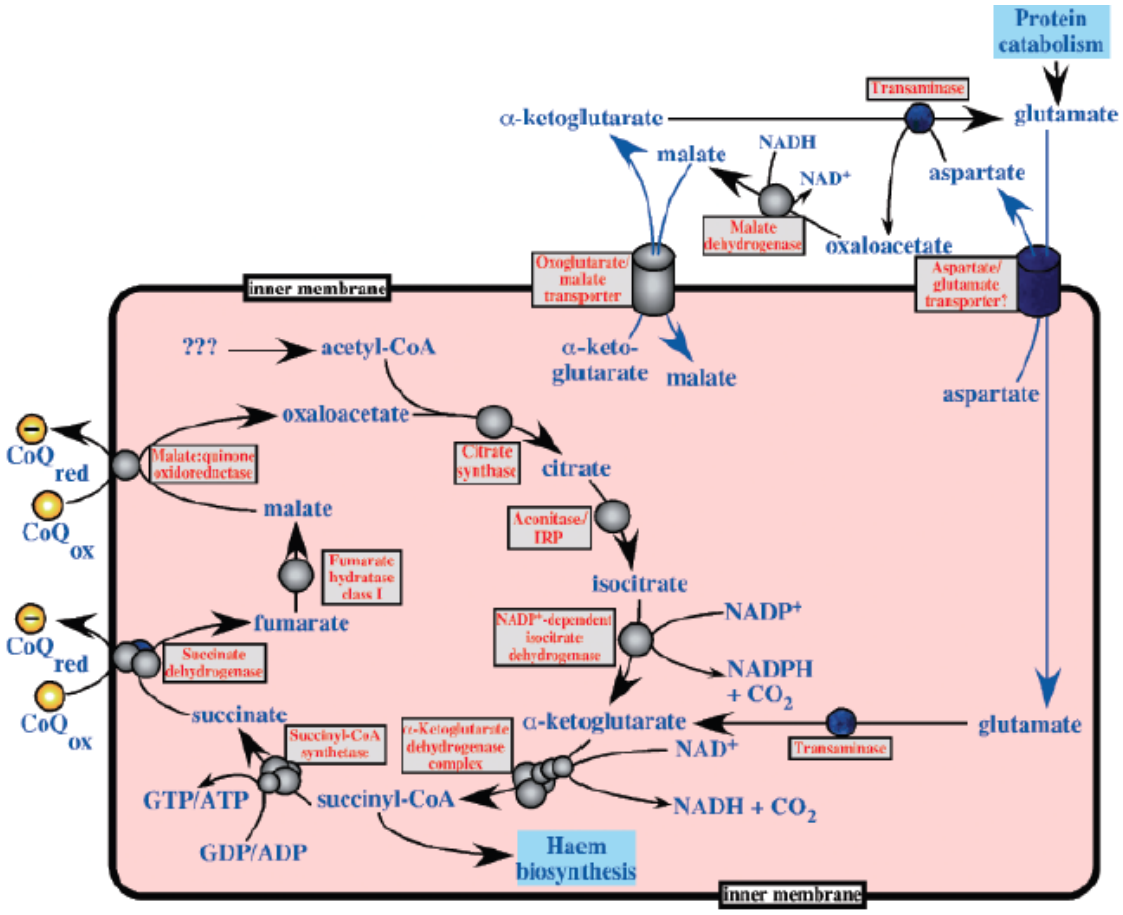

Figure 6: Proposed TCA cycle in *P. falciparum* parasites[50], with ubiquinol (CoQ) highlighted in yellow.

With respect to antimalarial therapy, both the Q_o and the Q_i site have been identified as potential targets for inhibition of cyt *bc₁*. The canonical Q_o site inhibitors are myxothiazol and stigmatellin, while antimycin A acts as a selective inhibitor of the Q_i site. Although inhibition at either site rapidly interrupts Q-cycle function, Q_i site inhibition is associated with unique non-enzymatic bypass reactions in yeast and bacterial models[51]. These bypass reactions take advantage of the cytochrome *b* reduction that can occur in the presence of Q_i inhibitors, and involve the passage of electrons from b_L and b_H to various alternative electron acceptors, including oxygen. As a result, superoxide production is a frequent result of Q_i site inhibition, and this process allows for continued, low-level reduction of cytochrome *c* that is not observed in following inhibition at the Q_o site.

Interestingly, attempts to inhibit the Q_i site of *Plasmodium* cytochrome *bc₁* have been generally unsuccessful. While the Q_o site is largely homologous between the *Plasmodium*, yeast, and human enzymes, genetic analysis has revealed that Q_i site residues with key roles in antimycin A inhibition are naturally mutated in *P. falciparum*, including the L214 and L217 residues that respectively correspond to F225 and K228 in yeast[52]. As a result, antimycin A requires mid-nanomolar concentrations to inhibit cyt *bc₁* in *P. falciparum* yet fully blocks the human or yeast enzymes in the sub-picomolar range[53].

CHAPTER ONE: INTRODUTION AND LITERATURE REVIEW

Atovaquone

ATV is the only cyt *bc*$_1$ inhibitor in current clinical use, and has been a mainstay of antimalarial therapy since its discovery in the early 1990s[54]. Structurally, ATV closely resembles ubiquinone and acts as a competitive inhibitor at the cyt *bc*$_1$ Q_o site[55,56]. In x-ray crystal structures derived from *S. cerevisiae*, it has been reported that the hydroxyl component of atovaquone's naphthoquinone core forms a polarized hydrogen bond with the His181 residue of the nearby ISP subunit, while other components of the core establish non-polar interactions with highly conserved Q_o site residues, including the P271 component of the integral "PEWY loop" (Figure 7)[56].

Despite its potency against *Plasmodium*, the major clinical limitation of ATV is its high propensity for drug resistance. When administered as monotherapy, Q_o site point mutations arise rapidly, including the Y268S substitution found in the *P. falciparum,* Tm90-C2B clinical isolate, which is associated with a more than 1000-fold loss of ATV potency[57,58]. Although resistance propensity has been substantially reduced by the use of Malarone, which combines ATV with the partner drug proguanil[59,60], the Y268S mutation has still been detected in several cases of Malarone treatment failure[61]. In these instances, the emergence of resistance may be linked to the prolonged half-life of ATV relative to proguanil (and its active metabolite, cycloguanil), which would expose parasites to

essential ATV monotherapy at late time points[33,62]. Ultimately, there is a need for novel cyt bc_1 inhibitors with the same multi-stage activity as atovaquone, but a dramatically reduced propensity for drug resistance.

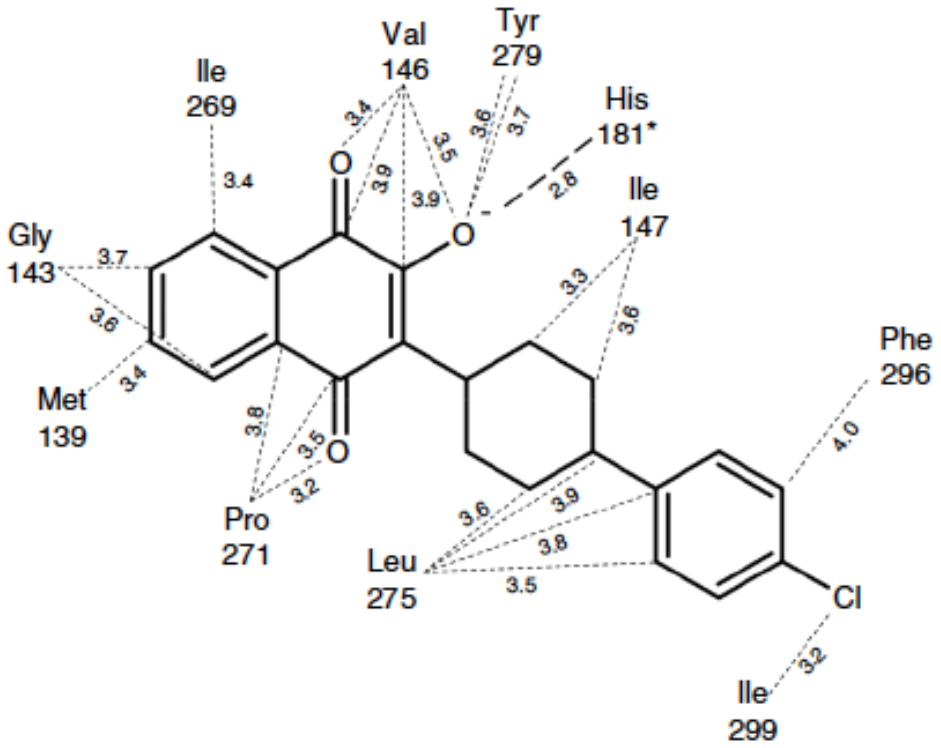

Figure 7: Interactions between atovaquone and the Q_o site of cyt bc_1 as identified by x-ray crystallography in *S. cerevisiae*. Hydrogen bonding to H181 illustrated by the thick, dashed line. Other depicted residues, including the Y279 residue (analogous to the Y268 in *P. falciparum*)[56], participate in non-polar interactions.

CHAPTER ONE: INTRODUTION AND LITERATURE REVIEW

Endochin-like Quinolones (ELQs)

Endochin was discovered by Hans Andersaag in the 1930s and is a 4(*1H*)-quinolone with known inhibitory activity at cyt bc_1[63,64]. Although endochin potently inhibited *P. falciparum* in vitro, it was inactive in preliminary human trials. As a result, optimization efforts were abandoned until the 1990s, when ATV was undergoing development, and the value of cyt bc_1 as a molecular target became apparent.

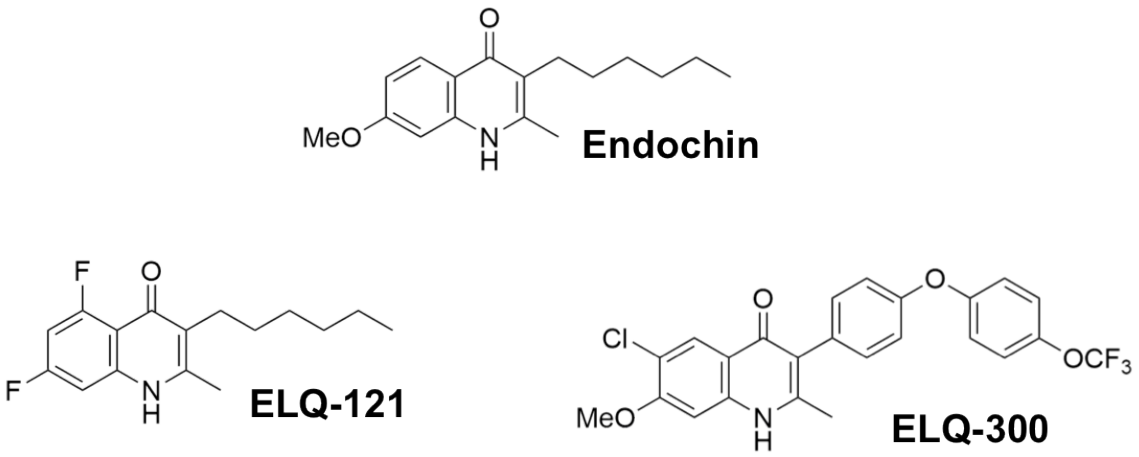

Figure 8: Structure of the 4(*1H*)-quinolone compounds, endochin, ELQ-121, and ELQ-300. The 3-diarylether side chain of ELQ-300 was critical for absorption and in vivo stability during the optimization of the ELQs.

One particular benefit of endochin as an antimalarial prototype is its surprising activity against ATV-resistant parasite strains, including Tm90-C2B. Several endochin variants, termed endochin-like quinolones (ELQs), have been designed in an attempt to maximize potency against various pan-sensitive and drug-resistant *P. falciparum* strains (Figure 8). To date, the most potent ELQ inhibitor of pan-sensitive parasites is the 5,7-difluoro compound, ELQ-121[64], while the most effective inhibitors of Tm90-C2B parasites are the 3-diarylether variants ELQ-271, ELQ-316[65], and ELQ-300[66].

ELQ-121

Like endochin, ELQ-121 was poorly active in mammalian models of malaria, likely due to extensive crystal formation and limited bioavailability. As can be seen in the ELQ-121 crystal structure, a number of intermolecular interactions occur between neighboring quinolone rings, including hydrogen bonds between oxygen, fluorine, and nitrogen components, and extensive aromatic, pi-pi stacking interactions (Figure 9). Consistently, the reduction of the 4-position ketone to an ether group in PEG-based, ELQ-121 prodrugs effectively decreased hydrogen bonding and was compatible with in vivo activity in mouse models[64].

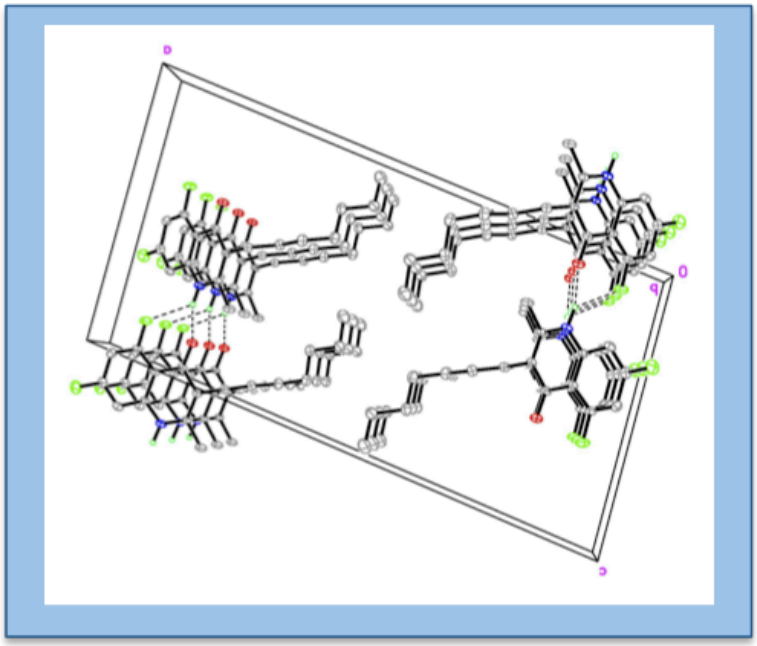

Figure 9: Crystal structure of ELQ-121 depicting intermolecular hydrogen bonds between 1-NH, 4-O, and 5-F residues, as well as pi-pi stacking interactions between the quinolone rings.

ELQ-300

The discovery of the 3-diarylether side chain represented a breakthrough for in vivo use of the ELQs. Like the ELQ-121 prodrug, the diarylether group likely interrupts crystal formation by introducing a steric obstacle to pi-pi stacking. This chemical group is also metabolically stable. Accordingly, the 3-diarylether ELQs are remarkably active in vivo, and the 6-chloro, 7-methoxy compound, ELQ-300, exceeds even the efficacy of ATV in murine models of malaria. ELQ-300 is also remarkable for its long in vivo half-life, low propensity for drug resistance, and

selective inhibition of *Plasmodium* cyt bc_1[66]. Like ATV, ELQ-300 demonstrates potent, single-dose prophylactic activity in murine models of malaria and it is likely that this property is a generalizable feature of highly potent cyt bc_1 inhibitors. Although ELQ-300 does not produce single-dose, blood-stage cures in murine models up to its solubility limit, a single 10 or 20 mg/kg dose could effectively delay recrudescence for more than one week following administration (Figure 10), suggesting that ELQs can potently inhibit parasites with a single exposure.

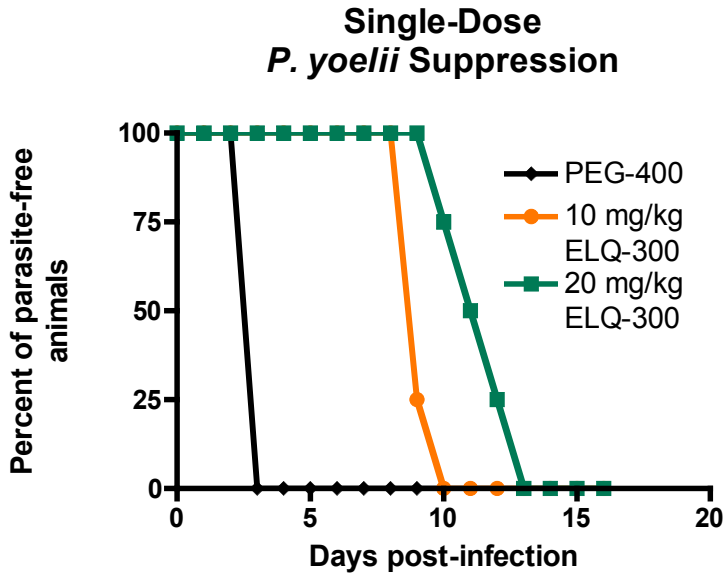

Figure 10: Recrudescence in blood-stage, *P. yoelii* infected mice following single-dose ELQ-300 treatment on day 1 post-infection vs. PEG-400 vehicle control. Both 10 and 20 mg/kg doses delayed recrudescence by more than one week relative to controls, but did not permanently clear infection.

CHAPTER ONE: INTRODUTION AND LITERATURE REVIEW

The primary goal of this project is to evaluate the ELQs as multi-stage, single dose therapies for malaria, and to determine the structural and biological mechanisms underlying single dose antimalarial activity at cyt *bc$_1$*.

Justification

Metabolic inhibitors, including those that function at cyt *bc$_1$*, are among the only compounds that effectively target liver-stage parasites and subsequently function as malarial prophylactics. Because all known prophylactics also exhibit some degree of activity against blood-stage parasites, prophylactic compounds are the logical choice for developing a multi-stage, single-dose therapy. Cyt *bc$_1$* is an especially valuable target because it coordinates multiple cellular processes and is sensitive to picomolar or nanomolar concentrations of several known inhibitors, including ATV, ELQ-300, and ELQ-121. Unlike ATV, all tested ELQs demonstrate a low propensity for drug resistance and many are active against clinically isolated, ATV-resistant parasites. Furthermore, because the ELQ library is easily diversifiable, new compounds can be readily designed to adjust and optimize single-dose ELQtherapies for eventual clinical use.

CHAPTER ONE: INTRODUTION AND LITERATURE REVIEW

Experimental Outline

This project involves two primary phases. In the first phase, a single-dose, cyt bc_1 antimalarial is synthesized as a proof of concept. Because activity against blood-stage parasites has been the failure point for single-dose activity of other metabolic inhibitors, in vivo assays in murine models serve as a preliminary screening tool, including the standard suppressive test that was used in the identification of the single-dose, blood-stage compounds OZ439 and NITD609. **Chapter three** describes this process and presents an initial characterization of the potent single-dose inhibitor, ELQ-400.

The second phase of this project focuses on the biological mechanism of ELQ-400 and the general theory that this compound functions as a dual, Q_o and Q_i site inhibitor of cyt bc_1. In **chapter four,** the relationship between ELQ structure and enzymatic site of action is assessed using various *P. falciparum* point mutants and molecular modeling techniques. Specific, dual-site inhibition by ELQ-400 is also verified via enzyme-level, cytochrome *b* reduction. Finally, this project explores alternatives to ELQ-400 treatment by using combination therapy to mimic the effects of simultaneous Q_o and Q_i site inhibition. **Chapter five** describes these combination therapy studies and highlights several features that may be uniquely associated with either Q_o or Q_i site inhibition in *Plasmodium*.

CHAPTER TWO: MATERIALS AND METHODS

The major experimental aims of this project are to: (1) Assess the single-dose antimalarial activity of the ELQs (2) Determine the mechanism of action of effective single-dose compounds, and (3) Explore alternate approaches to single-dose therapy. Experimentally, many of these research questions utilized similar techniques for chemical synthesis, in vitro/in vivo screening, and enzyme-level analysis, as described below.

Chemical Synthesis

ELQs were synthesized in house using one of two major synthetic methods. All 3-alkyl ELQs (approximate range: ELQ-100-ELQ-270) were synthesized by Rolf Winter as previously published[63,64]. The 3-aryl ELQs, including the 3-darylethers (approximate range: ELQ-271-ELQ-430) were synthesized by Aaron Nilsen, Galen Miley, and myself using the scheme outlined by Nilsen et al[66] (Figure 11). Briefly, aniline and ethyl acetoacetate were heated in benzene in the presence of p-tolulenesulfonic acid, and the condensation product was added to in boiling Dowtherm A at 250°C to produce a cyclized 4(*1H*)-quinolone precursor. The quinolone was then iodinated at the 3-position using a mixture of sodium bicarbonate and iodine in methanol, and protected at the 4-position using a heated mixture of potassium carbonate and ethyl iodide in DMF. Side chain groups were added to the protected intermediate via Suzuki coupling, and the product was obtained via deprotection in a heated mixture of HBr and acetic acid,

and filtration of the insoluble quinolone. All ELQ compounds were recrystallized from DMF and methanol and tested for purity using nuclear magnetic resonance imaging (NMR), high performance liquid chromatography (HPLC), and tandem mass spectrometry.

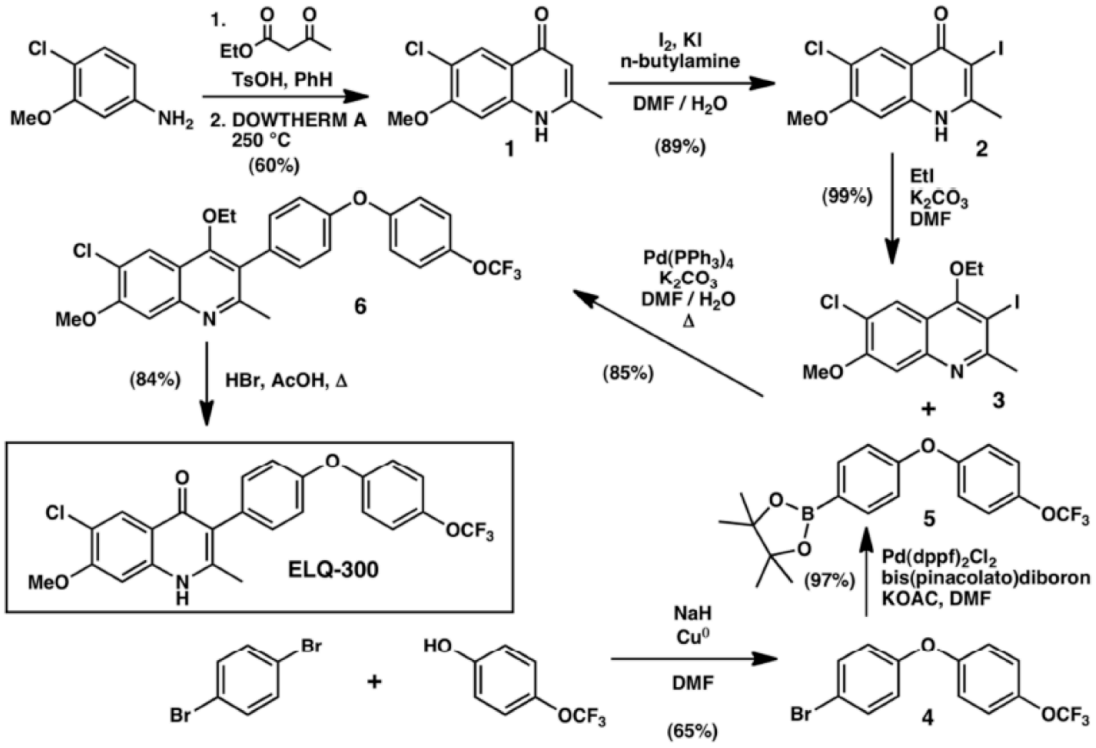

Figure 11: Reaction schema of ELQ-300[66] depicting synthesis of the 6-Cl, 7-methoxy substituted quinolone core, the 3-diarylether side chain, and the Suzuki cross-coupling procedure.

During the synthetic process, I identified an alternate catalyst that decreased reaction time and increased yield of the Suzuki cross-coupling reaction relative to

the tetrakis(triphenylphosphine)palladium(0) catalyst described above (Figure 11, $Pd(PPh_3)_4$). In this modified reaction, 1 equivalent of the protected, iodinated quinoline intermediate was reacted with 1.2 equivalents of the diarylether boronic ester, 2 equivalents of aqueous K_2CO_3, and 0.05 equivalents of [1,1'-bis(diphenylphosphino)ferrocene]dichloropalladium(II) under an inert argon atmosphere in DMF at 85°C. Reaction progress was monitored by GC/MS and full consumption of starting materials could be reliably detected within 1-2 hours. To isolate the coupled product, solvent was removed by rotary evaporation and precipitate was extracted with ethyl acetate and H_2O followed by column purification on a 2-20% ethyl acetate:hexanes gradient. Final yield ranged from 90-99%. Subsequent deprotection and isolation of final 4(*1H*)-quinolone compounds was performed as previously described[66].

In Vitro Drug Susceptibility (*P. falciparum*)

All *P. falciparum* strains were obtained as glycerol-frozen stocks from the MR4 malaria resource center. Parasites were thawed using a standard NaCl precipitation procedure, and incubated in HEPES-modified RPMI (supplemented with 50 mg/L hypoxanthine), in the presence of type A, human RBCs. Cultures were maintained at 2% hematocrit and 1-10% parasitemia at 37°C under blood gas conditions (5% O_2, 5% CO_2, 90% N_2). Parasitemia was monitored via thin smear and Giemsa-stain.

CHAPTER TWO: MATERIALS AND METHODS

In vitro drug susceptibility was determined using a fluorescence-based SYBR Green I assay[67]. Briefly, drugs were diluted in HEPES-modified RPMI and added to 96 well plates using two-fold, serial dilutions. Wells were seeded with parasites to give a final volume of 200µL, at 2% hematocrit and 0.2% parasitemia. After 72 hours of incubation under culture conditions, parasites were lysed and incubated with SYBR Green I nucleic acid stain for 30-60 minutes in the dark. SYBR Green signal was quantified using a Gemini-EM plate reader with excitation and emission bands centered at 497 and 520 nm, respectively. 50% inhibitory concentrations (IC_{50}) were determined using Graphpad Prism software. All final IC_{50} values represent averages from at least three independent experiments, with each compound run in triplicate.

In Vitro Onset of Action (*P. falciparum*)

P. falciparum stasis and cell death were quantified in vitro using an array of techniques. Specifically, the parasite reduction ratio (PRR) assay previously developed by GlaxoSmithKline (GSK)[68] was used to assess *Plasmodicidal* kinetics, while microscopy and washout assays were used to characterize parasite stasis.

CHAPTER TWO: MATERIALS AND METHODS

PRR

Stock cultures of Dd2 *P. falciparum* parasites were maintained at 0.5% parasitemia and 2% hematocrit in the presence of drug at 10x IC_{50}. Every 24 hours, an aliquot corresponding to 10^5 parasites was collected, washed with RPMI to remove drug, and clonally diluted on 96 well plates using 10-fold dilutions. Plates were incubated at 37°C under blood-gas conditions for 21 days, which was the minimum time necessary for replication of single cells to detectable levels.

Parasitemia of the initial aliquot was determined by SYBR Green I quantification. The signal from terminal wells (containing no parasites) was used to determine average SYBR Green background level, and wells were considered parasite positive if SYBR Green signal was more than three standard deviations above average background. The most dilute, parasite-positive well was interpreted as a clonal population, and back calculation revealed the number of parasites present in the initial plated inoculum. Overall kinetics were plotted as number of viable parasites at each time point and various parameters including lag-time, log(PRR), and 99.9% PCT were defined as follows: lag-time = time required to reach maximum killing rate, log(PRR) = log(reduction of parasitemia over one life cycle), and 99.9% PCT = time required to reduce the number of viable parasites by three log units (Figure 12).

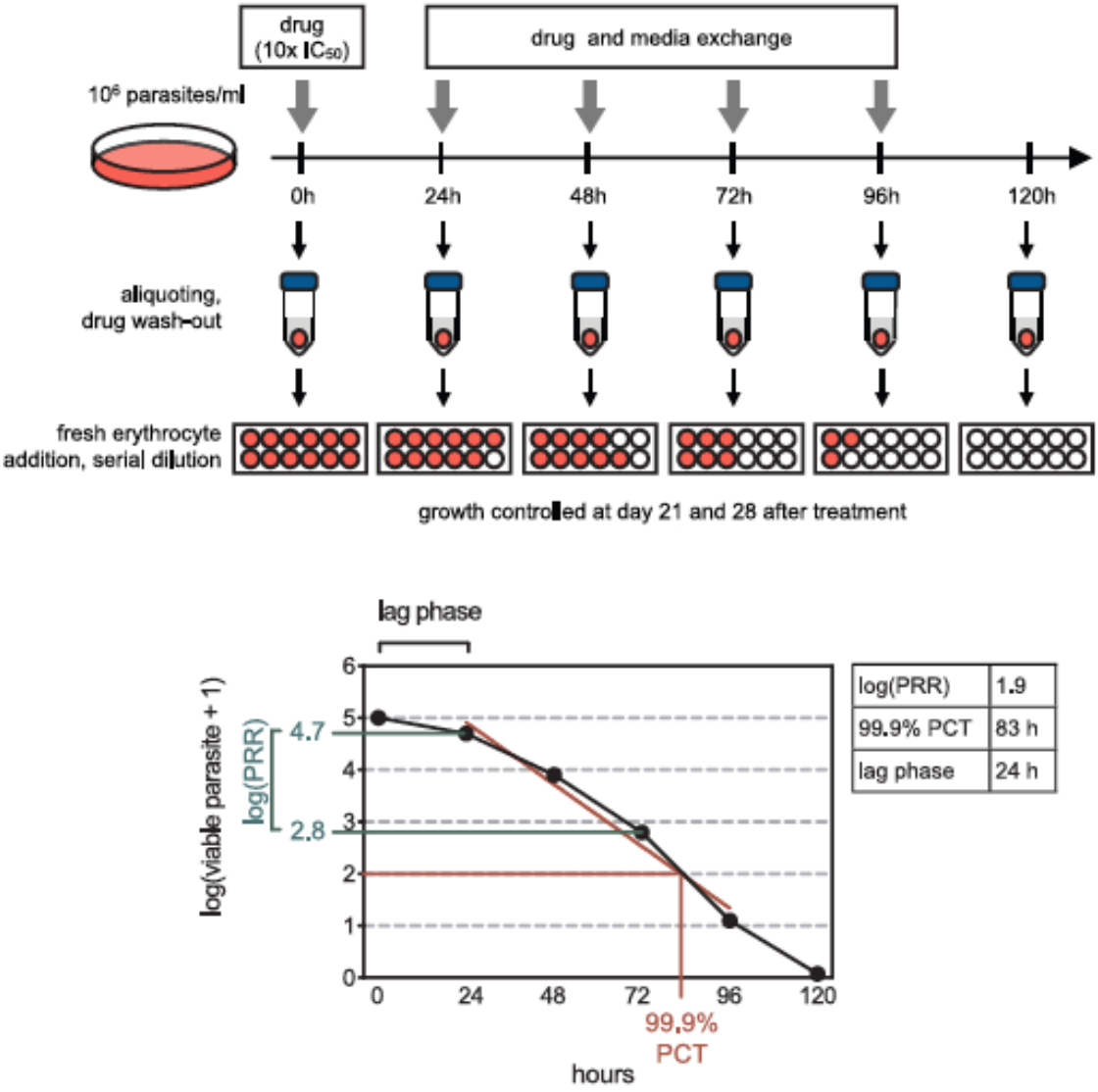

Figure 12: Graphical representation of the PRR assay[68]. Top panel outlines standard experimental setup and provides an example of raw, serial dilution data. Bottom panel is a numerical analysis of sample data with relevant output parameters highlighted in red and green.

CHAPTER TWO: MATERIALS AND METHODS

Microscopy

Dd2 *P. falciparum* parasites were synchronized in the presence of sorbitol, and incubated with drug at 10x IC_{50} as described above. Aliquots of 10^5 parasites were removed from stock cultures at various time points, washed, and visualized via Giemsa stain and thin smear. One hundred parasites per sample were classified by morphology (ring, early trophozoite, late trophozoite, or schizont) to assess progression through the parasite life cycle. Trophozoites were defined by the presence of a hemazoin-positive digestive vacuole, and size was used to distinguish early (<50% of total RBC volume) from late stage trophozoites (>50% of total RBC volume).

Washout

96-well plates were prepared for drug susceptibility screens as described above (initial parasitemia reduced to 0.1%). Drug was removed at predetermined time points by transferring well contents into microcentrifuge tubes, washing wells with fresh RPMI, and removing drug media by centrifugation. Each pellet was washed twice with fresh RPMI, then re-plated for continued incubation at 37°C. After 100 hours of incubation, IC_{50} values were determined as described above, and plotted as a function of drug incubation time. Duration of stasis was also determined by varying the total incubation time between 48 and 120 hours post-washout, and monitoring increases in IC_{50} over time.

CHAPTER TWO: MATERIALS AND METHODS

In Vivo Drug Susceptibility (*P. yoelii*)

Two major methods were used to assess the in vivo activity of the ELQs. A modified Peters suppressive test was used as an initial measure of activity, including ED_{50} and non-recrudescence dose determination, while an acute infection study was used to measure in vivo response to drug administration. All animal procedures were in accordance with regulations of the Portland VA Medical Center and the Institutional Animal Care and Use Committee.

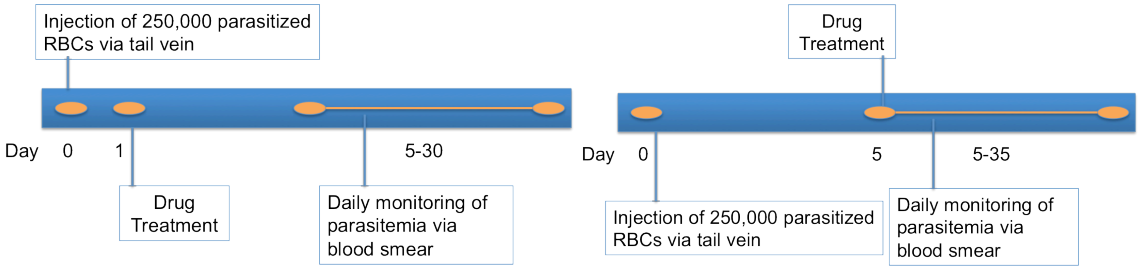

Figure 13: Schematic representation of 1-day Peters suppressive model (left) and 1-day acute treatment model (right).

Peters Suppressive Test

Six-week old, female CF-1 mice were obtained from Charles River and inoculated with $2.5x10^5$ blood-stage *P. yoelii* parasites via tail vein injection. Drug stocks were prepared as solutions in PEG-400 (calculated for 30g mice) or as solutions in DMSO, and administered to animals once daily for 1 or 4 days,

beginning 24 hours post-infection. For oral dosing, animals received 100-200μL of PEG solution via oral gavage. For transdermal administration, 10μL of DMSO solution was applied to the inner surface of each ear and allowed to absorb through the pinna. After treatment, daily blood samples were collected from the tail vein, beginning on post-infection day 5, and parasitemia was determined microscopically using Giemsa stain and NIS-Elements cell-counting software. Animals were treated in accordance with IACUC guidelines, and were sacrificed with parasitemia exceeded 30%. ED_{50} was calculated as the dose that effectively reduced day 5 parasitemia by 50% relative to controls and animals were considered cured if no parasitemia was detectable at post-infection day 30.

Acute Treatment Model

Mice were infected as above, and blood was monitored daily via thin smear until parasitemia reached 15-25%. At that time, drugs were administered via oral gavage as solutions in PEG-400, and parasitemia was monitored daily via thin smear and plotted as a function of time post-treatment. Lag time and clearance time were used as measures of in vivo kinetics. For animals that recrudesced post-treatment, resistance was assessed by re-treating animals with a second drug dose (at 10-25% parasitemia) and comparing parasite response to initial kinetics, lag time, and clearance time. Resistant parasites were collected via

cardiac puncture, frozen in 30% glycerol, and shipped to Drexel University for sequencing.

Cytochrome *bc$_1$* Assays

Mitochondrial preparations from several sources were used for enzyme-level cyt *bc$_1$* analysis. EC_{50} analysis was completed using isolated mitochondria from HEK-293 cells, while specific Q_i site activity was measured using a *Paracoccus denitrificans* model system. Inhibition of *P. falciparum* cytochrome *bc$_1$* was evaluated by the Vaidya group at Drexel University.

Isolation of HEK-293 Derived Mitochondria

HEK-293 cells were obtained from the Janowsky lab and cultured in DMEM containing 10% FCS. Cells were trypsinized and washed with 2x with ice-cold PBS, then transferred to isolation buffer containing 1mM PMSF, 25mM sucrose, 225mM mannitol, 5nM $MgCl_2$, 5mM KH_2PO_4, 1mM EDTA, and 5mM HEPES at pH 7.4. Cells were lysed via French press, debris was removed via low-speed centrifugation (800xg) for 10 minutes, and mitochondria were pelleted at 20000xg (40 minutes, 4°C). Pellets were re-suspended in 30% glycerol, 70% isolation buffer, and frozen at -80°C until the time of use.

CHAPTER TWO: MATERIALS AND METHODS

Measurement of Cytochrome bc_1 Complex Inhibition

Assays were performed in assay buffer containing 50mM Tricine and 100mM KCl at pH 8. Buffer was supplemented with 0.1 mg/mL n-dodecyl β-D-maltoside (DDM), 50μM oxidized cytochrome *c*, 4mM KCN, and tested inhibitors in a cuvette at 30°C. For each experiment, measurement began with the addition of 50μM decylubiquinol (prepared by reducing decylubiquinone with sodium borohydride and quenching with HCl), and a 20 second baseline reading was collected. Permeabilized mitochondria (prepared with 0.1 mg/mL DDM) were then added (amount adjusted so that signal was between 10^{-4} and 10^{-3} absorbance units/second), and cytochrome *c* reduction was monitored via absorbance at 550nM (542=set point). Percent inhibition was calculated as the difference between total signal and baseline signal relative to controls. EC_{50} was defined as the concentration of drug that resulted in 50% inhibition.

Isolation of P. denitfiricans cytochrome bc_1

Paracoccus denitrificans was cultured in standard nutrient broth at room temperature. Bacteria were concentrated via centrifugation, lysed in isolation buffer (described above) via French Press, and debris was pelleted at 20000xg. Following centrifugation, supernatant was collected, column purified on DEAE cellulose, and concentrated via filter centrifugation.

CHAPTER TWO: MATERIALS AND METHODS

Cytochrome b Reduction Assay

Cytochrome *b* reduction assays were performed in assay buffer (described above) containing 0.8 mg/mL DDM, 3 μM cyt bc_1, and variable concentrations of inhibitor. Baseline reduction was measured at 562nm (set point = 578) for 20 seconds and reaction was initated by the addition of 50 μM decylubiquinol.

DHODH Inhibition Assay

Isolation of DHODH

The n-terminal-truncated *P. falciparum* DHODH plasmid was obtained from the Phillips lab and transfected into BL21 *E. coli* using a heat shock technique. Cells were plated on LB agar and a colony was transferred to LB broth containing 1mM ampicillin and 1mM chloramphenicol. Once cells reached an optical density of 0.5, 1mM IPTG was added and cells were incubated with shaking for two hours. *E. coli* were isolated via centrifucation (800g x 10 minutes) and lysed via French Press in buffer containing 50mM Tris-HCl, 1mM DTT, 1mM EDTA, and 1mM PMSF at pH 7.5. Protein was column purified with Ni-NTA and eluted with imidazole in lysis buffer. Imidazole was removed via centrifugation in 1000 MW centrifuge filters and aliquots were frozen with 30% glycerol at -80°C

CHAPTER TWO: MATERIALS AND METHODS

DHODH Inhibition Measurement

For DHODH activity studies, reaction buffer containing 100 mM HEPES, pH 8.0, 150 mM NaCl, 0.1% Triton X-100, and 10% glycerol was supplemented with 0.8 mg/mL DDM, 120μM DCIP, 500μM L-DHO, 0.1 mg/mL glucose oxidase, 0.02 mg/mL catalase, 50mM glucose, and 20μM oxidized decylubiquinone. Reactions were initiated by addition of enzyme to a final concentration of 5–50 nM, and the temperature was maintained at 25 °C with a circulating water bath. Production of orotic acid was detected by a specific absorbance peak at 296nm (set point = 500), and all values were reported as percent of uninhibited activity. The known DHODH inhibitor, DSM1 was used as a positive control.

Molecular Modeling

The 1KYO (Q_o) and 1EZV (Q_i) crystal structures of *S. cerevisiae* cyt bc_1 were obtained from the protein data bank and modified as follows: Q_i site= F225L, K228L; Q_o site= C133V, C134L, V135P, Y136W, H141Y, and L275F. ELQ models were created using ChemBioDraw 3D, and docking was performed using the CLC drug discovery software. One thousand docking iterations were run per compound at each site.

CHAPTER TWO: MATERIALS AND METHODS

Chemical compounds

All ELQs and decylubiquinone were synthesized in house by Aaron Nilsen and Rolf Winter. Atovaquone was purchased from Sigma, and recrystallized from DMF and methanol before use. All other solvents and chemical reagents were purchased from commercial suppliers or the MR4 malaria research source.

Collaborator Contributions

Transmission blocking and prophylactic assays were performed by the Kim lab at Albert Einstein College of Medicine. In vivo resistance propensity, *P. falciparum* cyt bc_1 assays, and sequencing studies were performed by the Vaidya group at Drexel University. Toxicity assays were performed by Yuexin Li and Erin Meermeier at OHSU.

CHAPTER THREE: DEVELOPMENT AND CHARACTERIZATION OF ELQ-400 AS A MULTI-STAGE, SINGLE-DOSE ANTIMALARIAL THERAPY

Introduction

Although many well-tolerated and potent antimalarial drugs exist, drug therapy is often complicated by the complexity of the *Plasmodium* parasites that cause malaria and the difficulty of delivering uninterrupted drug therapy in areas where medical resources are limited. Interruptions in antimalarial dosing, including missed or incorrectly timed doses, can cause wide fluctuations in drug exposure, which puts patients at high risk for medication overdose[69,70], parasite recrudescence, or the development of drug-resistant *Plasmodium* infections[39,41].

The pursuit of single-dose antimalarial therapies is one leading strategy to simplify antimalarial treatment, reduce cost, and ensure compliance[39,71]. Several potential single dose cure antimalarials are currently in the developmental pipeline. The endoperoxide OZ439[42], the aminopyridine MMV390048[43], and the spiroindolone NITD609[44] all effectively clear asexual, blood-stage parasites in mouse models of malaria with a single oral dose, and also inhibit gametocyte development[30], which reduces the potential for malaria transmission. In contrast, several imidazolopiperazines[45,46], 8-aminoquinolines[72], and anti-respiratory compounds[73] have been identified as single-dose causal prophylactics, which inhibit the sporozoite and liver-stage parasites that are responsible for the earliest stages of *Plasmodium* infection[32]. While each of these antimalarials is

highly potent at select stages of the parasite life cycle, it has not yet been possible for a single agent to provide simultaneous cures for blood, liver, and transmissive stage malaria following a single oral dose.

A key step in developing a multi-stage, single-dose cure antimalarial is to identify a biological target that is essential throughout the parasite life cycle. One such target is complex III of the mitochondrial electron transport chain, which is also known as the cytochrome bc_1 complex (cyt bc_1) and is essential for pyrimidine biosynthesis in *Plasmodium*[47]. Several cyt bc_1 inhibitors, including the naphthoquinone atovaquone (ATV) and the 4(*1H*)-quinolone ELQ-300, are potent single-dose prophylactics[66,73], with remarkable multi-dose efficacy against blood-stage malaria parasites. Although it has not yet been possible to formulate these compounds as single-dose, blood-stage therapies, it is likely that this limitation is related to poor solubility, which restricts the plasma concentrations that can be achieved following a single oral dose. Practically, this exposure barrier could be overcome in one of two ways: (1) by increasing solubility or, (2) by increasing intrinsic potency so that a lower plasma concentration is required for maximal effect. Here, I specifically focus on maximizing the potency of the 4(*1H*)-quinolones to obtain a multi-stage, single dose cure for malaria.

CHAPTER THREE: DEVELOPMENT AND CHARACTERIZATION OF ELQ-400

Our group has developed an extensive library of 4(*1H*)-quinolones based on the general structure of the cyt bc_1 inhibitor, endochin. Within the endochin-like quinolone (ELQ) library, the most potent in vitro inhibitor is the 5,7-difluoro compound, ELQ-121, which inhibits growth of pan-sensitive, *P. falciparum* parasites at picomolar concentrations[63,64]. Although ELQ-121 is poorly active in vivo, recent work with ELQ-300 has suggested that the 3-diarylether side chain may be instrumental for improving metabolic stability and extending the potency of ELQ-121 to animal models[66]. In this chapter, I investigate a subset of highly potent 4(*1H*)-quinolone-3-diarylethers containing 5,7-difluoro substituents, and demonstrate that these compounds, including the prototype ELQ-400, provide single dose cures in murine models of malaria across various stages of parasite development.

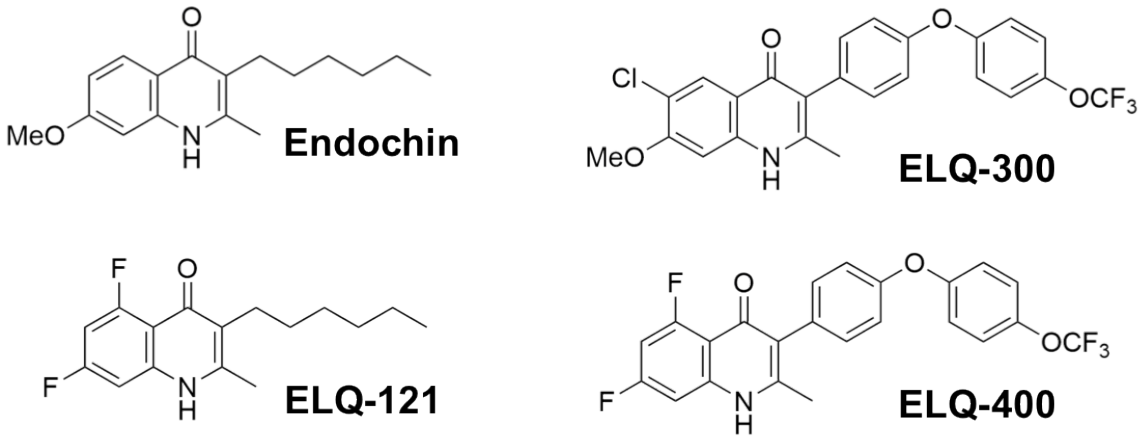

Figure 14: Structures of the 4(*1H*)-quinolones, endochin, ELQ-121, ELQ-300, and ELQ-400.

CHAPTER THREE: DEVELOPMENT AND CHARACTERIZATION OF ELQ-400

Results

Synthesis

ELQ-400 was synthesized by Aaron Nilsen, using the reaction scheme previously reported for the 3-diarylether compound, ELQ-300[66]. Compound identity was verified using HNMR and tandem LC/MS, and purity exceeded 99% prior to evaluation. Like other 4(*1H*)-quinolones, ELQ-400 exhibited minimal aqueous solubility, with a cLogP of 5.6 and a melting/decomposition point of 308-310°C[74].

In vitro activity against P. falciparum

I used a SYBR Green-based fluorescence assay to compare the in vitro activity of ELQ-400, ELQ-121 and ELQ-300 against various *P. falciparum* strains. In pan-sensitive and chloroquine-resistant parasites, ELQ-400 was only slightly less active than the parent compound ELQ-121 and was approximately 10-fold more potent than ELQ-300 (Table 1). Like ATV and the parent ELQs, ELQ-400 was inactive against transfected parasites expressing yeast dihydroorotate dehydrogenase (DHODH)[48], demonstrating that its predominant mechanism of action involves pyrimidine starvation secondary to cyt bc_1 inhibition. However, in contrast to ELQ-121, which demonstrated a nearly 1000-fold loss of potency against ATV-resistant Tm90-C2B parasites (which contain Y268S point mutations in cyt bc_1[57,75]) ELQ-400 retained substantial activity against this strain with an IC_{50} of 35nM.

CHAPTER THREE: DEVELOPMENT AND CHARACTERIZATION OF ELQ-400

Compound	Pan-sensitive		CQ-resistant		Anti-respiratory-resistant	
	D6	D10	Dd2	7G8	Tm90-C2B	D10yDHOD
ELQ-121	0.2	0.9	0.5	2.0	306.1	>2500
ELQ-300	7.2	20.4	6.6	33.3	4.6	>2500
ELQ-400	0.6	2.2	1.5	4.2	35.1	>2500

Table 1: In vitro IC_{50} values (nM) against standard *P. falciparum* clones. The 5,7-difluoro, 3-diarylether compound, ELQ-400, was more potent than ELQ-300 against pan-sensitive and chloroquine-resistant parasites, and was more effective against atovaquone-resistant Tm90-C2B parasites than the parent compound, ELQ-121. CQ: chloroquine. D10yDHOD: D10 strain expressing yeast DHODH.

In vivo activity against blood-stage P. yoelii

In vivo, ELQ-400 was highly active against blood-stage parasites. In these experiments, I utilized a modified Peter's test in which CF-1 mice were intravenously injected with blood-stage *P. yoelii*, treated orally with drug beginning 24 hours after infection, and monitored for parasitemia by thin smear. Although ELQ-121 was inactive in vivo, ELQ-300 and ELQ-400 were both highly

effective after 4 days of treatment, with 50% effective doses (ED_{50}) of 0.02 and 0.01 mg/kg, and curative doses of 0.3 and 0.1 mg/kg, respectively (Table 2).

Treatment	4-day dosing		1-day dosing	
	ED_{50}	NRD	ED_{50}	NRD
Oral ELQ-300	0.02	0.3	ND	>20
Oral ELQ-400	0.01	0.1	0.01	1
TD ELQ-400	0.01	1	0.06	1

Table 2: In vivo activity of ELQ-300 and ELQ-400 against blood-stage *P. yoelii*. ELQ-400 was more effective than ELQ-300 in both 1-day and 4-day tests as either an oral formulation in PEG-400 or a transdermal formulation in DMSO. Groups of n=4. All values in mg/kg. ED_{50} = 50% effective dose, NRD = non-recrudescence/curative dose, TD = transdermal.

Strikingly, ELQ-400 was also curative after a single oral dose. When administered 24 hours post-inoculation, a 1 mg/kg dose of ELQ-400 prevented recrudescence in all animals, and the single dose ED_{50} of 0.01 mg/kg was identical to that obtained from the 4-day test (Table 2). Interestingly, the single dose efficacy of ELQ-400 was not limited to oral administration. When applied topically to the surface of the inner ear as a solution in DMSO, ELQ-400 was also

fully curative following a single 1 mg/kg dose. As was observed in the oral dosing studies, additional days of ELQ-400 treatment provided little added benefit over single day therapy, suggesting that *Plasmodium* parasites respond rapidly and near-maximally to an initial dose of ELQ-400.

Onset of activity against blood-stage parasites

In order to determine the kinetics of the in vivo response to ELQ-400, I again used the *P. yoelii* model, but delayed ELQ-400 treatment until day 5 post-inoculation, when parasitemia ranged from 15-25%. I then followed parasitemia and parasite morphology by thin smear to determine how parasites responded to ELQ-400 over time. Oral doses of 5, 10, or 20 mg/kg of ELQ-400 effectively reduced parasitemia within 24 hours of treatment, and no observable parasites were present in any group by post-treatment day 5 (Figure 15). Ultimately, a single dose of 20 mg/kg was sufficient to universally prevent recrudescence, while doses of 5 and 10 mg/kg were curative in a subset of animals (2/3).

Morphologically, ELQ-400 treated parasites demonstrated several obvious abnormalities. In vivo, parasites exposed to ELQ-400 became arrested at the schizont stage, with evidence of hypopigmentation, pyknosis and RBC membrane rupture 24-48 hours following treatment (Figure 16). I was able to mimic this schizont stage arrest in vitro by incubating synchronized *P. falciparum*

parasites with ELQ-400 at 10x the IC_{50}. For this experiment, thin smears were taken at set time points, and morphology was used to determine the relative proportions of ring-stage, early trophozoite, late trophozoite, or schizont parasites. In contrast to control cultures, which followed a characteristic, 48-hour progression through the life-cycle, parasites in the ELQ-400 condition were arrested at the first schizont phase and failed to undergo asexual replication (Figure 17).

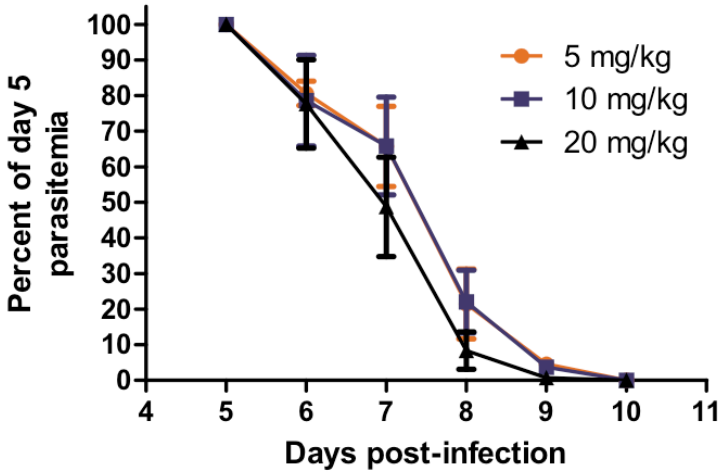

Figure 15: Clearance of *P. yoelii* parasites following single dose ELQ-400 treatment on post-infection day 5. In all treatment groups, parasitemia decreased within 24 hours of ELQ-400 administration and parasites were undetectable 5 days following ELQ-400 exposure. All animals treated with 20 mg/kg of ELQ-400 were permanently cured of parasites. Groups: 5 mg/kg (n=3), 10 mg/kg (n=3), or 20 mg/kg (n=6). Data represented as percentage of day 5 parasitemia (~20%).

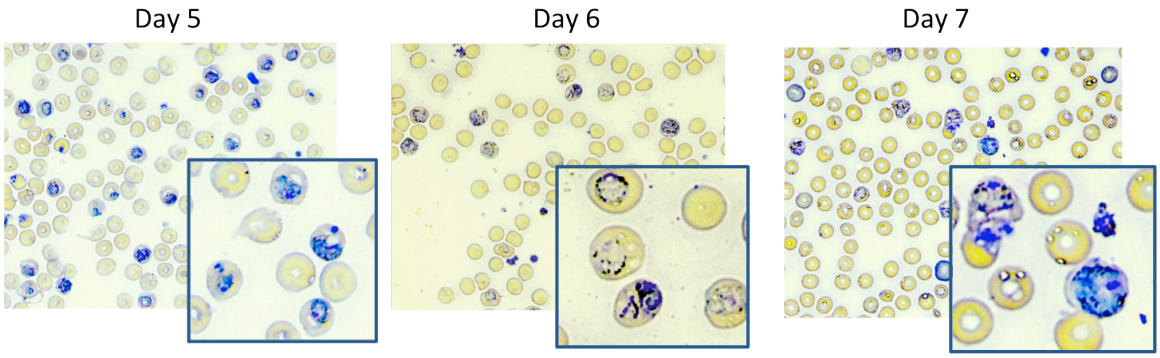

Figure 16: Representative Giemsa-stained smears from a *P. yoelii* infected animal treated with 20 mg/kg ELQ-400. Prior to treatment (day 5), parasites were morphologically normal and distributed across ring, trophozoite, and schizont stages. Within 24 hours of ELQ-400 administration (day 6), parasites became pyknotic and arrested at the schizont stage. Within 48 hours (day 7), many parasites were extracellular.

Although microscopy was a useful tool for assessing parasite morphology, it did not effectively distinguish between ELQ-400-treated and control parasites at early time points. To examine the early response to ELQ-400 exposure, I designed a washout assay based on the drug-susceptibility tests used for IC_{50} determination. In these studies, parasites were incubated in 96-well plates and exposed to serial dilutions of ELQ-400 as previously described. At various time points, well contents were collected, washed thoroughly to remove drug, and re-plated. IC_{50} values were determined 100 hours after set-up and compared to a control plate to determine the minimal incubation time necessary for full response

to ELQ-400. Surprisingly, even the shortest (2 hour) incubation was associated with an IC_{50} value in the low nanomolar range, and full potency was achieved after 60 hours of ELQ-400 exposure (Figure 18).

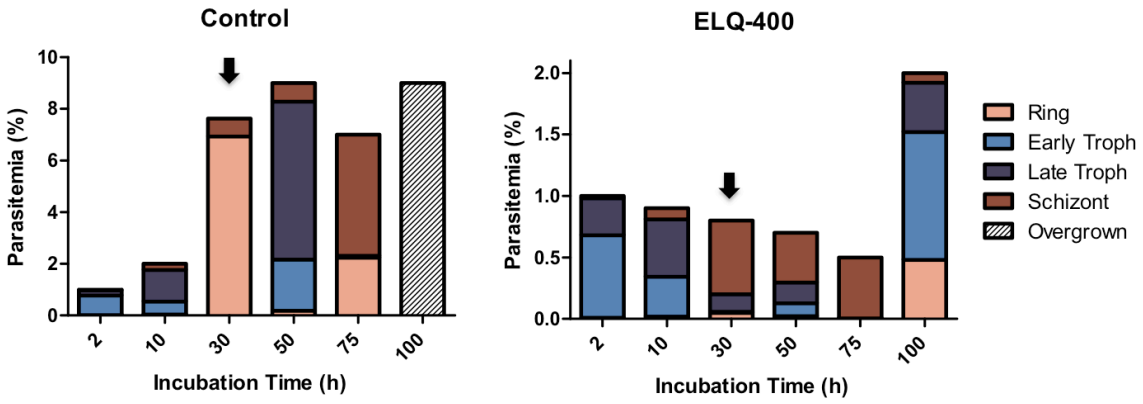

Figure 17: Stage-classification of synchronized, *P. falciparum* parasites treated with either 10nM ELQ-400 or RPMI vehicle (control). Vehicle-treated parasites followed a 48-hour replication cycle with normal increases in parasitemia. Parasites exposed to ELQ-400 became arrested at the schizont stage, but were able to resume normal growth 70 hours following drug washout. Troph = trophozoite. Arrows represent drug washout.

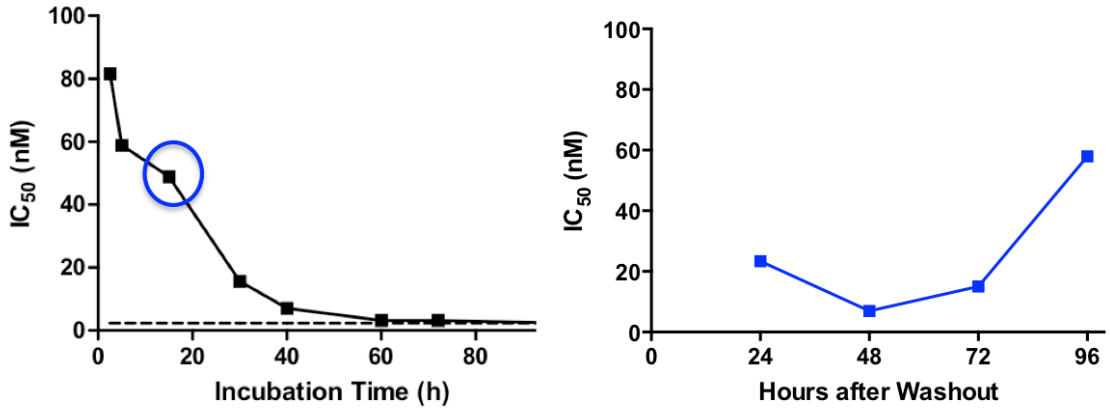

Figure 18: ELQ-400 washout assays. Left panel: Brief (2 hour) exposure to ELQ-400 effectively inhibited *P. falciparum* growth with an IC_{50} of 80nM. Right panel: ELQ-400 exposure resulted in long-lasting *P. falciparum* stasis, and 72-96 hours were required for growth to resume post-washout. Dotted line represents ELQ-400 IC_{50} under continuous ELQ-400 exposure. Circle indicates incubation time used for recovery assay (right panel).

Because microscopy and SYBR Green-based assays do not distinguish between parasite stasis and parasite death, I next used a Parasite Reduction Ratio (PRR) assay to assess viability[68]. In this experiment, 10^6 *P. falciparum* parasites/mL (Dd2 strain) were grown in the presence of ELQ-400 at 10x the IC_{50}. Each day, 10^5 parasites were removed, washed, and transferred to 96 well-plates using limiting dilution. After 21 days, parasites were lysed and detected using SYBR Green I nucleic acid stain, and back-calculation was used to determine the

original number of viable parasites. As previously reported for other cyt bc_1 inhibitors, ELQ-400 was associated with an in vitro lag phase and did not decrease the number of viable parasites until 48 hours post-exposure (Table 3). Consistent with this finding, parasites in both the microscopy or washout assays described above could resume normal growth if ELQ-400 was removed 24 hours post-exposure, although recovery was delayed by approximately 72-96 hours in both of these cases (Figures 17, 18). Taken together, this data demonstrates that ELQ-400 is associated with rapid parasite stasis and delayed cell-death in *Plasmodium*.

Compound	Dose	Lag Phase (h)	Log PRR	PCT 99.9% (h)
ATV	10 x IC_{50}	48	2.5	98
ELQ-300	10 x IC_{50}	48	3.25	89
ELQ-400	10 x IC_{50}	48	4.75	77

Table 3: Parasite reduction ratio (PRR) assessment of atovaquone, ELQ-300, and ELQ-400 in Dd2 *P. falciparum* parasites. All tested compounds demonstrated a 48 hour lag phase before the onset of parasite death. ATV = atovaquone

CHAPTER THREE: DEVELOPMENT AND CHARACTERIZATION OF ELQ-400

Single-dose causal prophylactic and transmission blocking activity

One major benefit of cyt bc_1 inhibition is the ability to inhibit *Plasmodium* parasites throughout multiple life cycle stages. Collaborators at Albert Einstein College of Medicine assessed the exoerythrocytic activity of ELQ-400 using luciferase-based *P. yoelii* models. As described in appendix A, these studies verified that ELQ-400 also potently blocked transmission and provided causal prophylactic protection at single doses of 0.1 and 0.08 mg/kg, respectively.

Resistance propensity

One major concern regarding the use of cyt bc_1 inhibitors as treatments for malaria is the propensity for *Plasmodium* drug resistance. Although ATV is the only cyt bc_1 inhibitor in clinical use, ATV resistance develops rapidly in the setting of monotherapy and several highly-resistant strains have emerged, including the clinical isolate Tm90-C2B, which contains a Y268S mutation at the cyt bc_1 Q_o site and is more than 1000-fold less sensitive to ATV. To assess the resistance propensity of ELQ-400, collaborators at Drexel University exposed cultured *P. falciparum* parasites to continuous drug pressure as described in appendix B. In these assays, mild ELQ-400 resistance was conferred by a V259L mutation at the cyt bc_1 Q_o site. However, unlike the Y268S mutation that confers ATV resistance, V259L mutant parasites were only 10-fold less sensitive to both ELQ-400 and ATV.

Compound	EC_{50} (nM)		TD_{50} (μM)	
	P. falciparum cytochrome bc_1	Human cytochrome bc_1	HFF	Murine T-cell activation
ATV	2.0	274	>37	8.9
ELQ-300	0.56	>10000	>37	>25
ELQ-400	6.7	108	>37	>25

Table 4: Cyt bc_1 inhibition and toxicity determinations for atovaquone, ELQ-300, and ELQ-400. ELQ-300 was highly selective for *Plasmodium* cytochrome bc_1, while atovaquone and ELQ-400 also inhibited HEK293-derived enzyme in the nanomolar range. All compounds were minimally toxic to HFF and murine T-cells. HFF = human foreskin fibroblast. ATV = atovaquone.

Cytochrome bc_1 inhibition and host vs. parasite selectivity

In addition to being expressed throughout the *Plasmodium* life cycle, the cyt bc_1 complex is highly conserved across eukaryotic species, and selectivity for *Plasmodium* is a desirable characteristic of new cyt bc_1 inhibitors. I assessed cyt bc_1 inhibition by ELQ-400 in permeabilized mitochondria isolated from HEK293 cells and determined that ELQ-400 inhibited the human enzyme at a 50% effective concentration (EC_{50}) of 108nM (Table 4). For comparison, ELQ-400 targeted the *P. falciparum* enzyme with an EC_{50} of 6.7nM (as determined by our collaborators at Drexel University). Despite this limited selectivity, ELQ-400 did

not demonstrate toxicity in whole-cell models. In toxicity screens with proliferating human foreskin fibroblasts and activated murine T-lymphocytes, the 50% toxic dose (TD_{50}) of ELQ-400 exceeded 25μM (Table 4, collaborator data), suggesting that ELQ-400 may have a multifaceted interaction with human cells that cannot be adequately estimated by isolated assessment of cyt bc_1.

Structure-activity relationship (SAR) of ELQs and HEK cyt bc_1 inhibition

In order to determine how general ELQ structure contributed to inhibition of HEK-derived cyt bc_1, I conducted a large-scale screen of various 3-diarlyether ELQs against the human enzyme. At 10μM concentrations, there was a clear effect of sterics on relative inhibition of human cyt bc_1; undecorated compounds were potent inhibitors of the human enzyme, while the presence of large groups at either the 6 or 7-position had a protective effect. Notably, ELQs containing either methoxy or cyano groups on the benzenoid ring were exceptions to this trend and were associated with undesirable inhibition of human cyt bc_1 (Figure 19).

6-position variants of ELQ-400

Because human cyt bc_1 inhibition was minimized in ELQs containing large substituents at the 6 or 7 positions, I next addressed the possibility of chemically modifying ELQ-400 to improve selectivity for the parasite target. As observed for other ELQs containing 6-position halogens, the 6-fluoro and 6-chloro analogs of

ELQ-400, ELQ-404 and ELQ-428 (Figure 20), demonstrated reduced inhibition of HEK-derived cytochrome bc_1 with EC_{50} values of 1.4μM and >10μM, respectively (Figure 21).

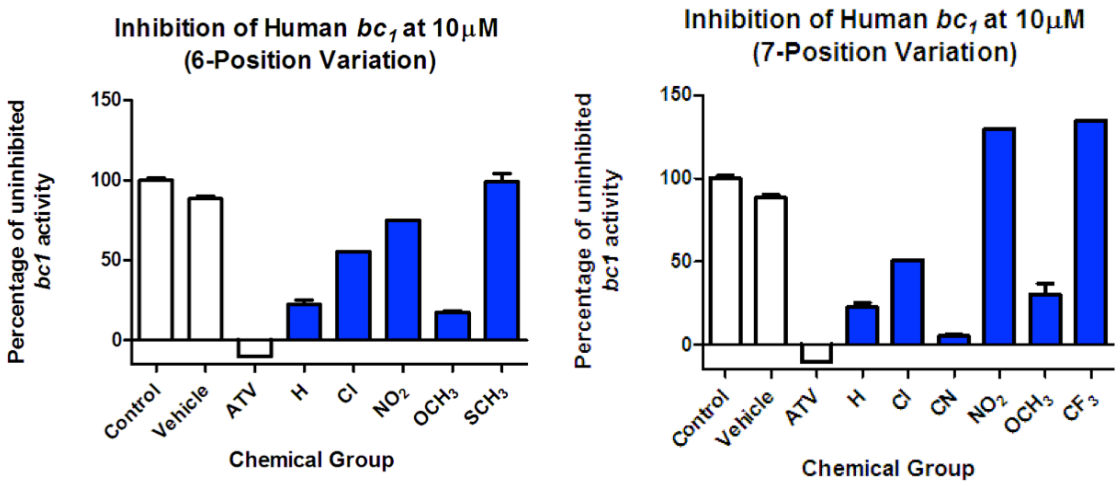

Figure 19: Inhibition of HEK293-derived cyt bc_1 by ELQs with various 6 and 7 position substituents. Substituent size was inversely correlated with human cyt bc_1 inhibition, except in ELQs containing methoxy or cyano groups. All tested compounds were 3-diarylether ELQs. n=2 replicates per compound.

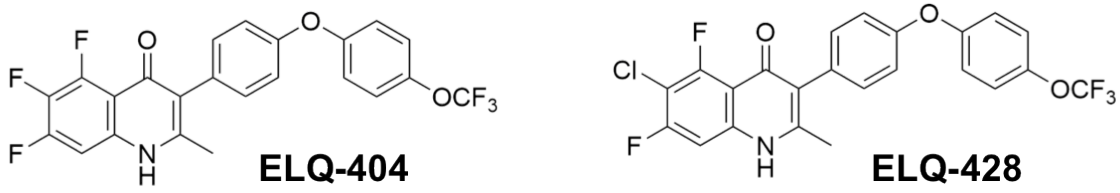

Figure 20: Structures of ELQ-400 analogs, ELQ-404 and ELQ-428.

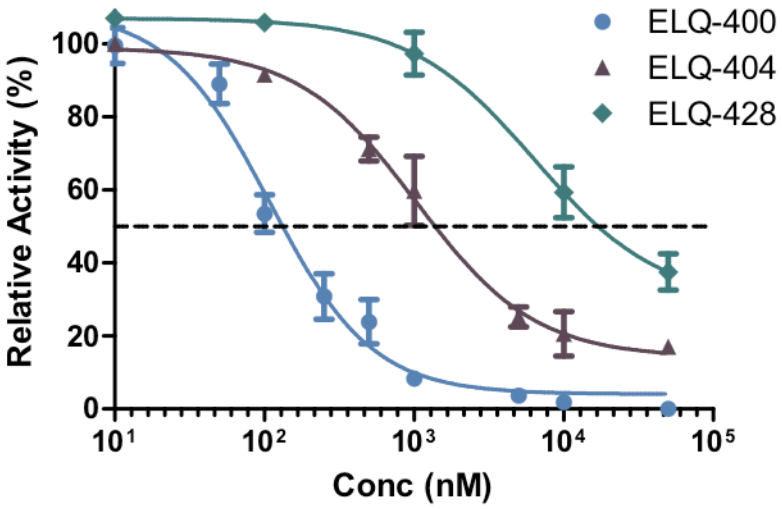

Figure 21: EC_{50} curves for ELQ-400, ELQ-404, and ELQ-428 against HEK293-derived cytochrome *bc*$_1$. ELQ-404 and ELQ-428 both exhibited reduced inhibition of the human enzyme relative to ELQ-400, with respective EC_{50} values of 1.4μM and >10μM. Dashed line represents 50% inhibition. n=2 replicates per point.

Although 6-position modification successfully increased the selectivity of the 5,7-difluoro ELQs, these adjustments were associated with a reduction in antiplasmodial activity and anti-malarial efficacy, and ELQ-404 and ELQ-428 were between 5 and 10-fold less active than ELQ-400 both in vitro and in vivo (Table 5). Encouragingly, both compounds were still capable of producing single

dose cures against blood-stage murine malaria in the 1-day suppressive test, although they required higher, 10 mg/kg doses to achieve this effect.

Compound	In vitro *P. falciparum* IC_{50} (nM)			In vivo 4-day dosing (mg/kg)		In vivo 1-day dosing (mg/kg)
	D6	Dd2	C2B	ED_{50}	NRD	NRD
ELQ-400	0.6	1.5	35	0.01	0.1	1
ELQ-404	0.9	6.2	27	0.03	1	10*
ELQ-428	5.8	11	34	0.1	1	10

Table 5: Comparison of in vitro and in vivo activity of ELQ-400, ELQ-404, and ELQ-428. Both ELQ-404 and ELQ-428 were less potent than ELQ-400 in vitro and in vivo, but effectively cleared blood-stage *P.yoelii* parasites with single oral doses of 10 mg/kg. NRD = non-recrudescence dose. n=4 animals per group. * = 10 mg/kg ELQ-404 was curative in 3/4 animals.

Discussion

ELQ-400 is a potent antimalarial, and the first single dose compound with combined prophylactic, treatment, and transmission blocking activity against malaria. In mouse models, ELQ-400 prevented malaria transmission and blocked the development of liver stage infections with single oral doses of 0.1 and 0.08 mg/kg, respectively. More impressively, ELQ-400 also effectively cleared

asexual, blood-stage parasites with a single 1 mg/kg dose, making it the most active single dose therapy to date, with a 20-fold to 100-fold increase in efficacy over other single dose compounds in the developmental pipeline.

Like other single dose antimalarials, I also found that ELQ-400 was capable of rapidly reducing blood-stage parasitemia in vivo. This finding was especially striking because cyt bc_1 inhibitors such as ELQ-400 have generally been classified as slow-onset antimalarials[68]. Although ELQ-400 did require at least 48 hours to initiate cell death in vitro, it triggered a rapid and long-lasting stasis in blood-stage parasites that was associated with clear morphological changes in vivo. These changes likely increased clearance by the spleen and allowed ELQ-400 to rapidly reduce parasite burden even before the onset of parasite death. Although I do not yet know the kinetics of ELQ-400's interaction with liver and sexual stage parasites, the finding that one hour of ELQ-400 exposure was sufficient to maximally inhibit oocyst development in fed mosquitoes suggests that the rapid inhibitory effects of ELQ-400 are likely conserved across multiple stages of *Plasmodium* development.

In addition to providing unprecedented, multi-stage single-dose cures for malaria, ELQ-400 may be ideally suited for topical formulation. In both 4-day and 1-day dosing tests against blood-stage parasites, transdermal administration of ELQ-

400 closely replicated the effects of oral delivery. Although oral therapy is the most common treatment route for uncomplicated malaria, IV drug administration is still the standard of care for infants and patients with severe disease[13,29]. My findings with ELQ-400 suggest that topical treatment may be a viable alternative, which could decrease the risk of bloodborne infections, reduce the medical training required to provide treatment, and ultimately provide safer, more accessible care for patients.

Biologically, the incredible single dose efficacy of ELQ-400 has yet to be fully explained. Although I initially attributed ELQ-400's single dose activity to its remarkable potency against *Plasmodium*, this cannot explain the response to ELQ-404 and ELQ-428, which are less potent than ELQ-300 both in vitro and in vivo. Therefore, I believe that the 5,7-difluoro quinolone scaffold plays a specific role in the activity of ELQ-400, ELQ-404, and ELQ-428. One possible explanation is that the 5,7-difluoro groups improve the pharmacokinetic properties of the ELQs and either increase absorption or extend in vivo half-life. It is also possible that the 5,7-difluoro configuration directly alters the interaction with cyt bc_1. Fluorine atoms are excellent hydrogen bond acceptors[83], and could potentially interact with cyt bc_1 residues to facilitate a more rapid or longer lasting inhibition. This could also explain the mild cross-resistance that Tm90-C2B parasites exhibit towards the 5,7-difluoro substituted ELQs because the mutated Y268

residue has been has been previously implicated in hydrogen bonding to the Q_o site of cyt *bc₁*.

The major obstacle to ELQ-400 development is its limited selectivity for *Plasmodium* cyt *bc₁*. Off-target inhibition of the mammalian enzyme was presented as a possible explanation for the failure of the recent GSK pyridone project, during which a prodrug form of the lead pyridone compound, GSK932121, produced acute toxicity in rats[76]. Although the pyridones do inhibit human cyt *bc₁* at levels comparable to ELQ-400, it is noteworthy that ELQ-400 has never produced toxicity in mice or in several primary cell culture models. Unlike immortalized cells, which rely primarily on glycolysis for metabolism, these primary cells are very sensitive to changes in mitochondrial function, and this observed lack of toxicity suggests that ELQ-400 does not inhibit cyt *bc₁* in intact cells.

In the case of ATV, which also potently inhibits human cyt *bc₁* but is clinically well-tolerated by patients[59], drug efflux has been proposed as a possible protective mechanism for human cells, based on the finding that atovaquone is a known substrate for several efflux transporters in yeast[77]. It is possible that a similar efflux process reduces the ELQ-400 concentration within host cells, and this could explain the discrepancy between enzyme-level EC_{50} and whole-cell

toxicity that has been observed in our HFF and T-cell models. Therefore, I believe that further investigation of ELQ-400 is warranted, and that its inhibition of permeablized, HEK293 mitochondria should not be used as a de facto indicator of human toxicity.

Ultimately, ELQ-400 provides the first evidence that cyt bc_1 inhibitors can function as single-dose, multi-stage antimalarials. In addition to providing several direct options for ongoing development, my work with ELQ-400 also raises the intriguing possibility that other potent single-dose curative compounds may exist within the broader library of anti-respiratory inhibitors. Direct assessment of these compounds, and specific formulation to maximize systemic exposure may be invaluable tools for the further development and evaluation of single-dose treatments for malaria.

CHAPTER FOUR: ASSESSMENT OF Q_O VS. Q_I SITE INHIBITION OF CYTOCHROME *BC_1* BY ENDOCHIN-LIKE QUINOLONES

Introduction

Complex III of the mitochondrial electron transport chain, also known as the cytochrome *bc_1* complex (cyt *bc_1*), is a validated target for multi-stage antimalarial therapy. Structurally, there are two known binding sites for antimalarial compounds within cyt *bc_1*: an oxidative (Q_o) site and a reductive (Q_i) site. Inhibition at either site is sufficient to block the catalytic cycle of cyt *bc_1* (Q cycle), which ultimately leads to pyrimidine starvation and cell death in *P. falciparum*[47]. Pyridone, naphthoquinone, acridone, and quinolone compounds have all been identified as potent inhibitors of *Plasmodium* cyt *bc_1*[34,78], including atovaquone (ATV), which targets the Q_o site[56] and is a key component of the clinical formulation Malarone.

To date, very few Q_i site inhibitors of cyt *bc_1* have been identified, and it has been especially difficult to isolate Q_i selective compounds with activity against *P. falciparum*. Sequencing studies have shown that the *P. falciparum* Q_i site is structurally distinct from that of other species and, as a result, even antimycin A, the prototype, sub-picomolar inhibitor of the Q_i site in bacteria, yeast, and mammalian cells, demonstrates decreased activity against *P. falciparum,* with an in vitro IC_{50} in the nanomolar range[52,79]. Incidentally, the uniqueness of the *P. falciparum* Q_i site may confer several therapeutic advantages. In addition to

retaining potency against ATV-resistant, Q_o mutant parasites, Q_i site inhibitors may be uniquely selective for parasite cyt bc_1[74], and would thus constitute a novel class of antimalarial compounds.

Ultimately, a major obstacle to the development of Q_i site inhibitors for malaria is the lack of effective screening tools to identify Qi-selective compounds. Although studies in yeast have suggested that the quinolone compounds ELQ-271[65] and HDQ (1-hydroxyl-2-dodecyl-4(*1H*)-quinolone)[80] function as Q_i site inhibitors, no Q_i site *P. falciparum* mutants have been available for verification. Furthermore, with such a small group of effective Q_i targeting antimalarials, it has not yet been possible to make any consistent associations between chemical structure and Q_i site preference.

Recently, our collaborators at Columbia University succeeded in producing the first *P. falciparum* clone with a mutation in the cyt bc_1 Q_i site. As described in appendix C, this clone was developed under incremental ELQ-300 pressure and contained a specific I22L substitution that reduced its sensitivity to ELQ-300 by approximately 25-fold. In this chapter, I use this mutant, “D1” clone in combination with the ATV-resistant Tm90-C2B[57] strain to conduct a detailed assessment of Q_i vs. Q_o targeting within the ELQ library. I highlight several structural features that are associated with preferential Q_i site activity, and use

homology modeling to probe the molecular basis of these effects. Finally, I conclude with direct enzyme-level assessment of Q_o and Q_i site inhibition by ELQ-400, by measuring direct cytochrome *b* reduction in a *Paracoccus denitrificans* model system and provide the first evidence that this single dose compound functions as a dual-site inhibitor of cyt bc_1.

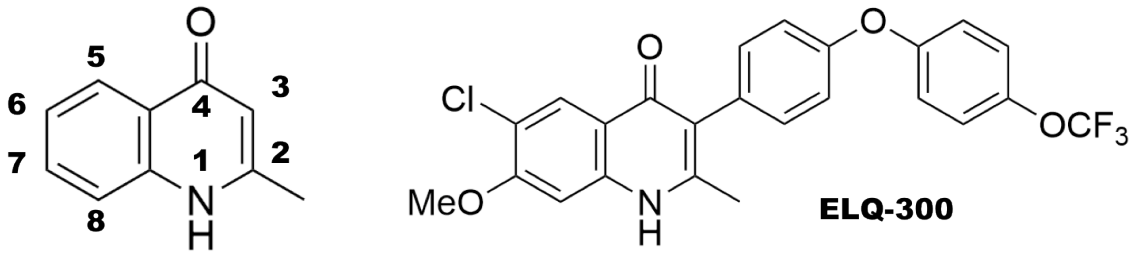

Figure 22: Left = general structure of 4(*1H*)-quinolones with numbered chemical positions. Right = structure of ELQ-300, the compound used to generate the Q_i mutant, D1 clone.

Results and Discussion

In vitro Q_o vs. Q_i preference of ELQs

In order to explore how chemical structure contributed to Q_i vs. Q_o site preference within the ELQ series, I conducted a large-scale assessment of our ELQ library using the D1 and Tm90-C2B *P. falciparum* drug-resistant clones. I used the fluorescence-based SYBR Green I assay to determine 50% inhibitory concentrations (IC_{50}) for each compound, and created cross-resistance indices (CRI) by normalizing D1 and Tm90-C2B activity against that of the Dd2 parental

strain. Because the D1 and Tm90-C2B strains respectively contain Q_i and Q_o site point mutations, I used D1 cross-resistance as an indicator of preferential Q_i site activity, and Tm90-C2B cross-resistance as an indicator of preferential Q_o site activity. Below, I describe the major structural features associated with Q_i vs. Q_o preference in the ELQs. Sensitivities of the D1 and Tm90-C2B strains to various comparison compounds are included in table 6.

Compound	Dd2 IC_{50} (nM)	Tm90-C2B IC_{50} (nM)	Tm90-C2B CRI	D1 IC_{50} (nM)	D1 CRI
ATV	0.41	>2500	>7800	0.71	1.7
ELQ-300	6.6	4.6	0.7	158	24
CQ	71	91	1.3	110	1.5
Antimycin A	72	39	0.5	35	0.5
Myxothiazol	1.7	320	188	3.5	2.0

Table 6: Sensitivity of the Dd2, Tm90-C2B, and D1 *P. falciparum* strains to atovaquone (ATV), ELQ-300, chloroquine (CQ), and the canonical Q_i and Q_o site inhibitors antimycin A and myxothiazol. Tm90-C2B parasites were highly cross-resistant to both ATV and myxothiazol, while D1 parasites were moderately resistant to ELQ-300. IC_{50} values averaged over at least 3 independent experiments run in triplicate. Standard deviation <10%. CRI = cross-resistance index.

CHAPTER FOUR: ASSESSMENT OF Q_O VS. Q_I SITE INHIBITION

6 and 7-positions

I assessed the role of 6-position and 7-position groups on Q_o/Q_i preference by first evaluating a set of ELQs containing the 3-position alkyl chain of endochin (Table 7). At the 7-position, all chemical groups were associated with an increase in Tm90-C2B cross-resistance relative to the undecorated compound ELQ-127. Electron-withdrawing substituents had the most dramatic effect, especially for the 7-Cl compound ELQ-109, which was more than 25 times less potent against the Tm90-C2B strain. In contrast, the effect of 6-position groups was dependent on electrostatic character; electron-donating groups (e.g. SCH_3, OH, OCH_3) dramatically reduced potency, but increased Tm90-C2B cross-resistance, while electron-withdrawing groups (e.g. halogens, NO_2) were universally associated with D1 cross-resistance and Q_i targeting. Overall, the most Q_i-selective compound was ELQ-130, which contained a 6-chloro substituent and was undecorated at the 7-position.

In a second compound set consisting of 3-diarylether ELQs, 6-position halogens had an even more dramatic effect on D1 cross-resistance and Q_i site preference (Table 8). While ELQ-130 was approximately 10-fold less active against the D1 clone, the corresponding 6-chloro, 3-diarylether, ELQ-296, was 15-fold less active, and a similar increase was observed for the 6-fluoro comparators, ELQ-131 and ELQ-314. Intriguingly, the combination of 6-halogen and 7-methoxy

groups produced an unanticipated increase in Q_i site preference among the 3-diarylether ELQs (Table 8). When compared to the 6-halogen compounds ELQ-314, ELQ-296, and ELQ-339, the corresponding 7-methoxy analogs demonstrated both increased potency and more pronounced D1 cross-resistance, which correlated with halogen size.

ELQ	3-Position	6-Position	7-Position	Dd2 IC_{50} (nM)	Tm90-C2B CRI	D1 CRI
131	C_7H_{15}	F	H	46.9	1.9	2.8
130	C_7H_{15}	Cl	H	29.2	0.9	9.7
162	C_7H_{15}	NO_2	H	257	1.4	4.6
150	C_7H_{15}	OCH_3	H	438	3.4	0.9
133	C_7H_{15}	SCH_3	H	283	5.9	1.5
127	C_7H_{15}	H	H	39.5	1.7	2.4
120	C_7H_{15}	H	F	9.6	19	1.0
109	C_7H_{15}	H	Cl	7.1	26	1.4
118	C_7H_{15}	H	CN	37.7	14	0.8
110	C_7H_{15}	H	NO_2	27.3	15	1.7
100	C_7H_{15}	H	OCH_3	5.2	6.1	0.9

Table 7: Comparative activity of 3-alkyl ELQs with various 6 and 7-position substituents. 7-position groups universally increased Tm90-C2B cross-resistance while electron-withdrawing 6-position substituents increased D1 cross-resistance and Q_i targeting. IC_{50} values averaged over at least 3 independent experiments run in triplicate. Standard deviation <10%. CRI = cross-resistance index

CHAPTER FOUR: ASSESSMENT OF Q_O VS. Q_I SITE INHIBITION

ELQ	3-Position	6-Position	7-Position	Dd2 IC_{50} (nM)	Tm90-C2B CRI	D1 CRI
271	DAE	H	H	12.5	2.8	0.2
298	DAE	H	OCH_3	5.5	0.7	0.8
314	DAE	F	H	33	1.3	3.4
316	DAE	F	OCH_3	3.1	1.1	3.6
296	DAE	Cl	H	29.1	0.9	16
300	DAE	Cl	OCH_3	6.6	0.7	24
339	DAE	Br	H	174	1.1	14
340	DAE	Br	OCH_3	25.4	0.4	65

Table 8: Comparative activity of 3-diarylether ELQs containing 6-Position halogens and 7-position methoxy groups. D1 cross-resistance was correlated with halogen size and the combination of 7-methoxy groups with 6-halogens increased both potency and associated Q_i site preference. DAE = para-OCF_3 diaryl ether side chain, as present in ELQ-300. IC_{50} values averaged over at least 3 independent experiments run in triplicate. Standard deviation <10%. CRI = cross-resistance index.

3-position side chains

The difference in D1 cross-resistance observed between the 3-alkyl and the 3-diarylether ELQs suggested that the 3-position side chain could play an integral role in Q_o vs. Q_i targeting for the ELQs. To assess this relationship, I next analyzed a series of 6-chloro ELQs containing various 3-position side chains (Table 9). Among these compounds, the most dramatic D1 cross-resistance was observed for the 3-biphenyl compound, ELQ-269, while the lowest degree of

cross-resistance was associated with ELQ-200, which contained a truncated 3-alkyl side chain. Generally, D1 cross-resistance correlated with side chain length and rigidity but was not noticeably altered by the presence of additional charged groups or heterocycles, as is demonstrated by the comparison between ELQ-296 and ELQ-317.

ELQ	3-Position	6-Position	7-Position	Dd2 IC_{50} (nM)	Tm90-C2B CRI	D1 CRI
220	Benzyl	Cl	H	508	4.1	2.7
200	C_4H_9	Cl	H	121	1.6	5.1
130	C_7H_{15}	Cl	H	29.2	0.9	9.7
296	DAE	Cl	H	29.1	0.9	16
317	Het- DAE*	Cl	H	57.7	0.5	15
269	Biphenyl	Cl	H	41.6	0.3	109

Table 9: Comparative activity of 6-chloro ELQs with various 3-position side chains. Degree of D1 cross-resistance generally correlated with side chain length and rigidity. DAE = para-OCF_3 diaryl ether side chain, as present in ELQ-300. Het-DAE = para-OCF_3 diaryl ether analog, containing a pyridyl inner ring. IC_{50} values averaged over at least 3 independent experiments run in triplicate. Standard deviation <10%. CRI = cross-resistance index.

5 and 7-positions

While 6-position halogens and aryl 3-position side chains were associated with the highest degree of Q_i site selectivity, Q_o site inhibition was strongly favored in ELQs containing 5,7-dihalogen groups (Table 10). The 5,7-difluoro compound

CHAPTER FOUR: ASSESSMENT OF Q_O VS. Q_I SITE INHIBITION

ELQ-121 was more than 600-times less potent against Tm90-C2B parasites and was the most Q_o selective compound within our ELQ library. Structurally, the 5-position fluorine contributed most strongly to this Q_o site preference; Tm90-C2B parasites were more cross-resistant to the 5-fluoro analog, ELQ-136, than to the 7-fluoro analog, ELQ-120. In contrast to the effect of isolated 7-position halogens, cross-resistance did not increase with 5,7-dihalogen size, and the 5,7-dichloro compound ELQ-124 was less Q_o selective than the difluoro compound ELQ-121.

Intriguingly, the Q_o-directing effects of the 5,7-difluoro configuration were effectively modulated by the addition of Q_i-directing chemical substituents (Table 10). Combination of a 3-position diarylether chain with 5,7-difluoro groups produced ELQ-400, which was associated with diminished Tm90-C2B cross-resistance relative to the 3-alkyl compound, ELQ-121. Tm90-C2B cross-resistance was further reduced by incorporation of halogens at the 6-position, and low levels of both D1 and Tm90-C2B cross-resistance were observed for the 5,7-difluoro, 6-chloro analog, ELQ-428. Conversely, addition of a 6-methoxy group between the flanking fluorine atoms increased Tm90-C2B cross-resistance relative to ELQ-400, which was consistent with the predicted effect of an electron donating, 6-position substituent.

CHAPTER FOUR: ASSESSMENT OF Q_O VS. Q_I SITE INHIBITION

ELQ	3-Position	5-Position	6-Position	7-Position	Dd2 IC_{50} (nM)	Tm90-C2B CRI	D1 CRI
136	C_7H_{15}	F	H	H	3.1	76.5	1.3
121	C_7H_{15}	F	H	F	0.5	612	0.6
124	C_7H_{15}	Cl	H	Cl	24	15.5	0.9
141	Benzyl	F	H	F	38	118	1.4
400	DAE	F	H	F	1.5	23.4	1.1
140	C_7H_{15}	F	F	F	2.8	34.1	1.1
404	DAE	F	F	F	4.9	5.80	1.4
428	DAE	F	Cl	F	11	3.40	3.3
429	DAE	F	OCH_3	F	46	26.4	2.0

Table 10: Comparative activity of ELQs containing 5 or 7-position halogens, with various Q_i-directing substituents. 5,7-difluoro compounds demonstrated the highest degree of Q_o site preference, and the presence of either a rigid, aryl side chain or a 6-position halogen increased D1 cross-resistance relative to the 3-alkyl comparator, ELQ-121. DAE = para-OCF_3 diaryl ether side chain, as present in ELQ-300. IC_{50} values averaged over at least 3 independent experiments run in triplicate. Standard deviation <10%. CRI = cross-resistance index.

Molecular Modeling

The dramatic impact of small chemical changes on site specificity suggested that ELQ substituents may divergently interact with key residues of cyt bc_1. Although there is no available crystal structure for the *Plasmodium* enzyme, I was able to use homology modeling in yeast to identify several potential ELQ binding interactions at both the Q_o and Q_i catalytic sites. For these models, I altered

several Q_o site residues to match those of *P. falciparum*, specifically at positions 133-136, 141, and 275, which have been shown to be important for sensitizing *S. cerevisiae* to both ATV and the quinolone compound RCQ06[81]. At the Q_i site, I incorporated F225L and K228L substitutions to reflect *P. falciparum* residues that play a known role in reduced sensitivity to canonical Q_i inhibitors, including antimycin A[52].

In my Q_i site model, there were multiple predicted interactions between cyt bc_1 and the ELQ core. In one potential conformation, the 4-oxygen and 1-NH components of the quinolone ring respectively formed predicted hydrogen bonds with S206 and H202 residues of the binding pocket (Figure 23). Alternately, another potential interaction predicted 1-NH binding to the local D229 residue (Figure 24). Although the first conformation is more energetically favorable and provides more anchoring interactions within the Q_i site, the alternate interaction with D229 places the 6-position of docked ELQs in close proximity to the I26 residue, which is analogous to the I22 residue mutated in ELQ-300-resistant, D1 parasites. In both cases, the involvement of the conserved quinolone core suggests that all ELQs are likely capable of Q_i site interaction, and specific bonds with the 1-NH group also provide a potential explanation for the increased Q_i site selectivity of ELQs containing 6-position, electron-withdrawing groups. Because the quinolone ring is aromatic in nature, electron-withdrawing groups located

para to the 1-position nitrogen (e.g. at the 6-position) would draw electron density away from the 1-NH group, making the associated hydrogen more acidic and available for hydrogen bond formation. Alternately, 6-position electron-donating groups would be expected to reduce the potential for hydrogen bonding, which is consistent with my finding that such compounds demonstrate a reduced Q_i site preference. With respect to the unique additive effect of 6-halogen and 7-methoxy groups, it is likely that 7-methoxy substituents also specifically interact with the Q_i binding pocket, although participating residues have yet to be identified.

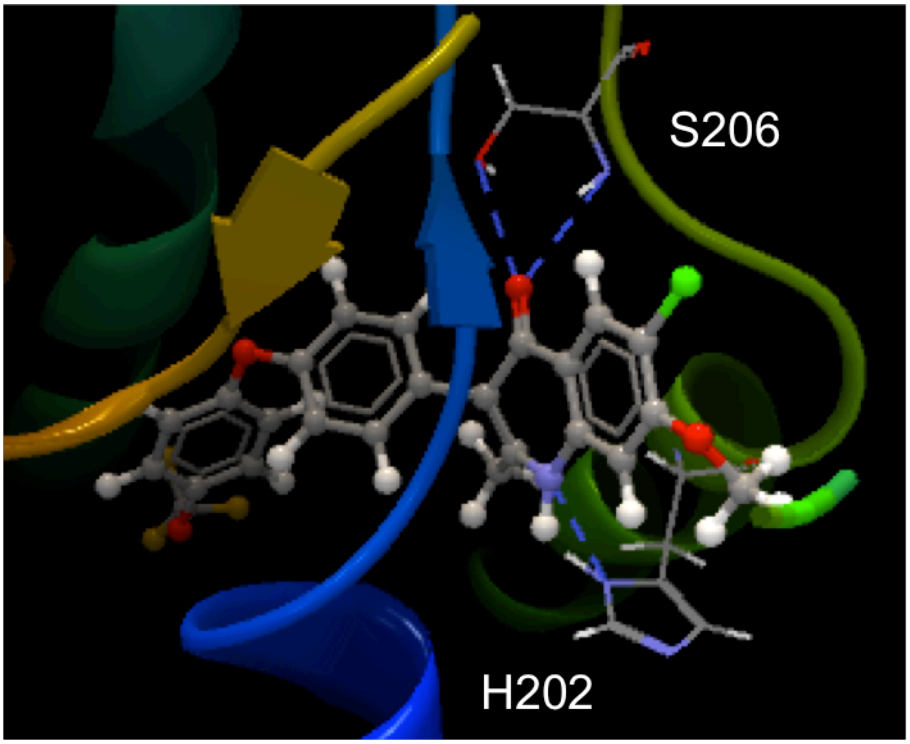

Figure 23: Docking of ELQ-300 to the *S. cerevisiae* Q_i site with predicted hydrogen bonds to S206 and H202 residues shown in blue.

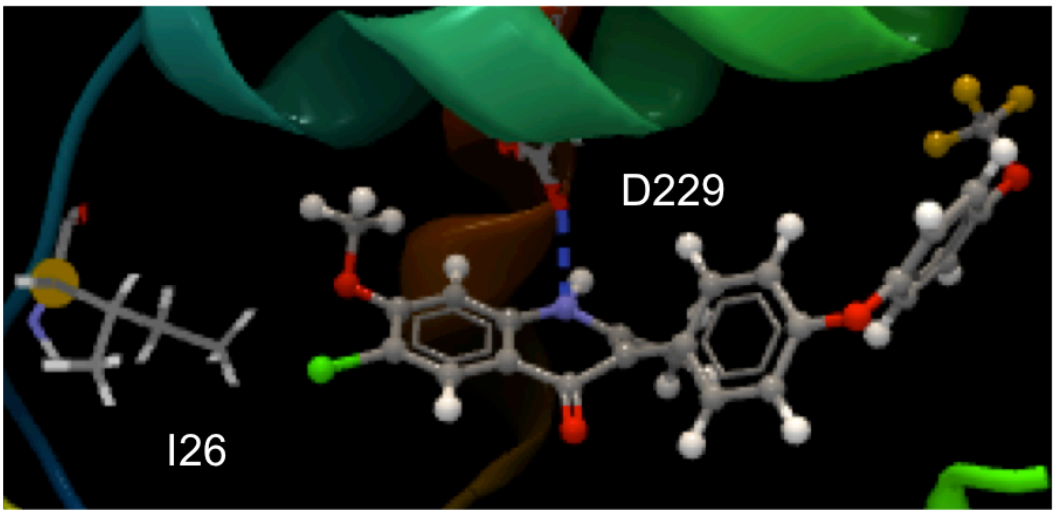

Figure 24: Alternate model of ELQ-300 interaction with the Q_i site, showing the 6-position chlorine in close proximity to the isoleucine residue mutated in the D1 *P. falciparum* clone.

While all tested ELQs made predicted hydrogen bonds within the Q_i site, similar interactions were only observed for a subset of compounds in my Q_o models. At the Q_o site, the major hydrogen bond participant was the conserved E272 residue, which is important for binding of both the natural cyt bc_1 substrate, ubiquinol, and the potent inhibitor stigmatellin[82] (Figure 25). At physiological pH, my models predicted a hydrogen bond between E272 and the quinolone 1-NH group. In this conformation, 7-position substituents were well tolerated and frequently formed additional predicted bonds with backbone atoms of the nearby M139 and G143 residues (Figure 25, right). In contrast, the presence of 6-position groups eliminated all predicted hydrogen bonds and these compounds

demonstrated no preference for tail-in vs. tail-out docking, which may explain the relative Q_i site selectivity of ELQs with less-flexible, aryl side chains.

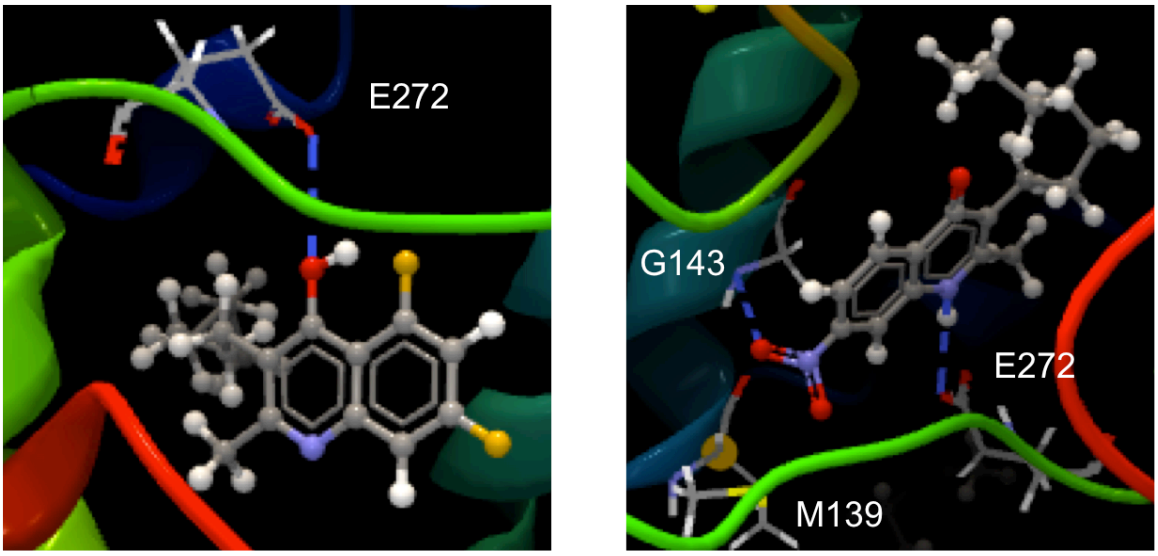

Figure 25: Predicted interactions of ELQ-121 (left) and ELQ-110 (right) with the Q_o site of *S. cerevisiae*. Both models involve potential hydrogen bonds with the conserved E272 residue. Predicted hydrogen bonds shown in blue.

Due to the inherent resonance potential of quinolone compounds, it is also possible that the 4-position oxygen of the quinolone core forms a hydrogen bond with E272. This alternate alignment is intriguing because it may allow the adjacent 5-fluorine substituent of highly Q_o selective compounds like ELQ-121 to coordinate with and stabilize the hydrogen bond interaction[83]. Although the role of fluorine in protein-based hydrogen bonding remains controversial, previous work with ELQ-121 has revealed that the adjacent 4-oxygen and 5-fluorine atoms do form collaborative hydrogen bonds with NH during the process of ELQ-121

crystal formation (Figure 9). If this interaction is maintained during binding to cyt *bc1*, it would explain both the unusual potency of the 5-fluoro and 5,7-difluoro ELQs, and the dramatic Tm90-C2B cross-resistance observed for these compounds.

Cytochrome b Reduction

Although modeling studies suggested that all ELQs should be capable of Q_i site inhibition, this was not fully reflected by observed D1 cross-resistance. In order to conclusively determine if ELQs interact with the Q_i site of cyt *bc1*, I next conducted a cytochrome *b* reduction assay that made use of the unique enzymatic mechanism of the cyt *bc1* complex. During the Q cycle, electrons are sequentially passed from the Q_o to the Q_i site of the cytochrome *b* subunit, where they are ultimately used to regenerate ubiquinol. Although electrons do not accumulate on cytochrome *b* during normal function, interruption of electron transfer by Q_i site inhibitors results in a dramatic overall reduction of the local b_H and b_L hemes, which can be spectrophotometrically detected by an absorbance peak at 562nM[84].

To assess cytochrome *b* reduction by the ELQs, I tested enzyme from the bacteria *Paracoccus denitrificans* in the presence of ELQ-400. This model system was selected because, unlike enzyme from either *P. yoelii* or *P.*

CHAPTER FOUR: ASSESSMENT OF Q_O VS. Q_I SITE INHIBITION

falciparum, bacterial cyt bc_1 could be collected in sufficient (3μM) quantities for direct cytochrome *b* assessment. In turn, ELQ-400 was used because of its relatively low, micromolar EC_{50} against the bacterial enzyme and because of its relevance as a potent, single-dose antimalarial therapy.

I tested the ability of ELQ-400 to reduce cytochrome *b* by incubating purified cyt bc_1 from *P. denitrificans* with 50μM ELQ-400 in the presence of ubiquinol. The known Q_i site inhibitor antimycin A served as a positive control, while the Q_o site inhibitor myxothiazol was used to detect any reverse electron accumulation via the Q_i site. As expected, antimycin A was associated with dramatic cytochrome *b* reduction, while myxothiazol had a more modest effect, equating to approximately 30% of the total antimycin A signal (Figure 26). Importantly, the combination of antimycin A and myxothiazol completely blocked cytochrome *b* reduction and verified that this effect was specifically associated with activity at the Q_o and Q_i binding sites.

In the presence of ELQ-400, cytochrome *b* was reduced to an intermediate extent relative to the Q_o and Q_i reference compounds, and this signal was effectively decreased by myxothiazol co-incubation, as would be expected in the setting of Q_i site inhibition (Figure 26).

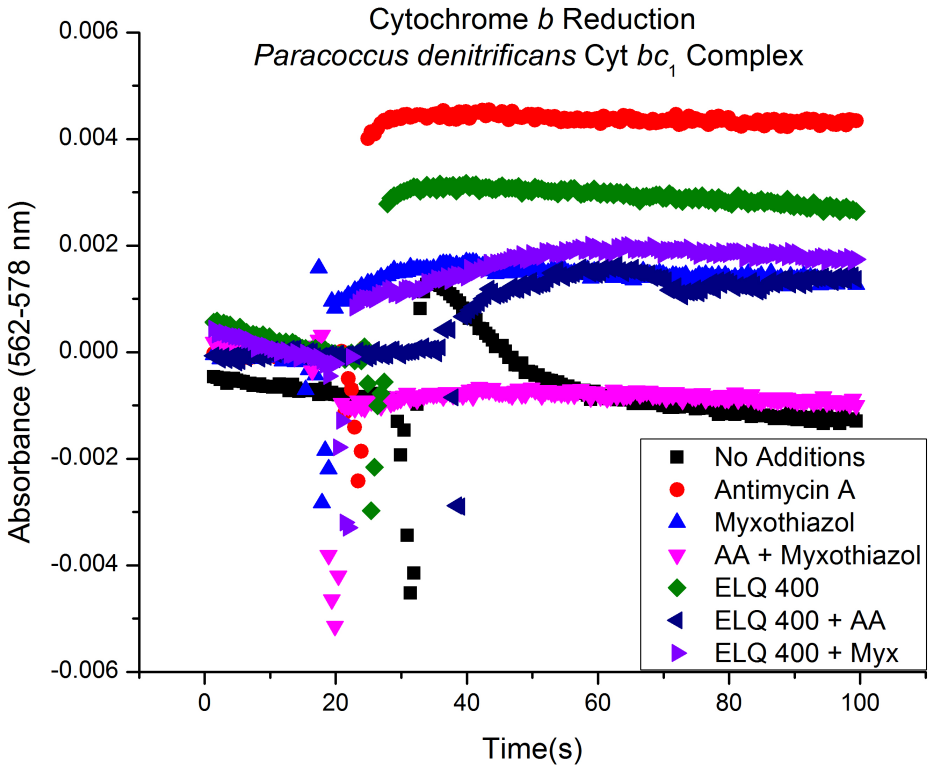

Figure 26: Cytochrome *b* reduction in *P. denitrificans* shown as adjusted absorbance at 562nM. Both ELQ-400 and antimycin A induced higher levels of cytochrome *b* reduction than the known Q_o site inhibitor, myxothiazol. Amplitude of the ELQ-400 signal decreased in the presence of either antimycin A or myxothiazol, which was suggestive of dual-side inhibition. Enzyme added 20 seconds into reading. AA = antimycin A. Myx = myxothiazol.

Although the ELQ-400 and ELQ-400+myxathiazol conditions did not perfectly replicate the behavior of the known Q_i site inhibitor, antimycin A, this was likely

the result of altered potency and binding stability. While antimycin A and myxothiazol are both considered irreversible inhibitors and block cyt *bc₁* function at sub-picomolar concentrations in *P. denitrificans*, ELQ-400 has an EC_{50} in the micromolar range. As a result, ELQ-400 may only partially block the Q_i site at soluble concentrations, which would explain both the decreased overall electron accumulation and the incomplete block of cytochrome *b* reduction in the presence of myxothiazol.

Interestingly, this cytochrome *b* reduction assay also provided evidence for inhibition by ELQ-400 at the Q_o site. As observed for the antimycin A+myxothiazol condition, cytochrome *b* reduction by antimycin A was disrupted by co-incubation with ELQ-400. Although this blunting effect was incomplete, this is again consistent with the lower affinity of ELQ-400 relative to myxothiazol and antimycin A.

Summary and Conclusions

Using a set of mutant *P. falciparum* strains, including the novel D1 clone, I have identified several key ELQ features associated with preferential Q_o or Q_i site inhibition of *Plasmodium* cyt *bc₁*. Primary contributors to Q_i site preference included: (1) Electron-withdrawing, 6-position substituents (including halogens) (2) Combined 6-halogen, 7-methoxy groups, and (3) Aryl 3-position side chains.

CHAPTER FOUR: ASSESSMENT OF Q_O VS. Q_I SITE INHIBITION

Alternately, 7-position groups were broadly associated with Q_o site targeting, especially in combination with 5-fluorine moieties, as was observed for the 5,7-difluoro ELQs.

Although my drug sensitivity model effectively identified several chemical characteristics associated with D1 and Tm90-C2B cross-resistance, one vital question is whether this observed cross-resistance is a true measure of Q_i vs. Q_o site selectivity. Unlike the Y268S mutation associated with the Tm90-C2B clone, which confers extensive ATV resistance and also decreases the potency of canonical Q_o site inhibitors like myxothiazol[57], the effect of the I22L mutation had relatively little impact on any tested compound. Because the I22L substitution is a minor chemical change and does not alter local charge, it is likely that D1 cross-resistance is the direct result of steric interference between the mutant leucine residue and the interfacing 6-position of bound ELQs (Figure 24). In addition to justifying the correlation between 6-substituent size and D1 cross-resistance, this hypothesis also suggests that the D1 clone underestimates the true extent of Q_i site inhibition and provides a compelling explanation for the lack of cross-resistance observed for several known Q_i site inhibitors, including antimycin A and ELQ-271.

CHAPTER FOUR: ASSESSMENT OF Q_O VS. Q_I SITE INHIBITION

It is also possible that the D1 and Tm90-C2B clones may not effectively classify compounds with the ability to inhibit both sites of cyt *bc₁*. Within the series of 5,7-difluoro ELQs, I found that the sequential addition of Q_i compatible features progressively decreased the degree of Tm90-C2B cross-resistance, suggesting that an adjustable balance exists between Q_o and Q_i site inhibition for these compounds. Cytochrome *b* reduction studies in my *P. denitrificans* model system supported the general theory that ELQs could function as dual-site inhibitors of cyt *bc₁*. In the case of ELQ-400, this could contribute to this compound's unparalleled single-dose efficacy in *P. yoelii* models and also explains why it retains nanomolar activity against all tested Q_o mutant strains, including Tm90-C2B.

Several avenues can be pursued for the future identification of Q_i targeting antimalarials. One strategy is to develop a more general Q_i site *P. falciparum* mutant, with greater sensitivity as a screening tool. Although this may be possible, my preliminary efforts to develop resistant parasites under either ELQ-271 or ELQ-298 pressure have thus far been unsuccessful. This finding, as well as the difficulty associated with developing the D1 clone, suggests that either dual-site inhibition by the ELQs is protective against drug resistance, or that there is simply limited genetic space for mutation within the cyt *bc₁* Q_i site. Alternately, it would be useful to develop *P. denitrificans, R. capsulatus,* or *S. cerevisiae*

strains with greater Q_i site homology to *Plasmodium*. While ELQ-400 effectively inhibited the *P. denitrificans* enzyme in this study, more *Plasmodium* selective compounds, such as ELQ-300 and ELQ-316 did not appreciably inhibit the bacterial enzyme and could therefore not be tested for cytochrome *b* reduction.

Ultimately, it will be necessary to parse the effects of isolated Q_i site inhibition from those of dual-site interaction so that cyt bc_1 inhibitors can be optimized for clinical use. Until then, the structural insight obtained from the ELQ library and the D1 clone has the potential to guide drug development efforts for several chemical families and advances our understanding of how these compounds interact with *P. falciparum* cyt bc_1.

CHAPTER FIVE: COMBINATION THERAPY AS A STRATEGY FOR DUAL-SITE INHIBITION OF CYTOCHROME BC_1

Introduction

The cytochrome *bc_1* complex (cyt *bc_1*) is well-established target for antimalarial therapy and is the known site of action of several potent inhibitors of *P. falciparum*, including atovaquone (ATV)[55] and the endochin-like quinolones (ELQs)[74]. Biologically, cyt *bc_1* plays a vital role in de-novo pyrimidine biosynthesis for *P. falciparum* by facilitating the activity of type II dihydroorotate dehydrogenase (DHODH). Because malaria parasites lack a functional pyrimidine salvage pathway, inhibition of cyt *bc_1* (and by extension, DHODH) is fatal and provides both treatment and prophylactic protection against malaria[47]. Currently, ATV is the only cyt *bc_1* inhibitor in clinical use, and is a major component of the antimalarial formulation, Malarone.

The major hurdle to the large-scale use of ATV is its high propensity for drug resistance. When administered as monotherapy, point mutations rapidly arise within the oxidative (Q_o) site of cyt *bc_1*. Parasites containing Y268S substitutions are the most clinically severe and these strains are more than 1000-fold less sensitive to ATV than wild-type parasites[57,58]. Although resistance propensity has been substantially reduced by the use of Malarone, which combines ATV with the partner drug proguanil[85], the Y268S mutation has still been detected in several

cases of Malarone treatment failure and drug resistance remains a major concern for the development of new cyt *bc*$_1$ inhibitor therapies[61].

Although ongoing drug development efforts have prioritized the identification of ATV-replacement drugs, little work has focused on the optimization of ATV combination therapy. The evaluation of novel ATV partner drugs is especially relevant in light of the recent discovery of ELQ-300[66], which potently inhibits the reductive (Q_i) site of cyt *bc*$_1$, rather than the oxidative (Q_o) site exploited by ATV. Because of this site specificity, ELQ-300 is fully active against ATV-resistant *P. falciparum* parasites. More importantly, resistance to ATV:ELQ-300 combination therapy would be evolutionarily unlikely, due to the requirement for two simultaneous mutations within a single target protein.

There are several secondary benefits to exploring ELQ-300 and ATV in combination. As previously described, ELQ-400 is a dual-site inhibitor of cyt *bc*$_1$. If ATV:ELQ-300 combination therapy replicates the in vivo effects of ELQ-400, this would offer a new approach for the development of single-dose, antimalarial therapies. On a more basic level, assessment of ELQ-300 against ATV also provides a unique opportunity to compare the biological effects of Q_i vs. Q_o inhibition *Plasmodium*. In this chapter, I used a murine system to compare the

potency and efficacy of ATV, ELQ-300, and the ATV:ELQ-300 combination in both 1-day and 4-day treatment models.

Results

ATV and ELQ-300 Combination Therapy – Peters Suppressive Test

I used in vivo models to test the synergistic activity of ATV and ELQ-300 in both 4-day and 1-day dosing experiments. For these studies, female CF-1 mice were inoculated with *P. yoelii* parasitized RBCs via tail vein injection and each animal received an initial dose of drug 24 hours post-infection, delivered orally as a solution in PEG-400. For combination therapies, doses were calculated with respect to total drug present such that a 20 mg/kg dose of the 3:1 ATV:ELQ-300 formulation would be equivalent to 15 mg/kg ATV + 5 mg/kg ELQ-300.

In the 4-day test, I found that either a 1:1 or a 3:1 combination of ATV:ELQ-300 increased both the potency and efficacy of treatment relative to ATV monotherapy (Table 11). In both combinations, daily 0.1 mg/kg doses suppressed parasitemia by >99% as compared to controls on post-infection day-5 (ED_{99}), while a 1 mg/kg dose was fully curative. Comparison values for ATV and ELQ-300 were consistent with previous reports.

CHAPTER FIVE: COMBINATION THERAPY

Treatment	4-Day Dosing (mg/kg)		1-Day Dosing (mg/kg)	
	ED_{99}	NRD	ED_{99}	NRD
ELQ-300	0.1	0.3	0.1	>20
ATV	1	10	1	10
(1:1) ATV:300	0.1	1	0.1	10
(3:1) ATV:300	0.1	1	1	1
(5:2) ATV:PG	1	1	1	1*
ELQ-400	0.03	0.1	0.1	1

Table 11: Comparative activity of ELQ-300, ATV, ELQ-400, and combination therapies in the murine Peters suppressive test. Co-formulation of ATV with either ELQ-300 or proguanil increased in vivo efficacy in both 4-day and 1-day studies. ELQ-400, ATV, ATV:ELQ-300, and ATV:proguanil were all capable of clearing parasites with a single oral dose. ED_{99} = 99% effective dose. NRD = nonrecrudescence dose. ATV = atovaquone, PG = proguanil. 300 = ELQ-300

* = ¾ animals cured at 1 mg/kg ATV:PG.

In the 1-day dosing-study, I also found evidence for increased activity of the combination therapy. In this model, the 3:1 ratio was most effective and cured all animals at a single dose of 1 mg/kg, while the 1:1 combination was curative at a higher, 10 mg/kg dose (Table 11). Although ELQ-300 did not prevent recrudescence in this test up to its solubility limit (20 mg/kg), ATV did demonstrate unanticipated single dose curative activity at a dose of 10 mg/kg. More surprisingly, the 1-day ED_{99} and nonrecrudescence values for ATV

perfectly matched those of the 4-day treatment study, suggesting that the maximum effectiveness of this compound was obtained following a single oral dose.

Clearance Kinetics and Resistance Propensity

To further assess the potential single dose efficacy of ATV and the ATV:ELQ-300 combination, I next tested these compounds in a model of acute infection, in which animals harbored a higher pre-treatment parasitemia. For these studies, mice were inoculated as described previously but treatment was delayed until initial parasitemia reached approximately 20%. Animals then received a single oral drug dose at the maximum soluble concentration (20 mg/kg), and parasite clearance was monitored via microscopic examination of stained blood smears.

Interestingly, use of the acute model highlighted several distinct differences between the in vivo response to the comparison compounds, ATV and ELQ-300. While both treatments successfully lowered initial parasitemia, the response to ATV was more rapid and lowered parasite burden within 24 hours of administration (Figure 27). In contrast, parasitemia initially remained static in ELQ-300 treated animals, and declines were not noticeable until 48-hours post-treatment. To determine if these effects extended to multi-day administration, I used a 4-day, acute comparison model and found that 4-day dosing of ELQ-300

effectively accelerated parasite clearance and prevented recrudescence, even at a reduced dose of 10 mg/kg (Figure 28). Importantly, as observed in the Peters model, repeated dosing did not impact the in vivo response to ATV and all animals recrudesced in both the 1-day and 4-day ATV treatment groups.

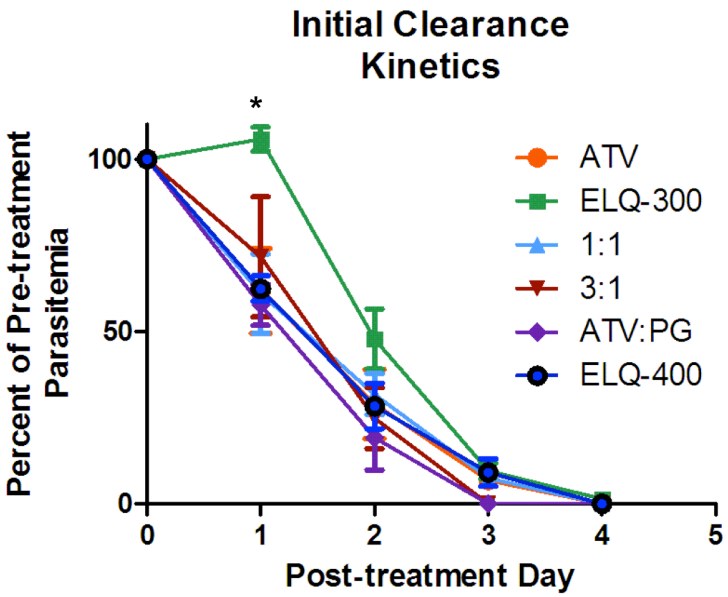

Figure 27: Onset of parasite clearance in the 1-day acute treatment model. ELQ-300 was associated with a 24 hour lag phase. All other groups effectively reduced parasitemia within 24 hours of drug administration. Averages of n=4 animals per group. Error bars represent SEM. Asterisk indicates $p<0.001$ for parasitemia in ELQ-300 treated animals vs. other groups on post-treatment day 1.

CHAPTER FIVE: COMBINATION THERAPY

In my acute infection studies, ATV and ELQ-300 also differed in terms of resistance propensity. While the single 20 mg/kg dose was sub-therapeutic for both compounds, resistance phenotypes were only associated with ATV treatment. To assess resistance, I exposed recrudescent animals to a second 20 mg/kg oral treatment, and compared parasite clearance kinetics to those of the first drug exposure. While recrudescent parasites in the ELQ-300 treatment group were fully responsive to a second dose of ELQ-300, the response of ATV-treated parasites to re-challenge was variable. In most cases, ATV resistant parasites were characterized by sustained, low-grade infections in the presence of ATV (Figure 28). However, I noted several instances of complete ATV insensitivity, which manifested as robust increases in post-treatment parasitemia and were highly reminiscent of the Y268S phenotype.

With respect to the combination therapy, I found that ATV:ELQ-300 co-administration merged the desirable clearance kinetics of ATV with the low resistance propensity and multi-day efficacy of ELQ-300. Animals in both the 1:1 and 3:1 treatment groups responded rapidly to initial drug therapy and recrudescent parasites were fully sensitive to a second, 20 mg/kg dose of ATV (Figure 29). Importantly, both combinations effectively delayed recrudescence relative to either the ATV or ELQ-300 monotherapy groups and, as was observed

for ELQ-300, 4-day administration of either formulation was fully curative at a dose of 10 mg/kg.

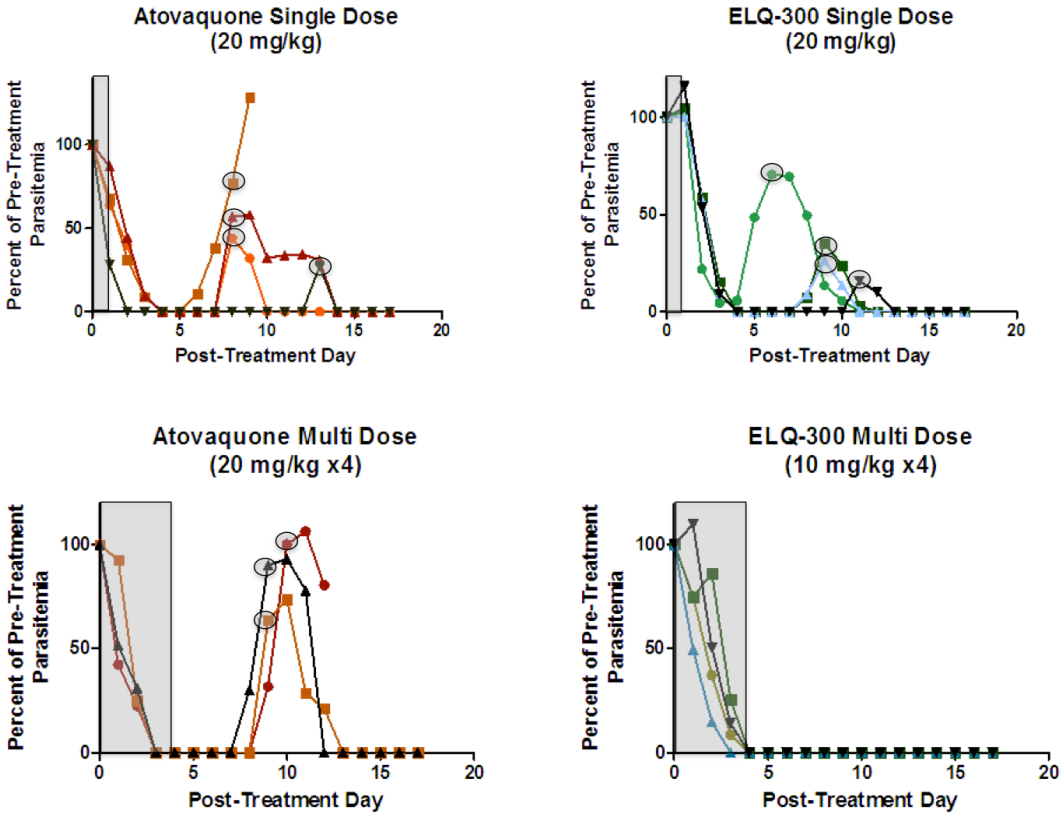

Figure 28: Impact of ATV or ELQ-300 therapy in 1-day (top) vs. 4-day (bottom) acute treatment models. ATV treatment was associated with a rapid onset of action, but high resistance propensity. ELQ-300 treatment demonstrated a cumulative multi-day dosing effect and no resistance was detected in ELQ-300 treated animals in either the 4-day or 1-day study. Grey bars/circles represent drug administration. Each trace represents a single animal.

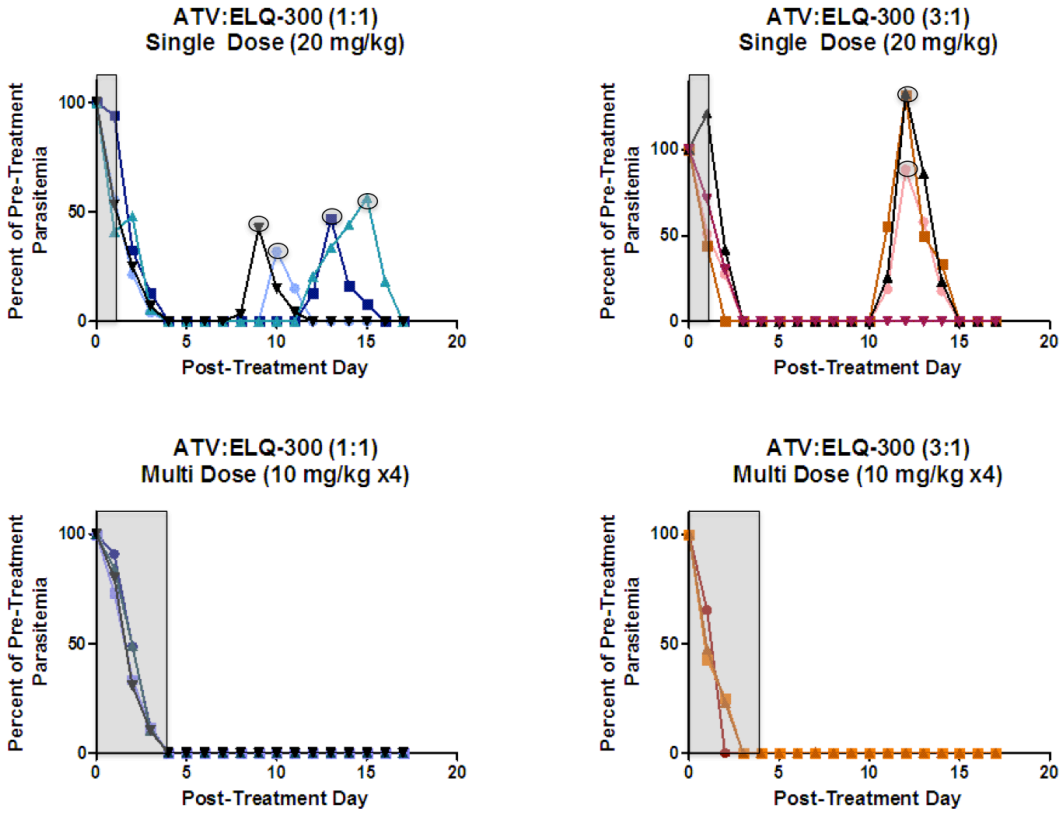

Figure 29: Impact of ATV:ELQ-300 combination therapy 1-day (top) vs. 4-day (bottom) acute treatment models. Both treatment groups demonstrated a rapid onset of parasite clearance, low resistance propensity, and multi-day dosing effect. Recrudescence was delayed relative to ATV or ELQ-300 comparison groups (Figure 28), and one animal in the 3:1 ATV:ELQ-300 group was fully cured with a single 20 mg/kg oral dose. Grey bars/circles represent drug administration. Each trace represents a single animal.

CHAPTER FIVE: COMBINATION THERAPY

Comparison to ELQ-400

In the suppressive test, ELQ-400 administration closely matched the effects of 3:1 ATV:ELQ-300 therapy and, in both cases, a 1 mg/kg dose was curative in all animals (Table 11). However, ELQ-400 was markedly more effective than ATV:ELQ-300 combination therapy in the acute treatment model, and either a single, 20 mg/kg dose or four sequential 10 mg/kg doses effectively prevented recrudescence (Figure 30).

Comparison to ATV:Proguanil Therapy

In order to determine how ELQ-400 or ATV:ELQ-300 combination therapy compared to the current standard of care, I next evaluated an ATV:proguanil co-formulation at the 5:2 ratio that is used in Malarone. Although ATV:proguanil treatment was more effective than ATV monotherapy in both 1-day and 4-day suppressive tests, with a nonrecrudescence dose of 1 mg/kg (Table 11), this combination did not fully counteract the high resistance propensity of ATV observed in the acute treatment model (Figure 30). Additionally, in contrast to the ATV:ELQ-300 groups, multi-day ATV:proguanil therapy was not curative in the 4-day, acute treatment test and did not delay recrudescence relative to the ATV comparison group.

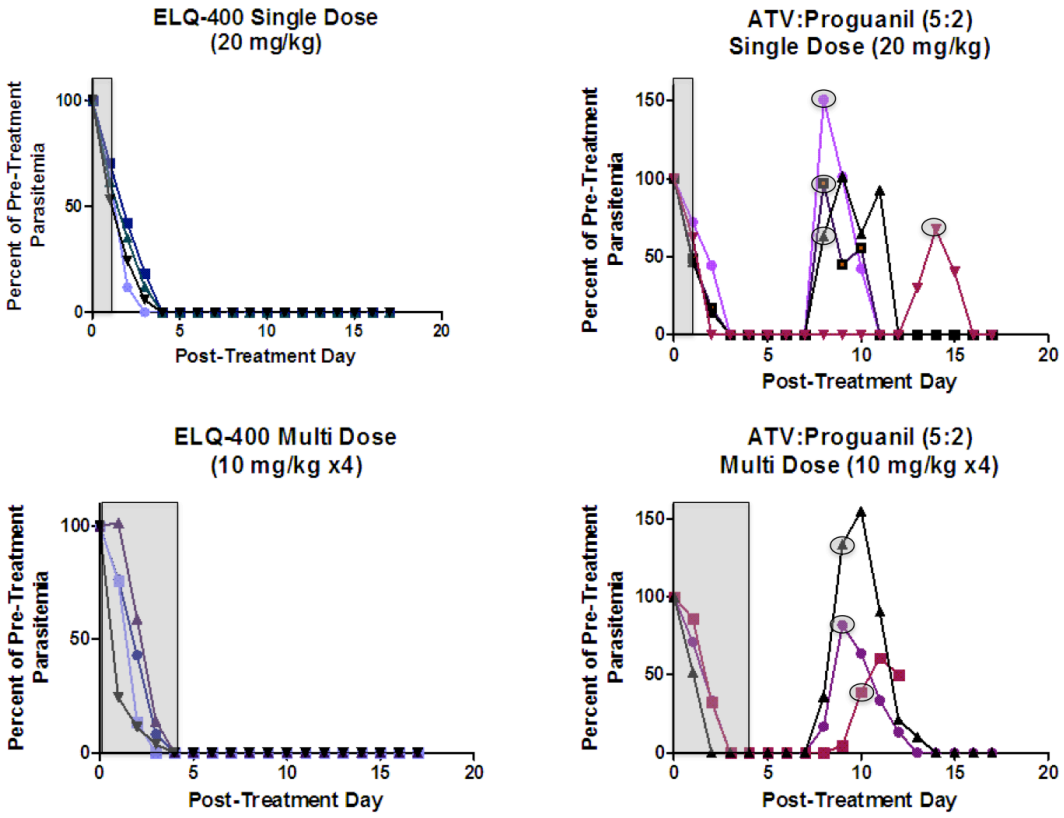

Figure 30: Impact of ELQ-400 or ATV:Proguanil combination therapy in 1-day (top) vs. 4-day (bottom) acute treatment models. ELQ-400 was more effective than ATV, ELQ-300, and combination therapy groups and effectively prevented recrudescence in both 1-day and 4-day models. Like ATV monotherapy, the ATV:proguanil formulation produced similar results in the 1-day and 4-day dosing tests and a subset of animals demonstrated mild ATV resistance in the 1-day study. Grey bars/circles represent drug administration. Each trace represents a single animal.

CHAPTER FIVE: COMBINATION THERAPY

Discussion

The therapeutic combination of ATV and ELQ-300 is the first example of an antimalarial formulation inhibiting two sites within a single target protein. In mouse models, this co-formulation was more effective than ATV alone in both 1-day and 4-day suppressive tests, and the 3:1 ratio of ATV:ELQ-300 was especially useful as a single-dose, blood-stage therapy. In comparison to ATV and proguanil, the key components of Malarone, the ATV:ELQ-300 formulation demonstrated a reduced propensity for in vivo drug resistance and increased efficacy in multi-day, acute treatment models, suggesting that this combination may be ideally suited to overcome the risk of treatment failure associated with both ATV and Malarone therapy.

Single-Dose ATV Therapy

One of the most surprising findings of this study is the previously unreported, single-dose activity of ATV. Although ATV was extensively tested in rodents at the time of its discovery in the late 1980s, the majority of these studies involved either multi-day dosing or prophylactic administration. Despite these differences, there were several initial indications that single dose ATV therapy could potently impact blood-stage parasites. An early study in rats by Davies et al. indicated that in addition to providing causal prophylactic protection, a single 10 mg/kg dose of ATV also delayed the development of blood-stage infection and reduced

peak parasitemia, even when administered 45 hours pre-inoculation[73]. The landmark Hudson et al. paper from 1991 provided further characterization of single dose ATV treatment and reported that 1-day and 7-day dosing schedules were similarly potent in a *P. yoelii* suppressive model, with ED_{50} values of 0.07 and 0.05 mg/kg, respectively[54].

Although it is likely that the single dose activity of ATV was simply not captured by previous studies due to selected dosing schedules and output measures, it is also possible that formulation played a key role in the response to ATV. In contrast to earlier studies, which delivered ATV as micro or nanoparticle suspensions, I prepared all compounds as solutions in PEG-400, which likely minimized the potential for crystal formation and subsequent precipitation within the alimentary canal. In addition to increasing the solubility of ATV, the PEG vehicle may have also directly aided absorption by limiting efflux from intestinal epithelial cells, which has previously been demonstrated for PEG-300 using a caco-2 model[86].

ATV vs. ELQ-300 Monotherapy

Despite their shared protein target, ATV and ELQ-300 elicited unique biological responses in both suppressive and acute treatment murine models. While the single-dose efficacy of ATV may simply be a reflection of its exceptional intrinsic

potency, which exceeds that of ELQ-300 by approximately 10-fold, my findings can also be explained in the context of respective Q_o vs. Q_i site inhibition by ATV and ELQ-300. In yeast and bacterial model systems, numerous bypass reactions partially compensate for Q_i site blockade by passing electrons to intermediate carriers such as oxygen[51]. Because similar pathways do not exist for Q_o site inhibition, ATV would be expected to more rapidly disrupt mitochondrial function, while ELQ-300 may disproportionately benefit from prolonged, multi-day exposure.

Another possibility is that off-target inhibition of other mitochondrial proteins may have contributed to the overall responses to ATV vs. ELQ-300 therapy. Structurally, the Q_i site of cyt bc_1 is similar to ubiquinone binding regions of both Complex I and dihydroorotate dehydrogenase (DHODH). Because ELQ-300 does moderately inhibit DHODH at micromolar concentrations (Figure 31), multi-day dosing may increase ELQ-300 exposure to levels compatible with multi-target inhibition, which would explain both the cumulative effects of multi-day dosing and the low resistance propensity observed following ELQ-300 administration.

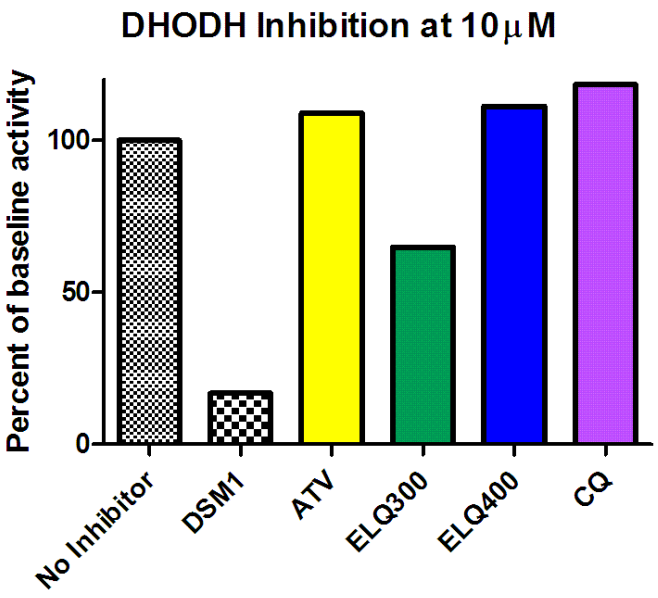

Figure 31: Inhibition of isolated DHODH enzyme by selected compounds in comparison to the known DHODH inhibitor, DSM1. The Q_i site inhibitor, ELQ-300, inhibited DHODH by approximately 40%. ATV = atovaquone, CQ = chloroquine. n=2 replicates per compound.

Clinical Implications

My work highlights several future possibilities for ATV combination therapy. I have shown that ATV:ELQ-300 co-formulations uniquely merge the potency of ATV with the low resistance propensity and multi-day dosing benefits of ELQ-300. Because of their well-matched, extended half-lives, formulations of ATV and ELQ-300 would be unlikely to expose patients to incidental monotherapy, which has been proposed as a possible contributing factor to Malarone treatment

failure[62]. As a preclinical candidate, ELQ-300 also has the potential to be rapidly partnered with ATV for evaluation in humans, which is important in the context of emerging resistance to artemisinin-based therapy. Ultimately, although this combination did not perfectly replicate the effects of ELQ-400 in vivo, it is likely that further adjustments to the ATV:ELQ-300 ratio may be useful for optimizing single-efficacy in the acute treatment model.

With respect to Malarone, my studies provide the first assessment of the ATV:Proguanil combination in a murine system and illustrate that the propensity for ATV-resistance can be experimentally reproduced in an acute infection model[61,87]. In addition to providing a potential new screening tool, the acute infection model also offers insight into potential changes to Malarone dosing frequency. Like ATV monotherapy, ATV:proguanil treatment had a similar impact on parasite clearance in both 1-day and 4-day tests, which suggests that Malarone may be equally effective with a reduced dosing schedule. Although several recent clinical studies have explored the potential for weekly prophylactic dosing[88], none have yet evaluated non-daily Malarone therapy in an acute setting. Because this would dramatically reduce treatment cost, reducing the frequency of Malarone treatment may be a useful strategy to pursue until new alternatives are available for clinical use.

CHAPTER FIVE: COMBINATION THERAPY

Finally, my work with ATV and ATV:ELQ-300 combination therapy supports the idea that cyt *bc*$_1$ is a useful target for single-dose antimalarial therapy. Like the 5,7-difluoro compound, ELQ-400, all ATV combinations demonstrated single-dose curative activity in the murine suppressive model. Intriguingly, both ELQ-400 and ATV have known activity at the Q_o site of cyt *bc*$_1$. Although Q_o site inhibition has become an undesirable feature in ongoing antimalarial drug development due to concerns over ATV resistance, it is possible that inhibition of this site has unique benefits in terms of single dose activity. It is also possible that many presumed Q_o-selective compounds may also exhibit some degree of Q_i site inhibition, which may explain the similarity between the response to ELQ-400 and the ATV:ELQ-300 combination, in vivo. Ultimately, it is clear that inhibition of cyt *bc*$_1$ is associated with a remarkable potency and scope of action that merits future research and may uniquely contribute to the goal of malaria eradication.

CHAPTER SIX: SUMMARY AND CONCLUSIONS

Summary

The major goal of this project was to evaluate inhibitors of the cytochrome bc_1 complex (cyt bc_1) as potential single-dose therapies for malaria. Despite the prevailing belief that metabolic inhibitors are limited by their slow onset of action against blood-stage parasites[68], this project identified several compounds as single-dose, rapid-onset antimalarials, including the 4(*1H*)-quinolone, ELQ-400, and the FDA-approved naphthoquinone, atovaquone (ATV). Single dose treatment with ELQ-400 resulted in initial parasite stasis and concomitant changes in cellular morphology that led to rapid clearance in vivo. Although similar kinetics were observed for ATV, ELQ-400 was associated with a lower resistance propensity and greater in vivo efficacy, as reflected by its 1 mg/kg curative dose in the standard Peter's suppressive test and its unique ability to clear acute infections with single doses of 5, 10, or 20 mg/kg.

Mechanistically, my studies have shown that ELQ-400 functions as a dual-site inhibitor of cyt bc_1, with activity at both the Q_o and Q_i catalytic sites. Structure activity relationship (SAR) analysis revealed that several specific chemical features were associated with Q_o vs. Q_i site inhibition in the ELQs; 7-position groups and 5-fluoro substituents were common features of Q_o-targeting compounds, while large aryl side chains and 6-halogens were generally associated with Q_i site inhibition. Although ELQ-400 contains both a Q_o-directing

5,7-difluoro-quinolone core, and a Q_i-directing diarylether side chain, the most direct evidence of dual-site inhibition came from cytochrome *b* reduction studies in *Paracoccus denitrificans*. Like the canonical Q_i site inhibitor antimycin A, incubation of cyt bc_1 with ELQ-400 resulted in substantial electron accumulation on cytochrome *b*. While this finding suggests that ELQ-400 effectively inhibits the Q_i site, it was also notable that the combination of ELQ-400 and antimycin A effectively blocked cytochrome *b* reduction, demonstrating that ELQ-400 also has secondary activity at the alternate, Q_o site.

Like ELQ-400, combination therapies designed to inhibit both the Q_o and Q_i catalytic sites were highly effective single dose, blood-stage treatments with a rapid onset of action and a low resistance propensity. In the case of ATV and ELQ-300, which inhibit the Q_o and Q_i sites, respectively, a 3:1 ATV:ELQ-300 formulation mimicked the in vivo behavior of ELQ-400 in murine suppressive models and effectively cured mice at a single dose of 1 mg/kg. Although ATV:ELQ-300 combination therapy was less effective than ELQ-400 in acute treatment tests, this co-formulation did delay recrudescence and combined the most desirable features of ELQ-300 and ATV monotherapy, including rapid onset of action, low resistance propensity, and the cumulative effect of multi-day dosing.

CHAPTER SIX: SUMMARY AND CONCLUSIONS

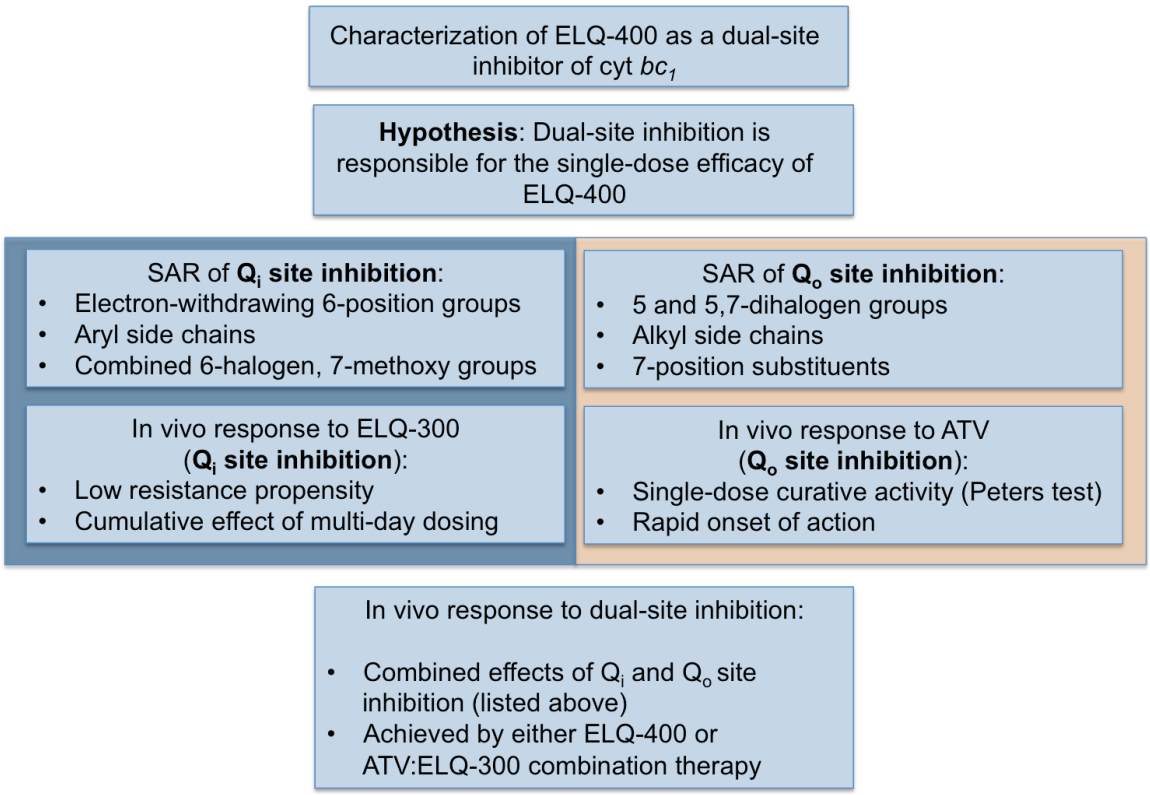

Figure 32: Summary of major experimental results.

Potential for Clinical Development

With the success of both ELQ-400 and ATV:ELQ-300 therapy in murine models, it possible that one or both of these formulations may be useful for the eventual treatment of human patients. In the case of ELQ-400, the major barrier for clinical development is its limited selectivity for *Plasmodium* cyt bc_1. Although I have demonstrated that 6-position variation is a potential strategy for decreasing inhibition of human cyt bc_1, these modifications were associated with an

undesirable loss of potency in both ELQ-404 and ELQ-428. Ultimately, this decreased activity, coupled with the limited solubility of the 4(*1H*)-quinolones, makes ELQ-404 and ELQ-428 unlikely candidates for clinical development. Therefore, the best option for ELQ-400 may be to comprehensively assess toxicity in additional whole-cell and animal models or to directly examine cellular pathways (e.g. efflux systems) that may play a role in human cell protection from ELQ-400.

In the short term, it may be more clinically feasible to develop ATV:ELQ-300 combination therapy for use in patients. Currently, ELQ-300 is in pre-clinical status and has undergone both toxicity and pharmacokinetic evaluation in a number of animal models. More importantly, ELQ-300 fails to inhibit HEK-derived cyt bc_1 and is not associated with the general selectivity concerns surrounding ELQ-400. Although ATV is a potent inhibitor of human cyt bc_1, this compound is FDA approved and clinically well-tolerated[59], suggesting that host toxicity would not be a major concern regarding ATV:ELQ-300 therapy.

Major Implications

In addition to identifying two possible approaches for single-dose, multi-stage antimalarial therapy, my work has highlighted several key features of cyt bc_1 inhibition that may significantly impact the field of antimalarial drug development:

CHAPTER SIX: SUMMARY AND CONCLUSIONS

- **Rapid onset of action**: In contrast to previously published in vitro studies, which classify cyt *bc$_1$* inhibitors as slow-onset antimalarials, I have shown that both ELQ-400 and ATV rapidly reduce parasitemia in mouse models. Because onset of action is a major concern for acute antimalarial therapy[39], this finding may extend the clinical utility of cyt *bc$_1$* inhibitors, especially in the developing world.

- **Weekly dosing potential**: In my acute treatment model, single doses of ATV, ELQ-300, ELQ-400, and various combination therapies all effectively reduced parasite burden and prevented recrudescence for at least one week following treatment. This timing suggests that cyt *bc$_1$* inhibitors may be ideally suited for reduced, weekly dosing schedules, which would significantly lower the associated cost of drug therapy.

- **Q_o inhibitors as single-dose therapies**: Although ATV:ELQ-300 combination therapy was an effective single-dose treatment in murine suppressive models, only ATV and ELQ-400 were capable of producing single dose cures when administered as monotherapy. Because both of these compounds have known activity at the Q_o site of cyt *bc$_1$*, it is possible that inhibition of this site is important for the rapid, single-dose effect exhibited by ATV and ELQ-400. If verified, this theory could have

striking implications for the ongoing development of cyt bc_1 inhibitors, and may encourage the re-evaluation of compounds that have previously been discarded due to Tm90-C2B cross-resistance.

- **Q_i inhibitors as potential multi-target therapies**: Unlike ATV, I found that the Q_i-targeting compound, ELQ-300, demonstrated a low propensity for drug resistance and exhibited unanticipated inhibition of the secondary target, dihydroorotate dehydrogenase (DHODH). Although it is unknown if this effect is broadly generalizable to Q_i site inhibitors, there is expected homology between ubiquinone binding sites on various mitochondrial proteins. Thus, it is possible that ELQ-300 (and other Q_i site inhibitors) have numerous sites of action, which may be relevant to the survival of *P. falciparum* and the treatment of malaria.

Priorities for Future Research

Although my work has expanded the arsenal of single-dose antimalarial therapies and provided preliminary insight into the roles of Q_o vs. Q_i site inhibition in *Plasmodium*, this field extends well beyond the scope of the ELQs. In order to make meaningful generalizations about the site-specific effects of cyt bc_1 inhibition, it will ultimately be necessary to evaluate other anti-respiratory compounds, including pyridones, acridones, and non-ELQ quinolones. However,

the challenge of identifying Q_i site inhibitors is nontrivial; as discussed previously, the D1 *P. falciparum* clone is not cross-resistant against all Q_i-targeting compounds, and cytochrome *b* reduction is only a useful tool for antimalarials with appreciable activity against either bacterial or yeast cyt bc_1.

For these reasons, one of the greatest contributions to this field of research would be the discovery of a high-throughput screening tool, such as a highly resistant Q_i site mutant akin to Tm90-C2B. Alternately, there may be great benefit in genetically modifying *Paracoccus*, *Rhodobacter, or Saccharomyces* model systems to create a Q_i mutant version of cyt bc_1 that closely mimics the drug sensitivity of *Plasmodium.*

Regardless of the approach, it will ultimately be necessary to identify common features of Q_i vs. Q_o site inhibition in vivo, and determine if dual-site targeting is broadly associated with increased potency, single-dose efficacy, and protection against drug resistance. In the short term, this information would support the process of drug development and aid in the identification of an optimal single-dose, antimalarial therapy. In the long term, we may gain greater insight into the full function of the *Plasmodium* mitochondrion, which may ultimately be applicable to other parasitic diseases or additional inhibitor families.

CHAPTER SIX: SUMMARY AND CONCLUSIONS

In conclusion, ELQ-400 and ATV:ELQ-300 combination therapy remain the first examples of multi-stage, single-dose treatments for malaria, and provide a powerful foundation for the optimization of single-dose, cyt bc_1 inhibitors.

REFERENCES

1. Fukuda, M.M., Klein, T.A., Kochel, T., Quandelacy, T.M., Smith, B.L., Villinski, J., Bethell, D., Tyner, S., Se, Y., Lon, C., Saunders, D., Johnson, J., Wagar, E., Walsh, D., Kasper, M., Sanchez, J.L., Witt, C.J., Cheng, Q., Waters, N., Shrestha, S.K., Pavlin, J.A., Lescano, A.G., Graf, P.C., Richardson, J.H., Durand, S., Rogers, W.O., Blazes, D.L., Russell, K.L., Akala, H., Gaydos, J.C., DeFraites, R.F., Gosi, P., Timmermans, A., Yasuda, C., Brice, G., Eyase, F., Kronmann, K., Sebeny, P., Gibbons, R., Jarman, R., Waitumbi, J., Schnabel, D., Richards, A. & Shanks, D. Malaria and other vector-borne infection surveillance in the U.S. Department of Defense Armed Forces Health Surveillance Center-Global Emerging Infections Surveillance program: review of 2009 accomplishments. *BMC public health* **11 Suppl 2**, S9 (2011).
2. Klein, E.Y. Antimalarial drug resistance: a review of the biology and strategies to delay emergence and spread. *International journal of antimicrobial agents* **41**, 311-317 (2013).
3. Miller, L.H, Baruch, D.I., Marsh, K., & Doumbo, O.K. The Pathogenic Basis of Malaria. *Nature* **415**, 673-679 (2002).
4. Antinori, S., Galimberti, L., Milazzo, L. & Corbellino, M. Biology of human malaria plasmodia including Plasmodium knowlesi. *Mediterranean journal of hematology and infectious diseases* **4**, e2012013 (2012).

REFERENCES

5. Menard, R. The journey of the malaria sporozoite through its hosts: two parasite proteins lead the way. *Microbes and Infection* **2**, 633-642 (2000).
6. Lew, V.L. Malaria: endless fascination with merozoite release. *Current biology : CB* **15**, R760-761 (2005).
7. Michalakis Y. & Renaud, F. Malaria: Evolution in vector control. *Nature* **462**, 298-300 (2009).
8. Liu Z, Miao, J., & Cui L. Gametocytogenesis in malaria parasite: commitment, development, and regulation. *Future Microbiology* **6**, 1351-1369 (2011).
9. Laishram, D.D., Sutton, P.L., Nanda, N., Sharma, V.L., Sobti, R.C., Carlton, J.M. & Joshi, H. The complexities of malaria disease manifestations with a focus on asymptomatic malaria. *Malaria journal* **11**, 29 (2012).
10. Oakley, M.S., Gerald, N., McCutchan, T.F., Aravind, L. & Kumar, S. Clinical and molecular aspects of malaria fever. *Trends in parasitology* **27**, 442-449 (2011).
11. Ralph, S.A. & Scherf, A. The epigenetic control of antigenic variation in Plasmodium falciparum. *Current opinion in microbiology* **8**, 434-440 (2005).
12. Flick, K. & Chen, Q. var genes, PfEMP1 and the human host. *Molecular and Biochemical Parasitology* **134**, 3-9 (2004).

REFERENCES

13. Trampuz, A., Jereb, M., Muzlovic, I. & Prabhu, R.M. Clinical review: Severe malaria. *Crit Care* **7**, 315-323 (2003).
14. Idro R., Marsh, K., John CC, & Newton CR. Cerebral malaria: mechanisms of brain injury and strategies for improved neurocognitive outcome. *Pediatric Research* **68**, 267-274 (2010).
15. Rowe, J.A. & Kyes, S.A. The role of Plasmodium falciparum var genes in malaria in pregnancy. *Molecular microbiology* **53**, 1011-1019 (2004).
16. Price R.N., Douglas, N.M., & Anstey NM. New Developments in Plasmodium vivax malaria: severe disease and the rise of chloroquine resistance. *Current Opinions in Infectious Disease* **22**, 430-435 (2009).
17. Galinski, M.R. & Barnwell, J.W. Plasmodium vivax: who cares? *Malaria journal* **7 Suppl 1**, S9 (2008).
18. Anstey, N.M., Russell, B., Yeo, T.W. & Price, R.N. The pathophysiology of vivax malaria. *Trends in parasitology* **25**, 220-227 (2009).
19. Ganesan, S., Chaurasiya, N.D., Sahu, R., Walker, L.A. & Tekwani, B.L. Understanding the mechanisms for metabolism-linked hemolytic toxicity of primaquine against glucose 6-phosphate dehydrogenase deficient human erythrocytes: evaluation of eryptotic pathway. *Toxicology* **294**, 54-60 (2012).
20. World Health Organization. *Roll Back Malaria Initiative* (Online). http://www.rbm.who/int (2014).

REFERENCES

21. Autino, B., Noris, A., Russo, R. & Castelli, F. Epidemiology of malaria in endemic areas. *Mediterranean journal of hematology and infectious diseases* **4**, e2012060 (2012).

22. Feachem R.G.A., Phillips, A.A., Hwang J., Cotter C., Wielgosz B., Greenwood B.M., Sabot O., Rodriguez M.H., Abeyasinghe R.R., Ghebreyesus T.A., & Show R.W. Shrinking the malaria map: progress and prospects. *Lancet* **376**, 1566-1578 (2010).

23. Zimmerman, P.A., Ferreira, M.U., Howes, R.E. & Mercereau-Puijalon, O. Red blood cell polymorphism and susceptibility to Plasmodium vivax. *Advances in parasitology* **81**, 27-76 (2013).

24. Allison, A.C. Genetic control of resistance to human malaria. *Current opinion in immunology* **21**, 499-505 (2009).

25. Najera, J.A., Gonzalez-Silva, M., & Alonso P.L. Some lessons for the future from the Global Malaria Eradication Programme (1955-1969). *PLoS medicine* **8** (2011).

26. Foley, M. & Tilley, L. Quinoline antimalarials: mechanisms of action and resistance and prospects for new agents. *Pharmacol. Ther* **79**, 55-87 (1998).

27. Nosten, F. & White, N.J. Artemisinin-based combination treatment of Falciparum malaria. *American Journal of Tropical Medicine and Hygeine* **77**, 181-192 (2007).

REFERENCES

28. Golenser, J., Waknine, J.H., Krugliak, M., Hunt, N.H. & Grau, G.E. Current perspectives on the mechanism of action of artemisinins. *International journal for parasitology* **36**, 1427-1441 (2006).

29. Hess, K.M., Goad, J.A., & Arguin, P.M. Intravenous artesunate for the treatment of severe malaria. *Ann Phamacother* **44**, 1250-1258 (2010).

30. Delves, M., Plouffe, D., Scheurer, C., Meister, S., Wittlin, S., Winzeler, E.A., Sinden, R.E. & Leroy, D. The activities of current antimalarial drugs on the life cycle stages of Plasmodium: a comparative study with human and rodent parasites. *PLoS medicine* **9**, e1001169 (2012).

31. Breman, J.G. Resistance to artemisinin-based combination therapy. *The Lancet* **12**, 820-822 (2012).

32. Derbyshire, E.R., Prudencio, M., Mota, M.M. & Clardy, J. Liver-stage malaria parasites vulnerable to diverse chemical scaffolds. *Proceedings of the National Academy of Sciences of the United States of America* **109**, 8511-8516 (2012).

33. Nixon, G.L., Moss, D.M., Shone, A.E., Lalloo, D.G., Fisher, N., O'Neill, P.M., Ward, S.A. & Biagini, G.A. Antimalarial pharmacology and therapeutics of atovaquone. *The Journal of antimicrobial chemotherapy* **68**, 977-985 (2013).

34. Ridley, R.G. Medical need, scientific opportunity and the drive for antimalarial drugs. *Nature* **415** (2002).

REFERENCES

35. Greenwood, B.M., Fidock, D.A., Kyle, D.E., Kappe, S.H., Alonso, P.L., Collins, F.H. & Duffy, P.E. Malaria: progress, perils, and prospects for eradication. *The Journal of clinical investigation* **118**, 1266-1276 (2008).

36. Sachs, J. & Malaney, P. The economic and social burden of malaria. *Nature* **415**(2002).

37. Abu-Raddad, L.J., Patnaik, P. & Kublin, J.G. Dual infection with HIV and malaria fuels the spread of both diseases in sub-Saharan Africa. *Science* **314**, 1603-1606 (2006).

38. Purdy, M., Robinson, M., Wei, K. & Rublin, D. The economic case for combating malaria. *The American journal of tropical medicine and hygiene* **89**, 819-823 (2013).

39. Burrows, J.N., van Huijsduijnen, R.H., Mohrle, J.J., Oeuvray, C. & Wells, T.N. Designing the next generation of medicines for malaria control and eradication. *Malaria journal* **12**, 187 (2013).

40. Anthony, M.P,, Burrows, J. N., Duparc, S., JMoehrle, J., & Wells, T.N.C. The global pipeline of new medicines for the control and elimination of malaria. *Malaria journal* **11**(2012).

41. Yeung, S. & White, N.J. How do patients use antimalarial drugs? A review of the evidence. *Tropical Medicine and International Health* **10**, 121-138 (2005).

REFERENCES

42. Charman, S.A., Arbe-Barnes, S., Bathurst, I.C., Brun, R., Campbell, M., Charman, W.N., Chiu, F.C.K., Chollet, J., Craft, J.C., Creek, D.J., Dong, Y., Matile, H., Maurer, M., Morizzi, J., Nguyen, T., Papastogiannidis, P., Scheurer, C., Shackleford, D.M., Sriraghavan, K., Stingelin, L., Tang, Y., Urwyler, H., Wang, X., White, K.L., Wittlin, S., Zhou, L., & Vennerstron, J.L. Synthetic oxonide drug candidate OZ439 offers new hope for a single-dose cure for uncomplicated malaria. *PNAS* **108**, 4400-4405 (2011).

43. Younis, Y., Douelle, F., Feng, T.S., Gonzalez Cabrera, D., Le Manach, C., Nchinda, A.T., Duffy, S., White, K.L., Shackleford, D.M., Morizzi, J., Mannila, J., Katneni, K., Bhamidipati, R., Zabiulla, K.M., Joseph, J.T., Bashyam, S., Waterson, D., Witty, M.J., Hardick, D., Wittlin, S., Avery, V., Charman, S.A. & Chibale, K. 3,5-Diaryl-2-aminopyridines as a novel class of orally active antimalarials demonstrating single dose cure in mice and clinical candidate potential. *Journal of medicinal chemistry* **55**, 3479-3487 (2012).

44. van Pelt-Koops, J.C., Pett, H.E., Graumans, W., van der Vegte-Bolmer, M., van Gemert, G.J., Rottmann, M., Yeung, B.K., Diagana, T.T. & Sauerwein, R.W. The spiroindolone drug candidate NITD609 potently inhibits gametocytogenesis and blocks Plasmodium falciparum transmission to anopheles mosquito vector. *Antimicrobial agents and chemotherapy* **56**, 3544-3548 (2012).

REFERENCES

45. Nagle, A., Wu, T., Kuhen, K., Gagaring, K., Borboa, R., Francek, C., Chen, Z., Plouffe, D., Lin, X., Caldwell, C., Ek, J., Skolnik, S., Liu, F., Wang, J., Chang, J., Li, C., Liu, B., Hollenbeck, T., Tuntland, T., Isbell, J., Chuan, T., Alper, P.B., Fischli, C., Brun, R., Lakshminarayana, S.B., Rottmann, M., Diagana, T.T., Winzeler, E.A., Glynne, R., Tully, D.C. & Chatterjee, A.K. Imidazolopiperazines: lead optimization of the second-generation antimalarial agents. *Journal of medicinal chemistry* **55**, 4244-4273 (2012).

46. Wu, T., Nagle, A., Kuhen, K., Gagaring, K., Borboa, R., Francek, C., Chen, Z., Plouffe, D., Goh, A., Lakshminarayana, S.B., Wu, J., Ang, H.Q., Zeng, P., Kang, M.L., Tan, W., Tan, M., Ye, N., Lin, X., Caldwell, C., Ek, J., Skolnik, S., Liu, F., Wang, J., Chang, J., Li, C., Hollenbeck, T., Tuntland, T., Isbell, J., Fischli, C., Brun, R., Rottmann, M., Dartois, V., Keller, T., Diagana, T., Winzeler, E., Glynne, R., Tully, D.C. & Chatterjee, A.K. Imidazolopiperazines: hit to lead optimization of new antimalarial agents. *Journal of medicinal chemistry* **54**, 5116-5130 (2011).

47. Vaidya, A.B. & Mather, M.W. Mitochondrial evolution and functions in malaria parasites. *Annual review of microbiology* **63**, 249-267 (2009).

48. Ganesan, S.M., Morrisey, J.M., Ke, H., Painter, H.J., Laroiya, K., Phillips, M.A., Rathod, P.K., Mather, M.W. & Vaidya, A.B. Yeast dihydroorotate

dehydrogenase as a new selectable marker for Plasmodium falciparum transfection. *Mol Biochem Parasitol* **177**, 29-34 (2011).

49. MacRae, J.I., Dixon, M.W.A, Dearnley, M.K., Chua, H.H., Chambers, J.M., Kenny, S., Bottova, I., Tilley, L., McConville, M.J. Mitochondrial metabolism of sexual and asexual blood stages of the malaria parasite Plasmodium falciparum. *BMC Biology* **11**(2013).

50. van Dooren, G.G., Stimmler, L.M. & McFadden, G.I. Metabolic maps and functions of the Plasmodium mitochondrion. *FEMS microbiology reviews* **30**, 596-630 (2006).

51. Muller, F., Crofts, A.R., & Kramer, D.M. Multiple Q-cycle bypass reactions at the Qo site of the cytochrome bc1 complex. *Biochemistry* **41**, 7866-7874 (2002).

52. Vaidya, A.B., Lashgari, M.S., Pologe, L.G., & Morrisey, J. Structural features of Plasmodium cytochrome b that may underlie susceptibility to 8-aminoquinolines and hydroxynaphthoquinones. *Molecular and Biochemical Parasitology* **58**, 33-42 (1993).

53. Li, H., Zhu, X.L., Yang, W.C. & Yang, G.F. Comparative kinetics of Qi site inhibitors of cytochrome bc1 complex: picomolar antimycin and micromolar cyazofamid. *Chemical biology & drug design* **83**, 71-80 (2014).

54. Hudson, A.T., Dickins, M., Ginger, C.D., Gutteridge, W.E., Holdich, T., Hutchinson, D.B.A., Pudney, M., Randall, A.W., & Latter, V.S. 566C80: A

potent broad spectrum anti-infective agent with activity against malaria and opportunistic infections in AIDS patients. *Drugs Under Experimental and Clinical Research* **17**, 427-435 (1991).

55. Srivastava, I.K., Rottenberg, H. & Vaidya, A.B. Atovaquone, a Broad Spectrum Antiparasitic Drug, Collapses Mitochondrial Membrane Potential in a Malarial Parasite. *Journal of Biological Chemistry* **272**, 3961-3966 (1997).
56. Birth, D., Kao, W.C. & Hunte, C. Structural analysis of atovaquone-inhibited cytochrome bc1 complex reveals the molecular basis of antimalarial drug action. *Nature communications* **5**, 4029 (2014).
57. Fisher, N., Abd Majid, R., Antoine, T., Al-Helal, M., Warman, A.J., Johnson, D.J., Lawrenson, A.S., Ranson, H., O'Neill, P.M., Ward, S.A. & Biagini, G.A. Cytochrome b mutation Y268S conferring atovaquone resistance phenotype in malaria parasite results in reduced parasite bc1 catalytic turnover and protein expression. *The Journal of biological chemistry* **287**, 9731-9741 (2012).
58. Vaidya, A.B. & Mather, M.W. Atovaquone resistance in malaria parasites. *Drug resistance updates : reviews and commentaries in antimicrobial and anticancer chemotherapy* **3**, 283-287 (2000).
59. Cordel, H., Cailhol, J., Matheron, S., Bloch, M., Godineau, N., Consigny, P.H., Gros, H., Campa, P., Bouree, P., Fain, O., Ralaimazava, P. &

REFERENCES

Bouchaud, O. Atovaquone-proguanil in the treatment of imported uncomplicated Plasmodium falciparum malaria: a prospective observational study of 553 cases. *Malaria journal* **12**, 399 (2013).

60. Musset, L., Pradines, B., Parzy, D., Durand, R., Bigot, P. & Le Bras, J. Apparent absence of atovaquone/proguanil resistance in 477 Plasmodium falciparum isolates from untreated French travellers. *The Journal of antimicrobial chemotherapy* **57**, 110-115 (2006).
61. Pimentel, S., Nogueira, F., Benchimol, C., Quinhentos, V., Bom, J., Varandas, L., do Rosario, V. & Bernardino, L. Detection of atovaquone-proguanil resistance conferring mutations in Plasmodium falciparum cytochrome b gene in Luanda, Angola. *Malaria journal* **5**, 30 (2006).
62. Edstein, M.D., Kotecka, B.M., Anderson, K.L., Pombo, D.J., Kyle, D.E., Rieckmann, K.H. & Good, M.F. Lengthy antimalarial activity of atovaquone in human plasma following atovaquone-proguanil administration. *Antimicrobial agents and chemotherapy* **49**, 4421-4422 (2005).
63. Winter, R.W., Kelly, J.X., Smilkstein, M.J., Dodean, R., Hinrichs, D. & Riscoe, M.K. Antimalarial quinolones: synthesis, potency, and mechanistic studies. *Experimental parasitology* **118**, 487-497 (2008).
64. Winter, R., Kelly, J.X., Smilkstein, M.J., Hinrichs, D., Koop, D.R. & Riscoe, M.K. Optimization of endochin-like quinolones for antimalarial activity. *Experimental parasitology* **127**, 545-551 (2011).

REFERENCES

65. Doggett, J.S., Nilsen, A., Forquer, I., Wegmann, K.W., Jones-Brando, L., Yolken, R.H., Bordon, C., Charman, S.A., Katneni, K., Schultz, T., Burrows, J.N., Hinrichs, D.J., Meunier, B., Carruthers, V.B., & Riscoe, M.K. Endochin-like quinolones are highly efficacious against acute latent experimental toxoplasmosis. *PNAS* **109**, 15936-15941 (2012).

66. Nilsen, A., LaCrue, A.N., White, K.L., Forquer, I.P., Cross, R.M., Marfurt, J., Mather, M.W., Delves, M.J., Shackleford, D.M., Saenz, F.E., Morrisey, J.M., Steuten, J., Mutka, T., Li, Y., Wirjanata, G., Ryan, E., Duffy, S., Kelly, J.X., Sebayang, B.F., Zeeman, A.M., Noviyanti, R., Sinden, R.E., Kocken, C.H., Price, R.N., Avery, V.M., Angulo-Barturen, I., Jimenez-Diaz, M.B., Ferrer, S., Herreros, E., Sanz, L.M., Gamo, F.J., Bathurst, I., Burrows, J.N., Siegl, P., Guy, R.K., Winter, R.W., Vaidya, A.B., Charman, S.A., Kyle, D.E., Manetsch, R. & Riscoe, M.K. Quinolone-3-diarylethers: a new class of antimalarial drug. *Science translational medicine* **5**, 177ra137 (2013).

67. Smilkstein, M., Sriwilaijaroen, N., Kelly, J.X., Wilairat, P. & Riscoe, M. Simple and Inexpensive Fluorescence-Based Technique for High-Throughput Antimalarial Drug Screening. *Antimicrobial agents and chemotherapy* **48**, 1803-1806 (2004).

68. Sanz, L.M., Crespo, B., De-Cozar, C., Ding, X.C., Llergo, J.L., Burrows, J.N., Garcia-Bustos, J.F. & Gamo, F.J. P. falciparum in vitro killing rates

allow to discriminate between different antimalarial mode-of-action. *PloS one* **7**, e30949 (2012).

69. Ball, D.E., Tagwireyi, D. & Nhachi, C.F. Chloroquine poisoning in Zimbabwe: a toxicoepidemiological study. *Journal of applied toxicology : JAT* **22**, 311-315 (2002).

70. Ursing, J., Kofoed, P.E., Rodrigues, A., Bergqvist, Y. & Rombo, L. Chloroquine is grossly overdosed and overused but well tolerated in Guinea-bissau. *Antimicrobial agents and chemotherapy* **53**, 180-185 (2009).

71. Muller, J.M., Simonet, A.L., Binois, R., Muggeo, E., Bugnon, P., Liet, J., Duong, M., Chavanet, P. & Piroth, L. The respect of recommendations provided in an international travelers' medical service: far from the cup to the lips. *Journal of travel medicine* **20**, 78-82 (2013).

72. Li, Q., O'Neil, M., Xie, L., Caridha, D., Zeng, Q., Zhang, J., Pybus, B., Hickman, M., & Melendez, V. Assessment of the Prophylactic Activity and Pharmacokinetic Profile of Oral Tafenoquine Compared to Primaquine for Inhibition of Liver Stage Malaria Infections. *Malaria journal* **13** (2014).

73. Davies, C.S., Pudney, M., Matthews, P.J., & Sinden, R.E. The causal prophylactic activity of the novel hydroxynaphthoquinone 566C80 against Plasmodium Berghei infections in rats. *Acta Leidensia* **58**, 115-128 (1989).

REFERENCES

74. Nilsen, A., Miley, G.P., Forquer, I.P., Mather, M.W., Katneni, K., Li, Y., Pou, S., Pershing, A.M., Stickles, A.M., Ryan, E., Kelly, J.X., Doggett, J.S., White, K.L., Hinrichs, D.J., Winter, R.W., Charman, S.A., Zakharov, L.N., Bathurst, I., Burrows, J.N., Vaidya, A.B. & Riscoe, M.K. Discovery, Synthesis, and Optimization of Antimalarial 4(1H)-Quinolone-3-Diarylethers. *Journal of medicinal chemistry* **57**, 3818-3834 (2014).

75. Musset, L., Bouchaud, O., Matheron, S., Massias, L. & Le Bras, J. Clinical atovaquone-proguanil resistance of Plasmodium falciparum associated with cytochrome b codon 268 mutations. *Microbes and infection / Institut Pasteur* **8**, 2599-2604 (2006).

76. Bueno, J.M., Herreros, E., Angulo-Barturen, I., Ferrer, S., Fiandor, J.M., Gamo, F.J., Gargallo-Viola, D., & Derimanov, G. Exploration of 4(1H)-pyridones as a novel family of potent antimalarial inhibitors of the plasmodial cytochrome bc1. *Future Med Chem* **4**, 2311-2323 (2012).

77. Hill, P., Kessl, J., Fisher, N., Meshnick, S., Trumpower, B.L. & Meunier, B. Recapitulation in Saccharomyces cerevisiae of Cytochrome b Mutations Conferring Resistance to Atovaquone in Pneumocystis jiroveci. *Antimicrobial agents and chemotherapy* **47**, 2725-2731 (2003).

78. Barton, V., Fisher, N., Biagini, G.A., Ward, S.A., & O'Neill. P.M. Inhibiting Plasmodium cytochrome bc1: a complex issue. *Current Opinion in Chemical Biology* **14**, 440-446 (2010).

REFERENCES

79. Smilkstein, M.J., Forquer, I., Kanazawa, A., Kelly, J.X., Winter, R.W., Hinrichs, D.J., Kramer, D.M. & Riscoe, M.K. A drug-selected Plasmodium falciparum lacking the need for conventional electron transport. *Mol Biochem Parasitol* **159**, 64-68 (2008).

80. Vallieres, C., Fisher, N., Antoine, T., Al-Helal, M., Stocks, P., Berry, N.G., Lawrenson, A.S., Ward, S.A., O'Neill, P.M., Biagini, G.A. & Meunier, B. HDQ, a potent inhibitor of Plasmodium falciparum proliferation, binds to the quinone reduction site of the cytochrome bc1 complex. *Antimicrobial agents and chemotherapy* **56**, 3739-3747 (2012).

81. Vallieres, C., Fisher, N. & Meunier, B. Reconstructing the Qo site of Plasmodium falciparum bc 1 complex in the yeast enzyme. *PloS one* **8**, e71726 (2013).

82. Wenz, T., Hellwig, P., MacMillan, F., Meunier, B., & Hunte, C.. Probing the role of E272 in quinol oxiation of mitochondrial complex III. *Biochemistry* **45**, 9042-9052 (2006).

83. Zhou, P., Zou, J., Tian, F., & Shang, Z. Fluorine Bonding - How Does it Work in Protein-Ligand Interactions? *Journal of Chemical Information and Modeling* **49**, 2344-2355 (2009).

84. Berry, E.A., Huang, L.S., Lee, D.W., Daldal, F., Nagai, K. & Minagawa, N. Ascochlorin is a novel, specific inhibitor of the mitochondrial cytochrome bc1 complex. *Biochimica et biophysica acta* **1797**, 360-370 (2010).

REFERENCES

85. Looareesuwam, S., Chulaty, J.D., Canfield, C.J., & Hutchinson, D.B.A. Malarone (Atovaquone and Proguanil Hydrochloride): A Review of its Clinical Development for Treatment of Malaria. *The American journal of tropical medicine and hygiene* **60**, 533-541 (1999).

86. Hugger, E.D., Audus, K.L., & Borchardt, R.T. Effects of poly(ethylene glycol) on efflux transporter activity in caco-2 cell monolayers. *Journal of Pharmaceutical Sciences* **91**(2001).

87. Happi, C.T., Gbotosho, G.O., Folarin, O.A., Milner, D., Sarr, O., Sowunmi, A., Kyle, D.E., Milhous, W.K., Wirth, D.F. & Oduola, A.M. Confirmation of emergence of mutations associated with atovaquone-proguanil resistance in unexposed Plasmodium falciparum isolates from Africa. *Malaria journal* **5**, 82 (2006).

88. Deye, G.A., Miller, R.S., Miller, L., Salas, C.J., Tosh, D., Macareo, L., Smith, B.L., Fracisco, S., Clemens, E.G., Murphy, J., Sousa, J.C., Dumler, J.S. & Magill, A.J. Prolonged protection provided by a single dose of atovaquone-proguanil for the chemoprophylaxis of Plasmodium falciparum malaria in a human challenge model. *Clinical infectious diseases : an official publication of the Infectious Diseases Society of America* **54**, 232-239 (2012).

APPENDIX A:
EXOERYTHROCYTIC ACTIVITY OF ELQ-400

In order to determine if ELQ-400 functioned as a single-dose prophylactic and transmission-blocking agent, collaborators at Albert Einstein College of Medicine tested this compound in a range of exoerythrocytic assays.

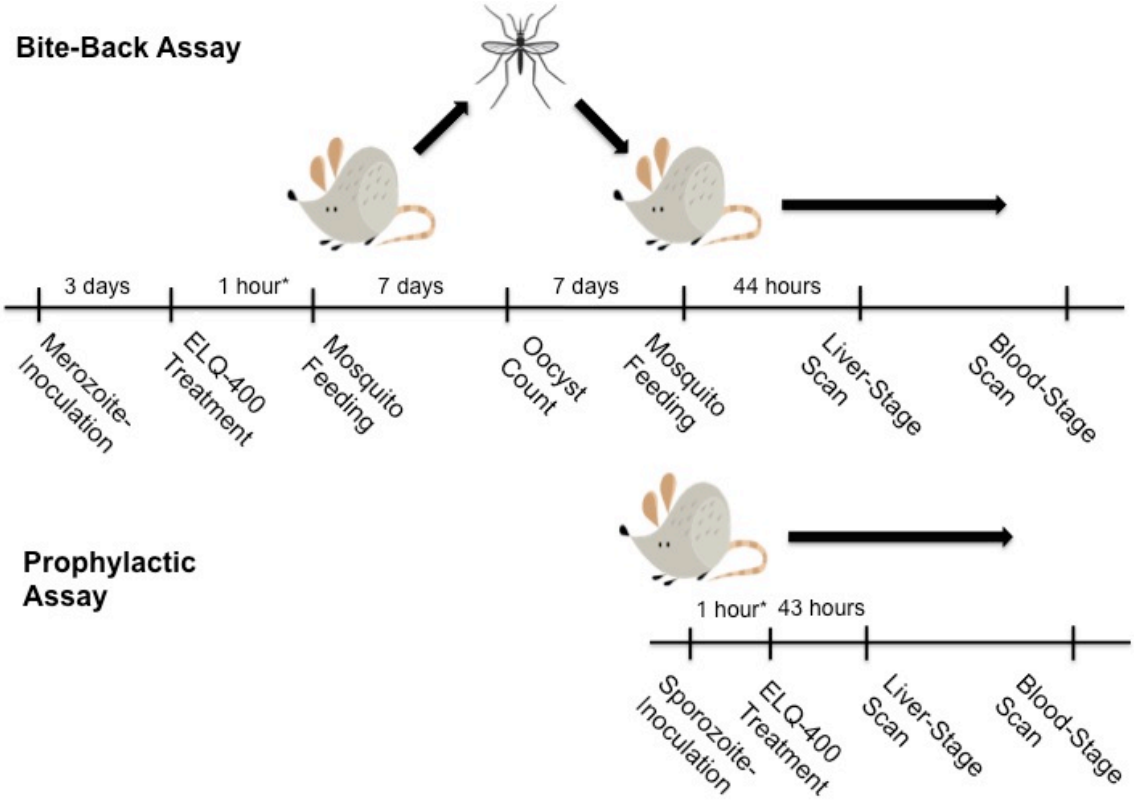

Figure 33: Schematic of prophylactic and transmission-blocking assays

ELQ-400 was first tested in a causal prophylaxis assay, which evaluated its ability to block the establishment of liver-stage infection by firefly luciferase-expressing *P. yoelii* (*Py*Luc) sporozoites. A single dose of ELQ-400 administered

APPENDIX A

1 hour following sporozoite inoculation completely prevented the development of both liver and blood-stage infections at oral doses as low as 0.08 mg/kg. Addition of a second treatment 24 hours later further enhanced ELQ-400's efficacy, and complete prophylaxis was achieved at individual doses of 0.016 mg/kg (Figure 34).

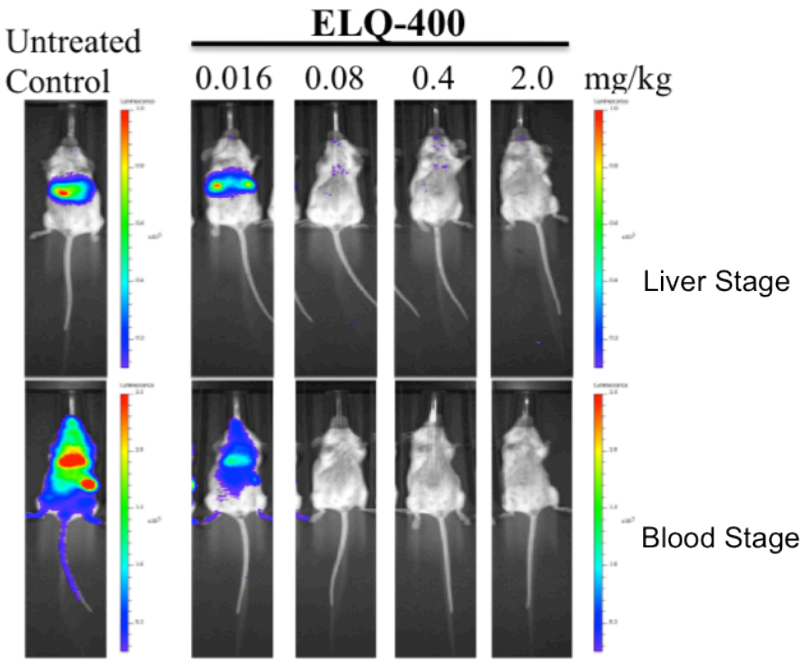

Figure 34: Whole-animal bioluminescence of animals infected with *Py*Luc sporozoites and treated with single oral doses ELQ-400 1 hour post-inoculation (Prophylactic assay). A single oral dose of 0.08 mg/kg ELQ-400 fully blocked the establishment of both liver and blood-stage infections.

ELQ-400 was also highly effective at blocking disease transmission by mosquitoes. In this assay, ELQ-400 was administered to mice with established

blood-stage *Py*Luc infections, and mosquitoes were allowed to feed on infected mice either one hour or 24 hours post-treatment. Malaria transmission was then measured by determining oocyst number in the midgut of dissected mosquitoes (Figure 35), and by assessing the ability of fed mosquitoes to initiate infections in untreated, immunologically naïve mice (Figure 36). A single 0.1 mg/kg dose of ELQ-400 was sufficient to fully inhibit both oocyst formation and transmission to naïve mice, whether administered 1 hour or 24 hours prior to mosquito feeding.

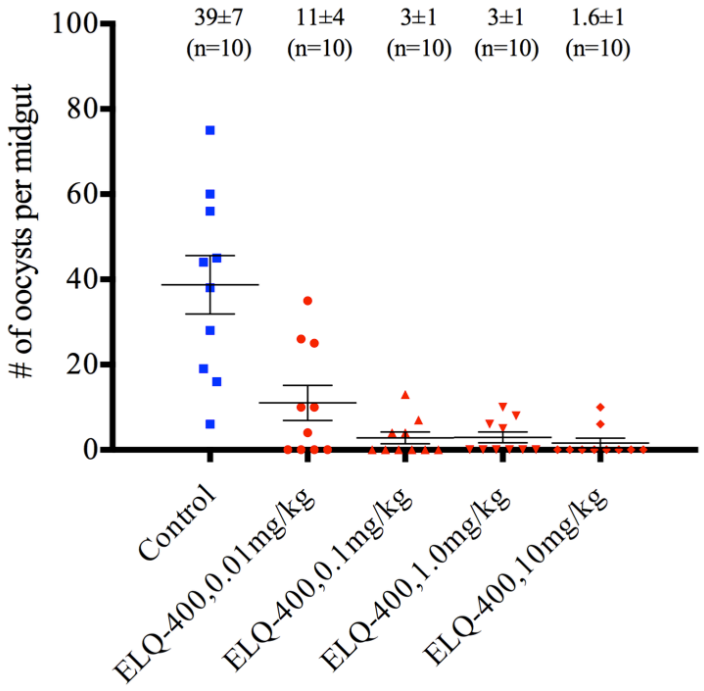

Figure 35: Oocyst counts from mosquitos fed on blood-stage, *Py*Luc-infected mice 1 hour following ELQ-400 treatment (bite-back assay). A single oral dose of 0.1 mg/kg ELQ-400 maximally suppressed oocyst development.

APPENDIX A

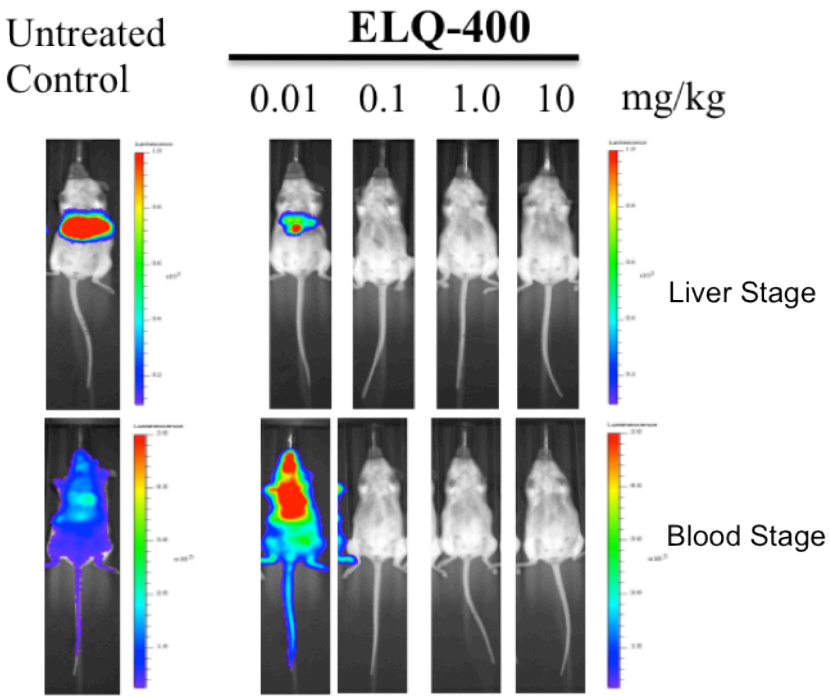

Figure 36: Whole-animal bioluminescence of mice in the bite-back assay. All animals were exposed to mosquitoes that had previously fed on *Py*Luc-infected mice one hour after treatment with ELQ-400. As in figure 35, a single dose of 0.1 mg/kg ELQ-400 was fully effective at blocking parasite transmission and prevented the development of both liver and blood-stage infections in mosquito-exposed, naïve mice.

APPENDIX B:
IN VITRO RESISTANCE PROPENSITY OF ELQ-400

Resistance propensity of ELQ-400 was assessed by collaborators at Drexel University. This was done by maintaining hypermutable Dd2 *P. falciparum* parasites under drug pressure and monitoring parasite outgrowth. In this model, atovaquone-resistant parasites developed from an initial population of 10^8 parasites within 16 days of 10nM drug pressure, yet ELQ-400 resistance required a higher parasite load (10^9 parasites), a higher concentration of drug (100nM), and an extended period of time (47 days) to develop (Table 12). More importantly, although the V259L mutation that confers ELQ-400 resistance also mapped to the cyt bc_1 Q_o site (Figure 37), mutant parasites were only 10-fold less sensitive to both ELQ-400 and atovaquone (Table 13).

Treatment	Initial Parasite Count	Days to Parasite Emergence
10 nM atovaquone	10^8	16
10 nM atovaquone	10^8	23
10 nM atovaquone	10^8	26
100 nM ELQ400	10^9	47
100 nM ELQ400	10^8	--
100 nM ELQ400	10^8	--
100 nM ELQ400	10^8	--

Table 12: Comparative resistance propensity of atovaquone and ELQ-400 in Dd2 *P. falciparum* parasites. ELQ-400 required both longer incubation time and a larger initial parasite population for resistance to develop as compared to atovaquone.

APPENDIX B

```
Query  241  SHPDNAIVVNTYVTPSQIVPEWYFLPFYAMLKTVPSKPAGLVIVLLSLQLLFLLAEQRSL  300
            SHPDNAIVVNTYVTPSQI+PEWYFLPFYAMLKTVPSKPAGLVIVLLSLQLLFLLAEQRSL
Sbjct  241  SHPDNAIVVNTYVTPSQILPEWYFLPFYAMLKTVPSKPAGLVIVLLSLQLLFLLAEQRSL  300
```

Figure 37: Sequence alignment of Dd2 and ELQ-400 resistant *P. falciparum* parasites. Highlighting indicates the V259L substitution associated with ELQ-400 resistance. This residue was located near the PEWY loop that defines the cyt bc_1 Q_o site.

Compound	IC_{50} (nM)	
	Dd2	ELQ-400 R
ELQ-400	4.8	52
ELQ-300	8.5	7.9
Atovaquone	0.9	11.2

Table 13: IC_{50} values (nM) of ELQ-400, ELQ-300, and atovaquone against the V259L *P. falciparum* mutant and Dd2 parental strain. ELQ-400-resistant parasites were only 10-fold less sensitive to ELQ-400 and atovaquone than the parental strain, and were fully sensitive to ELQ-300. Values were determined by the Vaidya lab, using a 48-hour [^{3}H]hypoxanthine incorporation method.

APPENDIX C:
DEVELOPMENT OF THE ELQ-300-RESISTANT D1 CLONE

To generate the D1 clone, our collaborators at Columbia University cultured hypermutable Dd2 *P. falciparum* parasites in the presence of low, 25nM concentrations of ELQ-300 (approximately 4x the 50% inhibitory concentration, IC_{50}). They monitored parasitemia daily, and gradually increased ELQ-300 concentration until parasite growth was fully inhibited and parasitemia dropped below the limit of detection. After two weeks at this final concentration of 70nM, parasites were detected and the clonally isolated.

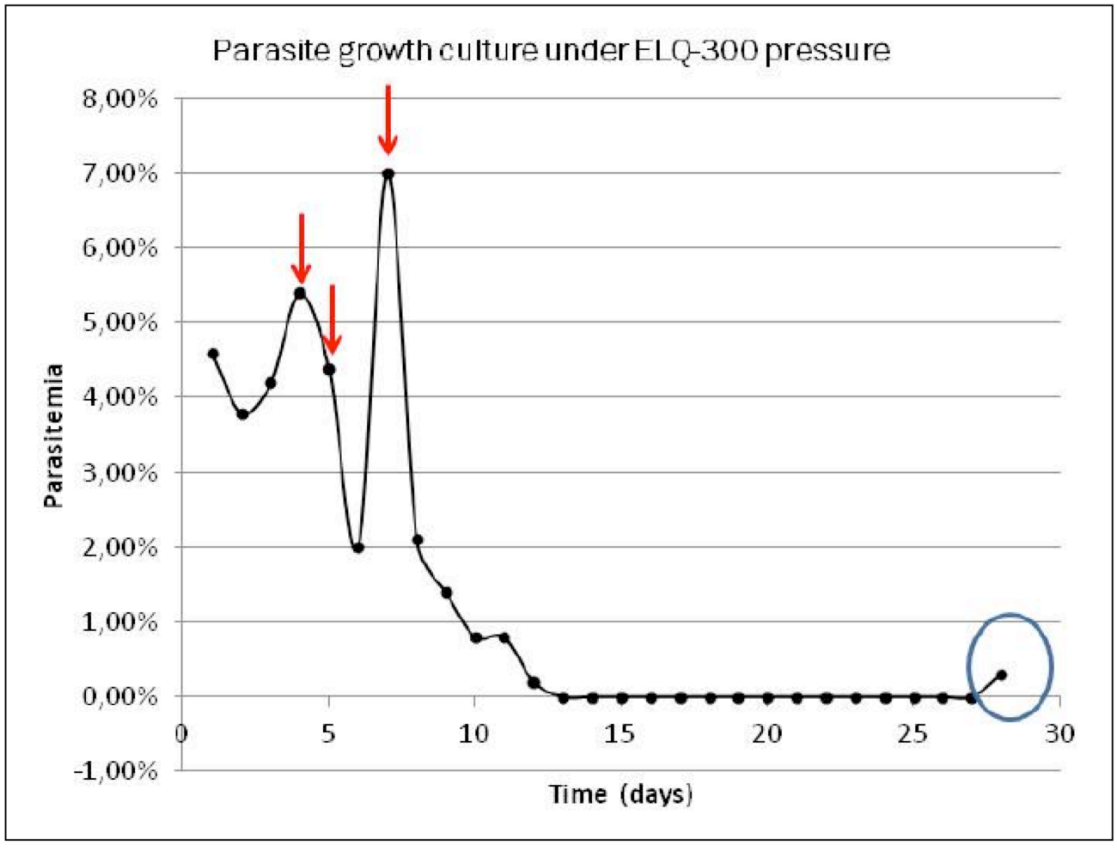

Figure 38: Generation of the ELQ-300-resistant, D1 *P. falciparum* clone. Arrows indicate gradual increases in ELQ-300 pressure to a final concentration of 70nM.

APPENDIX D:
H-NMR SPECTRA OF RELEVANT ELQ COMPOUNDS

ELQ-100: ^{1}H NMR (400 MHz, DMSO-d_6): δ 11.16 (s, 1H), 7.93 (d, *J* = 9.6 Hz, 1H), 6.84-6.81 (m, 2H), 3.83 (s, 3H), 2.45-2.41 (m, 2H), 2.33 (s, 3H), 1.38-1.24 (m, 10H), 0.87-0.84 (m, 3H).

ELQ-109: ^{1}H NMR (400 MHz, DMSO-d_6) δ 11.42 (s, 1H), 8.04 (d, *J* = 8.7 Hz, 1H), 7.49 (d, *J* = 2.0 Hz, 1H), 7.25 (dd, *J* = 8.7, 2.0 Hz, 1H), 2.49-2.44 (m, 2H), 2.38 (s, 3H), 1.41-1.25 (m, 10H), 0.88-0.84 (m, 3H).

ELQ-110: ^{1}H NMR (400 MHz, DMSO-d_6) δ 11.86 (s, 1H), 8.36 (d, *J* = 2.2 Hz, 1H), 8.26 (d, *J* = 8.9 Hz, 1H), 7.99 (dd, *J* = 8.9, 2.2 Hz, 1H), 2.50-2.49 (m, 2H), 2.44 (s, 3H), 1.43-1.25 (m, 10H), 0.88-0.85 (m, 3H).

ELQ-118: ^{1}H NMR (400 MHz, DMSO-d_6) δ 8.17 (d, *J* = 7.94 Hz, 1H), 7.89 (d, *J* = 1.22 Hz, 1H), 7.57 (dd, *J* = 7.94, 1.22 Hz, 1H), 2.48 (t), 2.47 (s, 3H), 1.2-1.4 (m, 10H), 0.85 (t, *J* =6.7 Hz, 3H).

ELQ-120: ^{1}H NMR (400 MHz, DMSO-d_6) δ 11.4 (s, 1H), 8.08 (dd, *J* = 8.5, 6.1 Hz, 1H), 7.17 (dd, *J* = 2.44, 10.37 Hz, 1H), 7.08 (ddd *J* = 8.5, 8.5, 2.44 Hz, 1H), 2.36 (s, 1H), 2.45 (t, 2H), 1.2-1.4 (m, 10H), 0.85 (t, *J* = 2.3 Hz, 3H).

APPENDIX D

ELQ-121: ^{1}H NMR (400 MHz, DMSO-d_6): 11.4 (bs, 0.85H), 7.0 (ddd, *J* = 10.0, 2.5, 1.4 Hz, 2H), 6.95 (ddd, *J* = *12.0, 10.0, 2.5 Hz,* 1H), 2.41 (dist. t, 2H), 2.33 (s, 3H), 1.2–1.4 (m, 10H), 0.87 (t, *J* = 6.8 Hz, 3H).

ELQ-124: ^{1}H NMR (400 MHz, DMSO-d_6): *δ* 11.42 (s, 1H), 7.44 (d, *J* = 2.1 Hz, 1H), 7.27 (d, *J* = 2.0 Hz, 1H), 2.42-2.39 (m, 2H), 2.33 (s, 3H), 1.39-1.23 (m, 10H), 0.88-0.85 (m, 3H).

ELQ-130: ^{1}H NMR (400 MHz, DMSO-d_6): *δ* 11.54 (s, 1H), 7.97 (d, *J* = 2.4 Hz, 1H), 7.60 (dd, *J* = 8.8, 2.5 Hz, 1H), 7.50 (d, *J* = 8.8 Hz, 1H), 2.38 (s, 3H), 2.48 (dist. t, 2H), 1.17–1.45 (m, 10H), 0.86 (t, *J* = 6.9 Hz, 3H).

ELQ-131: ^{1}H NMR (400 MHz, DMSO-d_6): *δ* 11.52 (s, 1H), 7.67 (dd, *J* = 9.5, 3.2 Hz, 1H), 7.55-7.45 (m, 2H), 2.49-2.45 (m, 2H), 2.38 (s, 3H), 1.40-1.24 (m, 10H), 0.88-0.84 (m, 3H).

ELQ-133: ^{1}H NMR (400 MHz, DMSO-d_6): *δ* 11.39 (s, 1H), 7.85 (d, *J* = 2.2 Hz, 1H), 7.49 (dd, *J* = 8.8, 2.2 Hz, 1H), 7.42 (d, *J* = 8.6Hz, 1H), 2.51 (s, 3H), 2.49-2.45 (m, 2H), 2.37 (s, 3H), 1.42-1.22 (m, 10H), 0.88-0.84 (m, 3H).

APPENDIX D

ELQ-136: ^{1}H NMR (400 MHz, DMSO-d_6): δ 11.38 (s, 1H), 7.50 (td, J = 8.2, 5.3 Hz, 1H), 7.25 (d, J = 8.4 Hz, 1H), 6.88 (ddd, J = 12.1, 8.0, 0.8 Hz, 1H), 3.18 (s, 1H), 2.45-2.40 (m, 2H), 2.35 (s, 3H), 1.40-1.23 (m, 10H), 0.88-0.85 (m, 3H).

ELQ-140: ^{1}H NMR (400 MHz, DMSO-d_6): δ 11.53 (s, 1H), 7.22 (ddd, J = 11.4, 6.3, 1.8 Hz, 1H), 2.44-2.39 (m, 2H), 2.34 (s, 3H), 1.39-1.23 (m, 10H), 0.88-0.85 (m, 3H).

ELQ-141: ^{1}H NMR (400 MHz, DMSO-d_6): δ 11.60 (s, 1H), 7.25-7.18 (m, 4H), 7.15-7.11 (m, 1H), 7.06-6.98 (m, 2H), 2.83 (s, 2H), 2.31 (s, 3H).

ELQ-150: ^{1}H NMR (400 MHz, DMSO-d_6): δ 11.33 (s, 1H), 7.46 (d, J = 2.9 Hz, 1H), 7.42 (d, J = 9.0 Hz, 1H), 7.21 (dd, J = 9.0, 2.9 Hz, 1H), 3.81 (s, 3H), 2.50-2.46 (m, 2H), 2.37 (s, 3H), 1.41-1.24 (m, 10H), 0.88-0.84 (m, 3H).

ELQ-162: ^{1}H NMR (400 MHz, DMSO-d_6): δ 11.92 (s, 1H), 8.83 (d, J = 2.7 Hz, 1H), 8.26 (dd, J = 9.2, 2.7 Hz, 1H), 7.64 (d, J = 9.2 Hz, 1H), 2.50-2.48 (m, 2H), 2.42 (s, 3H), 1.44-1.23 (m, 10H), 0.88-0.85 (m, 3H).

APPENDIX D

ELQ-200: ^{1}H NMR (400 MHz, DMSO-d_6): δ 11.54 (s. 1H), 7.97 (d, *J* = 2.3 Hz, 1H), 7.60 (dd, *J* = 8.8, 2.3 Hz, 1H), 7.50 (d, *J* = 8.8 Hz, 1H), 2.50-2.46 (m, 2H), 2.39 (s, 3H), 1.40-1.29 (m, 4H), 0.90 (t, *J* = 6.8 Hz, 3H).

ELQ-220: ^{1}H NMR (400 MHz, DMSO-d_6) δ 11.70 (s, 1H), 8.03 (d, *J* = 2.5 Hz, 1H), 7.64 (dd, *J* = 8.8, 2.5 Hz, 1H), 7.54 (d, *J* = 8.8 Hz, 1H), 7.25-7.19 (m, 4H), 7.15-7.11 (m, 1H), 3.90 (s, 2H), 2.36 (s, 3H).

ELQ-269: ^{1}H NMR (400 MHz, DMSO-d_6): δ 11.87 (s, 1H), 8.04 (d, *J* = 2.5 Hz, 1H), 7.74-7.68 (m, 5H), 7.60 (d, *J* = 9.0 Hz, 1H), 7.50 (tt, *J* = 7.4, 1.7 Hz, 2H), 7.41-7.34 (m, 3H), 2.30 (s, 3H).

ELQ-271: ^{1}H NMR (400 MHz, DMSO-d_6) δ 11.65 (s, 1H), 8.09 (d, *J* = 7.2 Hz, 1H), 7.64 (td, *J* = 7.6, 1.4 Hz, 1H), 7.54 (d, *J* = 8.1 Hz, 1H), 7.42 (d, *J* = 8.5 Hz, 2H), 7.27-7.31 (m, 3H), 7.15-7.18 (m, 2H), 7.07-7.09 (m, 2H), 2.27 (s, 3H).

ELQ-296: ^{1}H NMR (400 MHz, DMSO-d_6) δ 11.85 (s, 1H), 8.00-8.03 (m, 1H), 7.66-7.70 (m, 1H), 7.57-7.61 (m, 1H), 7.39-7.45 (m, 2H), 7.28-7.32 (m, 2H), 7.15-7.20 (m, 2H), 7.06-7.11 (m, 2H), 2.27 (s, 3H).

APPENDIX D

ELQ-298: ^{1}H NMR (400 MHz, DMSO-d_6) δ 11.65 (s, 1H), 8.09 (d, *J* = 7.2 Hz, 1H), 7.64 (td, *J* = 7.6, 1.4 Hz, 1H), 7.54 (d, *J* = 8.1 Hz, 1H), 7.42 (d, *J* = 8.5 Hz, 2H), 7.27-7.31 (m, 3H), 7.15-7.18 (m, 2H), 7.07-7.09 (m, 2H), 2.27 (s, 3H).

ELQ-300: ^{1}H NMR (400 MHz, $CDCl_3$) δ 11.97 (s, 1H), 8.05 (s, 1H), 7.42 (d, *J* = 8.7 Hz, 2H), 7.29 (d, *J* = 8.3 Hz, 2H), 7.17 (d, *J* = 8.3 Hz, 2H), 7.12 (s, 1H), 7.08 (d, *J* = 8.7 Hz, 2H), 3.97 (s, 3H), 2.26 (s, 3H).

ELQ-314: ^{1}H NMR (400 MHz, DMSO-d_6) δ 11.83 (s, 1H), 7.71-7.74 (m, 1H), 7.62 (dd, *J* = 9.1, 4.7 Hz, 1H), 7.56 (td, *J* = 8.6, 3.0 Hz, 1H), 7.42 (d, *J* = 8.5 Hz, 2H), 7.28-7.31 (m, 2H), 7.15-7.19 (m, 2H), 7.06-7.10 (m, 2H), 2.27 (s, 3H).

ELQ-316: ^{1}H NMR (400 MHz, DMSO-d_6) δ 11.78 (s, 1H), 7.69-7.74 (m, 1H), 7.40-7.43 (m, 2H), 7.29 (d, *J* = 8.5 Hz, 2H), 7.15-7.19 (m, 2H), 7.10-7.15 (m, 1H), 7.06-7.09 (m, 2H), 3.96 (s, 3H), 2.25 (s, 3H).

ELQ-317: ^{1}H NMR (400 MHz, DMSO-d_6) δ 11.95 (s, 1H), 8.03 (dd, *J* = 8.9, 2.4 Hz, 2H), 7.80 (dd, *J* = 8.3, 4.1 Hz, 1H), 7.69-7.72 (m, 1H), 7.61 (d, *J* = 8.9 Hz, 1H), 7.42-7.47 (m, 2H), 7.30-7.35 (m, 2H), 7.12-7.16 (m, 1H), 2.29 (s, 3H).

APPENDIX D

ELQ-339: ^{1}H NMR (400 MHz, DMSO-d_6) δ 8.16 (d, *J* = 2.4 Hz, 1H), 7.72 (dd, *J* = 8.8, 2.4 Hz, 1H), 7.59 (d, *J* = 8.8 Hz, 1H), 7.42 (dd, *J* = 9.0, 0.8 Hz, 2H), 7.29 (dt, *J* = 8.7, 2.1 Hz, 2H), 7.16 (dt, *J* = 9.1, 2.4 Hz, 2H), 7.07 (dt, *J* = 8.7, 2.1 Hz, 2H), 2.26 (s, 3H).

ELQ-340: ^{1}H NMR (400 MHz, DMSO-d_6) δ 8.164 (s, 1H), 7.42 (d, *J* = 9.3, 0.9 Hz, 2H), 7.30-7.26 (m, 3H), 7.16 (dt, *J* = 9.2, 2.4 Hz, 2H), 7.06 (dt, *J* = 8.7, 2.2 Hz, 2H), 3.93 (s, 3H), 1.65 (s, 3H).

ELQ-400: ^{1}H NMR (400 MHz, DMSO-d_6) δ 7.40 (d, *J* = 8.7 Hz, 2H), 7.25 (d, *J* = 8.5 Hz, 2H), 7.20-6.92 (m, 6H), 2.19 (s, 3H).

ELQ-404: ^{1}H NMR (400 MHz, DMSO-d_6): *δ* 11.83 (s, 1H), 7.43 (d, *J* = 8.9 Hz, 2H), 7.34-7.30 (m, 1H), 7.27 (dt, *J* = 8.7, 1.9 Hz, 2H), 7.17 (dt, *J* = 8.1, 2.3 Hz, 2H), 7.08 (dt, *J* = 8.6, 2.0 Hz, 2H), 2.22 (s, 3H).

ELQ-428: ^{1}H NMR (400 MHz, DMSO-d_6) δ 11.90 (s, 1H), 7.47-7.38 (m, 2H), 7.33-7.23 (m, 3H), 7.20-7.13 (m, 2H), 7.12-7.05 (m, 2H), 2.22 (s, 3H).

APPENDIX D

ELQ-429: ^{1}H NMR (400 MHz, DMSO-d_6) δ 11.68 (s, 1H), 7.42 (d, *J* = 8.8 Hz, 2H), 7.26 (d, *J* = 8.5 Hz, 2H), 7.19-7.15 (m, 3H), 7.08 (d, *J* = 8.5 Hz, 2H), 3.90 (s, 3H), 2.20 (s, 3H).